FINAL REPORT OF THE ULTRA LIGHT AIRCRAFT TESTING

NAG1-345

NASA Langley Research Center
Grant #NAG 1-345

Howard W. Smith
Professor
Department of Aerospace Engineering
University of Kansas

FINAL REPORT OF THE ULTRA LIGHT AIRCRAFT TESTING

I. Report on the Test Set-up for the Structural Testing of the Airmass Sunburst Ultralight Aircraft

II. Load Test Set-up for the Airmass Sunburst Ultra-light Aircraft

III. Nastran Analysis for the Airmass Sunburst Model "C" Ultralight Aircraft

IV. Construction, Wind Tunnel Testing and Data Analysis for a 1/5 scale Ultra-light Wing Model

V. Static Test of an Ultralight Airplane

VI. Selection and Static Calibration of the Marsh J1678 Pressure Gauge

VII. Design of Static Reaction Gantry for an Ultralight Airplane Destruction Test

NASA Langley Grant NAG1-345
Research on Aerodynamics and Flight Dynamics of Subsonic Aircraft

Bibliography

Natural Laminar Flow and Cruise Flap

October 1984
Vijgen, Paul; Ken Williams; Bob Williams
"Design Considerations of Natural Laminar Flow Airfoils for Medium-Speed Regional Aircraft," KU-FRL-6131-1, 236 pgs.

June 1985
Williams, Bob
"User's Guide to CLCDCM: FORTRAN program to Calculate Airplane Drag and Elevator Deflection as a Function of Lift Coefficient," KU-FRL-6131-2

June 1985
Williams, Bob
"A Streamline Curvature Method for Modifying Airfoils," KU-FRL-6131-3, 37 pgs.

June 1985
Williams, Bob
"Progress Report on the Development of a Flight Control System to Optimize Airplane Life-to-Drag Ratio," KU-FRL-6131-4, 56 pgs.

July 1985
Williams, Ken L.
"Natural Laminar Flow and Regional Aircraft: A Performance Assessment," KU-FRL-6131-5, M.S. Thesis

Paper
1984
Williams, Ken; Paul Vijgen; Jan Roskam
Natural Laminar Flow and Regional Aircraft," KU-FRL-6131-P1, 11 pgs.
SAE Paper

Ride Quality Augmentation System

July 1984
Hammond, Terry A; Shailesh P. Amin; James D. Paduano; D. R. Downing
"Design of a Digital Ride Quality Augmentation System for Commuter Aircraft," KU-FRL-6132-1, 364 pgs.
NASA #CR-172419, October 1984
D.E. Dissertation, Terry A. Hammond

February 1986
Davis, Donald J.; Dennis J. Linse; David P. Entz; David R. Downing (P.I.)
"Preliminary Control Law and Hardware Designs for A Ride Quality Augmentation System for Commuter Aircraft: Phase 2 Report," KU-FRL-6132-2, 257 pgs.
NASA #CR 4014, September 1986

May 1986
Donaldson, Kent E.; J. Roskam
"Study on Using a Digital Ride Quality Augmentation System to Trim an Engine-Out in a Cessna 402B," KU-FRL-6132-3, 36 pgs.

May
Linse, Dennis J.; D. Downing (P.I.)
"ICAD: The Interactive Control Augmentation Design Program User's Manual (preliminary)," KU-FRL-6132-4

October 1986
Suikat, Reiner
"Modification of a Panel Method Computer Program to Optimize the Shape of a Nacelle to Obtain Minimum Configuration Drag in Supersonic Flight: User's Manual," KU-FRL-6132-5, 64 pgs., (Supplement to Reiner Suikat's M.S. Thesis).

August 1987
Suikat, Reiner
"Subsonic and Supersonic Configuration Analysis and Design Program: SSCAD (Program Description)" KU-FRL-6132-6, 161 pgs.

November 1988
Suikat, Reiner; Kent Donaldson; David R. Downing
"Detailed Design of a Ride Quality Augmentation System for Commuter Aircraft (Final Report)," KU-FRL-6132-7, 114 pgs.
NASA CR-4230, May 1989

Papers
August 1984
Hammond, Terry A.; David R. Downing; Shailesh P. Amin; Jim Paduano
"Design of a Digital Ride Quality Augmentation System for a Commuter Aircraft," KU-FRL-6132-P1, 7 pgs.
AIAA Paper 84-1958-CP, presented at AIAA Guidance & Control Conference, Seattle, Washington, August 1984

April 1987
Downing, David R.
"A Ride Quality Augmentation System for Commuter Aircraft," KU-FRL-6132-P2, 21 pgs., (viewgraphs for oral presentation only; no text)
Presented at the 119th Annual Meeting of the Kansas Academy of Science, April 3, 1987

September 1987
Suikat, Reiner, Kent Donaldson, & David R. Downing
"An Analysis of a Candidate Control Algorithm for a Ride Quality Augmentation System," KU-FRL-6132-P3, 8 pgs.
AIAA Paper 87-2936, presented at AIAA/AHS/ASEE Aircraft Design, Systems, and Operations Meeting, St. Louis, MO, Sept. 14-16, 1987. Published in AIAA *Journal of Guidance, Control, and Dynamics*, Vol. 12, No. 4, July-August 1989, pgs. 505-513.

Ultra Light Structural Testing

October 1983
Blacklock, Carlos
"Determination of the Static Performance of a Cuyuna 430 CC Model UL-43044 Engine," KU-FRL-6135-1, 200 pgs.

November 1983
Woltkamp, John A.; Carlos L. Blacklock; Jan Roskam
"Weight and Balance for the Airmass Incorporated Sunburst Model 'C' Ultralight," KU-FRL-6135-2, 91 pgs.

February 1984
Braun, Gary
"Concepts for an Ultralight Aircraft Flight Test Data Acquisition System," KU-FRL-6135-3, 45 pgs.

February 1984
Anderson, Gary A.
"Drag Prediction of an Ultralight Airplane: The Airmass Sunburst (Model C)," KU-FRL-6135-4, 53 pgs.

December 1984
Hunt, J. Turner; Perry N. Rea; Carlos Blacklock
"A Determination of the Stability and Control Characteristics of the Airmass Sunburst Ultralight Model 'C', KU-FRL-6135-5, 314 pgs.

July 1984
Rea, Perry N.; Carlos L. Blacklock; Jan Roskam
"Steps Outlining the Assembly of the Airmass Sunburst Ultralight Model 'C', KU-FRL-6135-6, 478 pgs.

Sub-report
February 1984
Blacklock, Carlos L.
"Progress Report Showing Results Obtained in the Airfoil Analysis of an Airmass Sunburst Ultralight model 'C'," KU-FRL-6135-S1, (a "sub-report"; subsequently incorporated into progress report KU-FRL-6135-5), 58 pgs.

Paper

August 1984
Blacklock, Carlos L., Jr., and Jan Roskam
"Summary of the Weight and Balance and the Drag Characteristics of a Typical Ultralight Aircraft," KU-FRL-6135-P1, 18 pgs.
SAE Paper 841021, presented at the West Coast International Meeting & Exposition, San Diego, CA, August 6-9, 1984

Oct. 14, 1985
Smith, Howard W.
"Design of Static Reaction Gantry for an Ultralight Airplane Destruction Test," AIAA paper #85-4022, 6 pgs.

January 1988
Smith, Howard W.
"Static Test of an Ultralight Airplane," *J. Aircraft,* Vol. 25, No. 1, 4 pgs.

Unpublished reports

March 1986
Oxendine, Charles R., and Howard W. Smith
"Selection and Static Calibration of the Marsh J1678 Pressure Gauge," 30 pgs.

December 1988
James, Michael D., and Howard W. Smith
"Construction, Wind Tunnel Testing and Data Analysis for a 1/5 Scale Ultra-light Wing Model," 40 pgs.

October 1991
Nastran Analysis for the Airmass Sunburst Model "C" Ultralight Aircraft," 31 pgs.

May 1992
Zimmerman, William, and Howard W. Smith
"Report on the Test Set-Up for the Structural Testing of the Airmass Sunburst Ultralight Aircraft," 4 pgs.

May 1992
Krug, Daniel W., and Howard W. Smith
"Load Test Set-up for the Airmass Sunburst Ultra-light Aircraft," 40 pgs.

I. REPORT ON THE TEST SET-UP FOR THE STRUCTURAL TESTING OF THE AIRMASS SUNBURST ULTRALIGHT AIRCRAFT

William Zimmerman
Graduate Student

Howard W. Smith
Professor
Department of Aerospace Engineering
University of Kansas

May 1992

Partially supported by
NASA Langley Research Center
Grant #NAG 1-345

ABSTRACT

This report reviews the test set-up and procedure for the structural testing of the Airmass Sunburst Ultralight Aircraft.

INTRODUCTION

In general aviation today, there is a growing need for more stringent design criteria for ultralight aircraft. Unlike most general aviation aircraft, the ultralight lacks sufficient design criteria and more importantly it lacks sufficient certification enforcement. The Airmass Sunburst ultralight that is currently being tested at the University of Kansas, by William Zimmerman, Suman Sappali, and Dan Kurg, is responsible for over a dozen deaths. It is believed that had there been a more stringent criteria and certification process, this might have been prevented. Our attempt is to show that the failing loads of the aircraft in question are so far below that of the current design criteria, that the laws need to be changed.

PROGRESS (WORK DONE)

After an initial survey of the ultralight aircraft, located at the Lawrence Municipal Airport, the following jobs were outlined and performed.

1.) Since the aircraft had been sitting in the hanger for many years, it was decided that the whole aircraft should be cleaned. This was done by first using a power blower to whisk away most of the dirt, and then it was

dusted by hand.

2.) In order to work on the ultralight, a scafolding was needed. This was obtained through Dr. Smith and delivered to the airport by the Facilities and Operations personnel. It was then set up.

3.) After the ultralight was hoisted using the hand hoist, the scaffolding was moved under the ultralight. The next step was to assemble the whiffle trees. The whiffle trees are what the aircraft is to be supported with along its span, and when the aircraft is pulled from below, it simulates a lift load. The whiffle trees were first dusted and then they were assembled. There were twelve whiffle trees. Six for each wing. It was determined during this process, that additional turnbuckles were needed. They were obtained and all twelve whiffle trees positioned.

4.) Upon review of the above work, it was noted that the aircraft needed to be leveled both lateraly and longitudinaly. The longitudinal balancing was obtained by placing billets on the forward section of the whiffle trees near the front spar. These billets, weighing 25 pounds each, were drilled by Andy Pritchard to obtain a 0.5 inch hole through them. This allowed the billets to be attached quite easily. They were bolted firmly to prevent any accident, and helmets were worn at all times. The lateral leveling was obtained through a lengthy process of adjusting the turnbuckles, and wedging the outboard whiffle trees. In some cases, the turnbuckles had to be sawed down to a smaller length. The main problem

was that the load on the wings due to the ultralights weight, was not semmetric. This process took three weeks.

5.) The next step was to set up the actuator and load cell that would be used to apply a load to fail the aircraft structure. 175 pounds of sand was installed in the cockpit to simulate the weight of the pilot. Then the actuator and load cell were installed. To do this, the attachement bars that attach between the floor and the load cell were trimmed and drilled. Andy prichard provided the tooling and expertise required to machine the attachment bars.

6.) The next two weeks involved the testing and repair of the strain guages. During the process of attaching the whiffle trees, several of the strain guages were damaged. The wires were resoldered. The guages were then tested with a digital multimeter and the process of resoldering the guages continued untill all but three were fixed. These three were so badly damaged, that we were unable to fix them. Two of them are on the far inboard station and after discussion with Dr. Smith, it was agreed they were not critical to the test. The third was located at the rear spar, directly over the mounting point of one of the whiffle trees.

7.) The next step was to attach the guages to the recording equipment. Jerry Hanson was informed of our progress, and met with us out at the airport. After obtaining the equipment, it was determined that to hook up the guages, each guage would require a full wheat stone bridge. After

describing the theory of the bridge and how it allows the measurement of the strain in the guages, a sample bridge was mapped out and constucted. In attempting to zero out the equipment a show stopper had arisen. The resisters used to balance the bridge were not precise enought to allow a proper balance. In order to procede, preccision resistors will be needed. Currently they have been ordered by Jerry Hansen from a company in Kansas City and are expected soon.

CONCLUSION

The ultralight test set-up is nearly complete. All that is left is to balance the wheatstone bridges for each guage. When this is complete, and the tests are run, it is believed that the failing load of the ultralight will be far below that of the certifiable failing load. With our results, we will show the need for new design criteria and more importantly the need for stricter enforcement of the design criteria. The designer of this ultralight has fled the country. He obviously only cared about making a fast buck. In the future, we as an industry must work to prevent accidents like those attributed to the Airmass Sunburst. In all acutuality, they weren't accidents. They were negligent actions that could have been spotted had there been a stricter process of certification and enforcement been achieved.

II. LOAD TEST SET-UP FOR THE AIRMASS SUNBURST ULTRA-LIGHT AIRCRAFT

Daniel W. Krug
Graduate Student

Howard W. Smith
Professor
Department of Aerospace Engineering
University of Kansas

May 1992

Partially supported by
NASA Langley Research Center
Grant #NAG 1-345

Introduction

The purpose of this one hour AE 592 Special Project class was to set up, instrument, and test the Sunburst Ultra-Light aircraft at the Lawrence Municipal Airport for the University of Kansas Aerospace Engineering Dept. and the Center for Research Inc. (CRINC). The intentions of the project were that the aircraft would need to be suspended from the test stand, leveled in the stand, the strain gauges tested and wired to the test equipment, and finally, the aircraft would be broke to obtain the failing loads.

All jobs were completed except to break the aircraft. This notebook shows the progress of Suman, Bill, and myself as these tasks were completed and the following section attempts to explain the photographs in the notebook. All work done, was done as a team effort, so that no one person was required to do more work than the others.

Work Done

1.) The first task was that of cleaning the aircraft and equipment to be used in the test. To start this process, a gasoline powered leaf blower was used to dust the aircraft and test stand off. Next the wings and cockpit were dusted by hand. Finally, the whiffle-tree sections were assembled and dusted to determine what additional equipment was needed.

2.) The next set of tasks included setting up the scaffolding, hoisting the aircraft, hanging it from the whiffle-trees, and hanging the balance weights. The scaffolding proved very helpful in hanging the aircraft, though if it was done again, it is recommended that a second set be obtained to make the job easier. This set of tasks appeared to be difficult, but ended up being relatively easy.

3.) Leveling the ultra-light in the whiffle-trees was the next task and it proved to be just the opposite of the previous group of tasks. It looked relatively easy and ended up taking about three weeks to get an even loading on the aircraft. Most of this work was performed in the weeks following spring break.

4.) Approximately two weeks were spent to examining the strain gauges, resoldering the broken ones, and then testing the gauges with a digital multimeter. After this was done, three strain gauges were determined to be unfixable but were in locations that did not merit replacement. One was the most inboard strain gauge on the front spar and another was located on the underside of the rear spar directly over the mounting point for one of the whiffle-trees. Also at this point, the actuator was attached to

the aircraft and it was determined that new flat iron pieces would be required so that the actuator assembly would reach from plane to floor.

5.) At this point, Jerry Hanson came to the airport to help set up the test equipment and it was determined that resistors to make wheatstone bridges for strain gauges were needed. This is where the project stands at the time of this report. Some work will be performed the first week of finals so that the aircraft will be completely set up such that Suman can finish the test himself or with the help of Todd and Steve this summer or next fall.

Conclusions

The actual test was not completed in this semester due to the last minute problem of not having resistors in the last three weeks. These were the only major piece of equipment that we did not have, but when these come in, the final test of the aircraft should not take a large quantity of time.

This project proved to be very interesting and I enjoyed finally to be able to work on a project at the airport. I think I will find the work done on this airplane useful in the future, as I plan to attend law school at the University of Kansas this summer. Testing an airplane that carries with it the legal problems that this ultra-light does will give me experience that most in the legal field will not have.

CLEANING THE ULTRA-LIGHT WITH
A POWER LEAF BLOWER

CLEANING THE ULTRA-LIGHT WITH
A POWER LEAF BLOWER

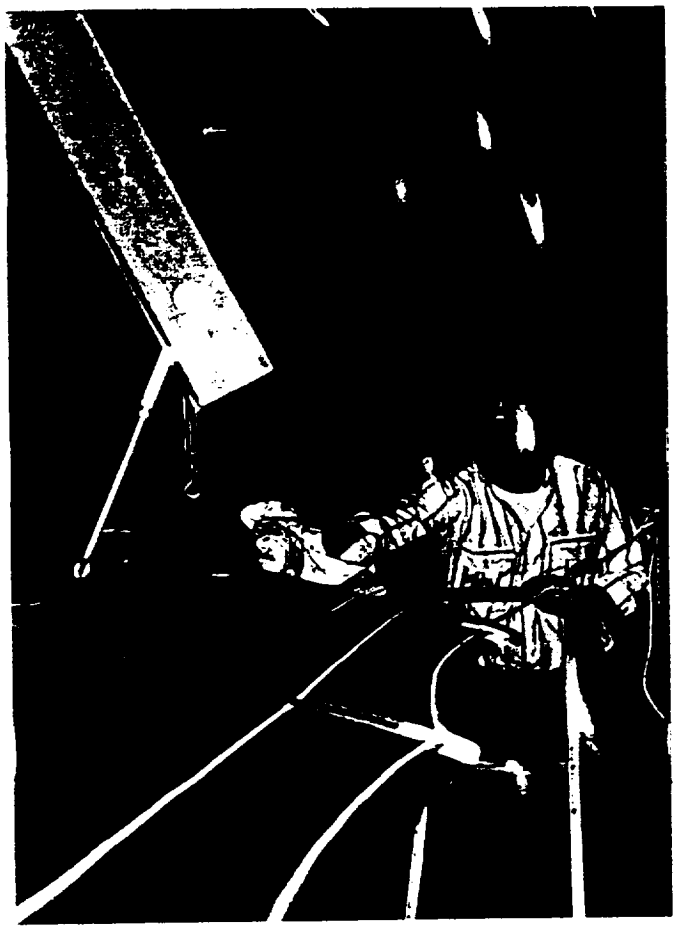

DUSTING THE WINGS AND WHIFFLE-TR ES

SETTING UP THE SCAFFOLDING

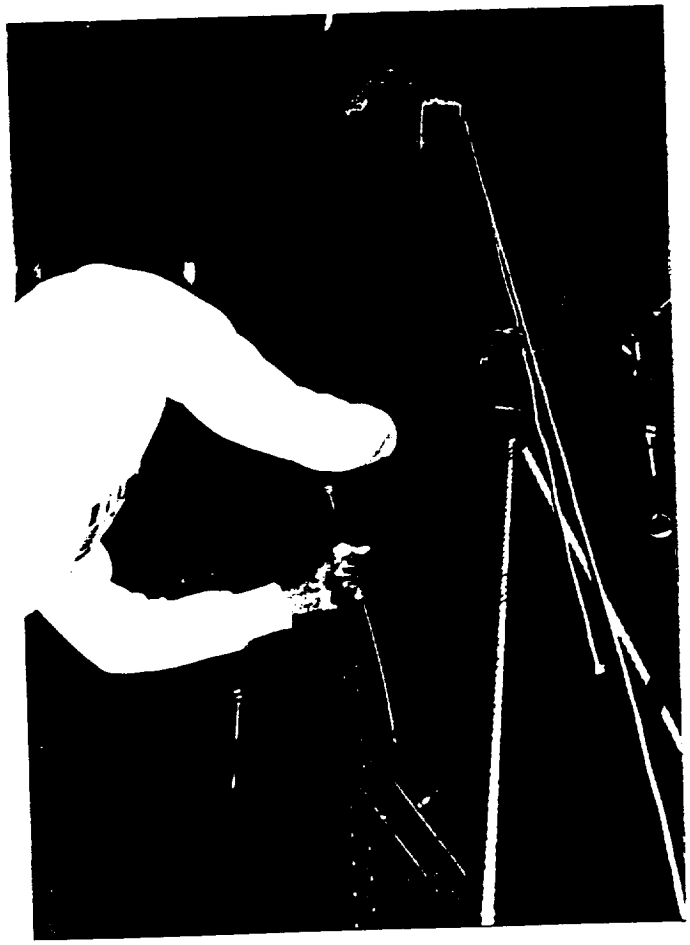

HOISTING THE ULTRA-LIGHT

ALIGNING 2ND RANK OF WHIFFLE-TREES

ATTACHING THE 1ST RANK OF THE WHIFFLE-TREES
TO SUSPEND THE ULTRA-LIGHT FROM THE TEST STAND

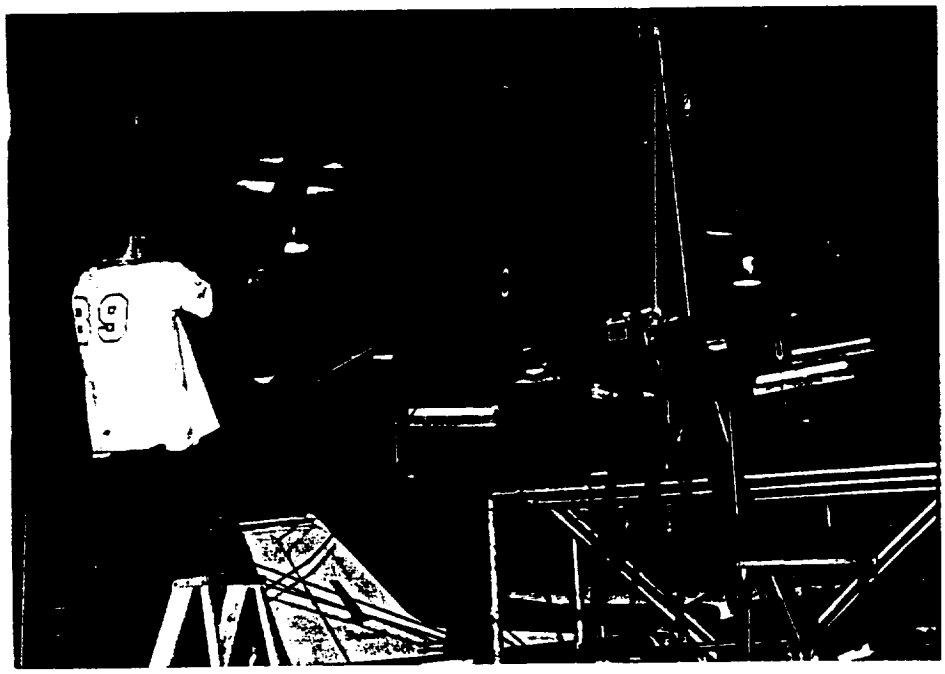

ATTACHING THE 1ST RANK OF THE WHIFFLE-TREES
TO SUSPEND THE ULTRA-LIGHT FROM THE TEST STAND

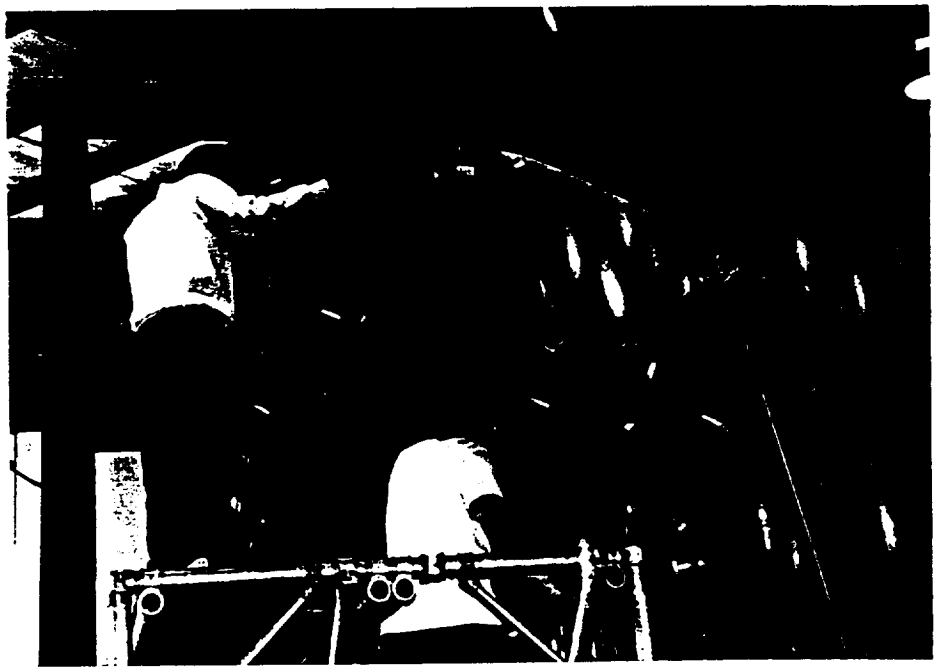

ATTACHING THE 1ST RANK OF THE WHIFFLE-TREES
TO SUSPEND THE ULTRA-LIGHT FROM THE TEST STAND

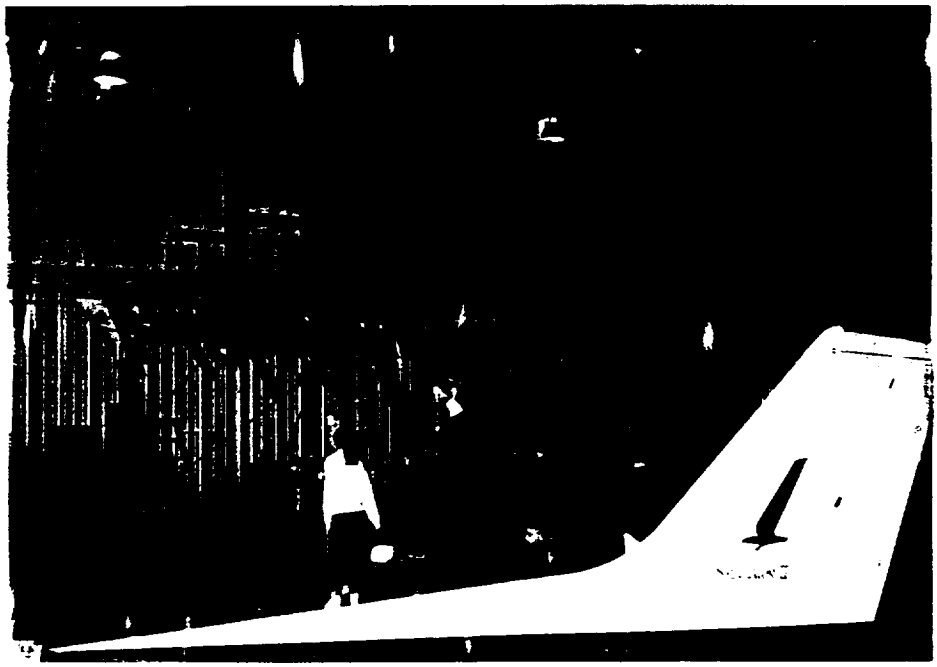

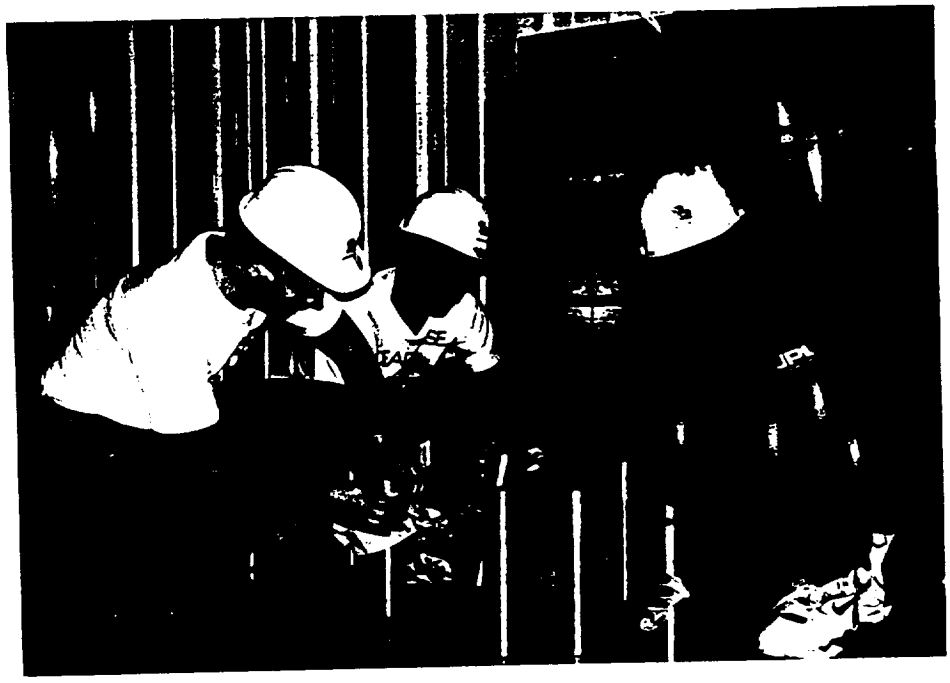

CLEANING THE BALANCE WEIGHTS

HANGING THE BALANCE WEIGHTS

HANGING THE WEIGHTS

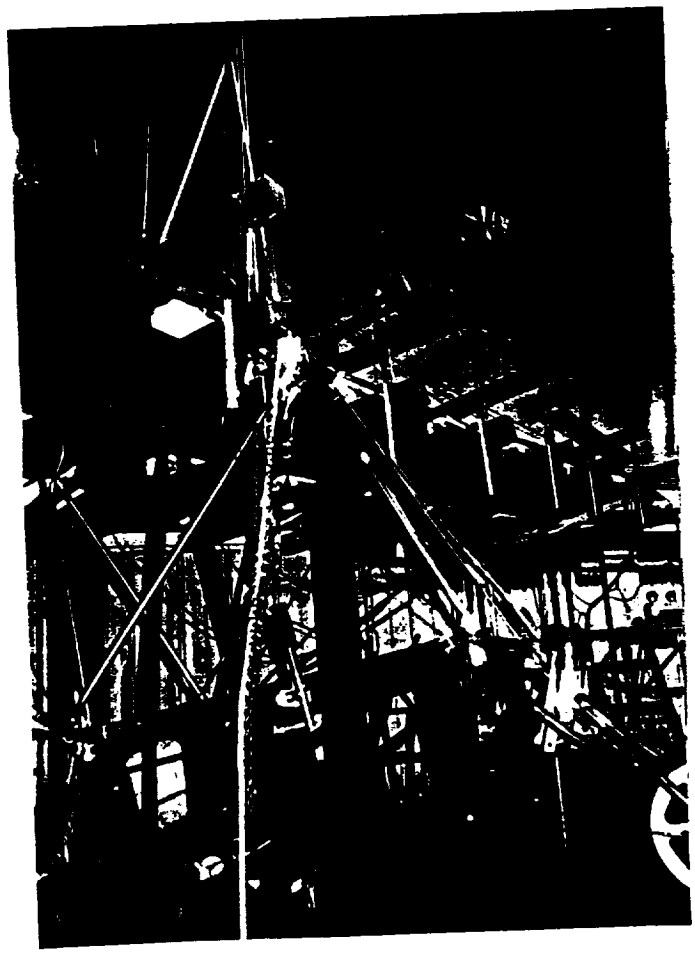

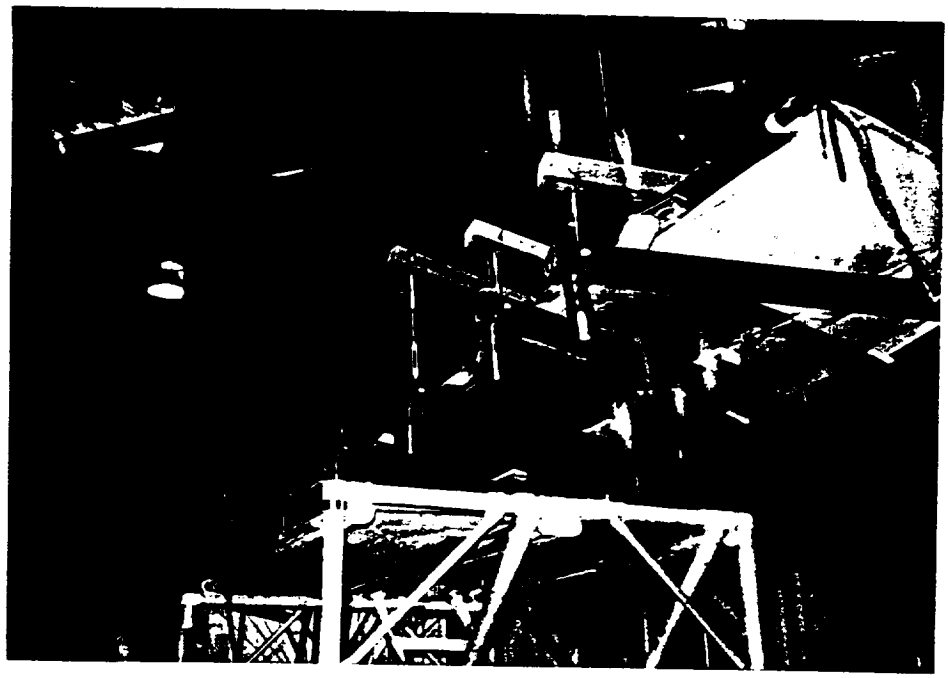

THE ULTRA-LIGHT WITH WEIGHTS HUNG

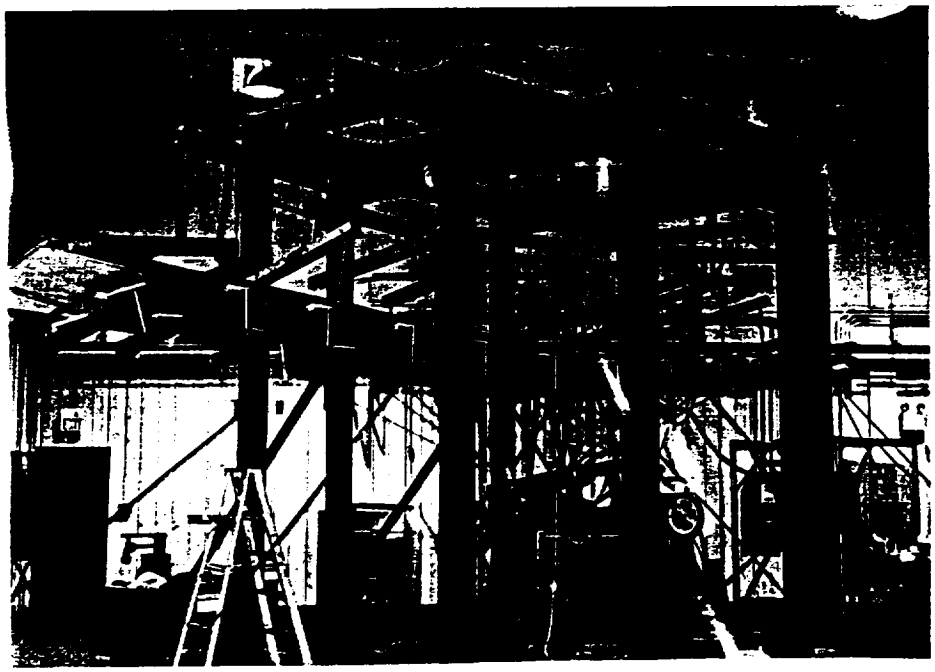

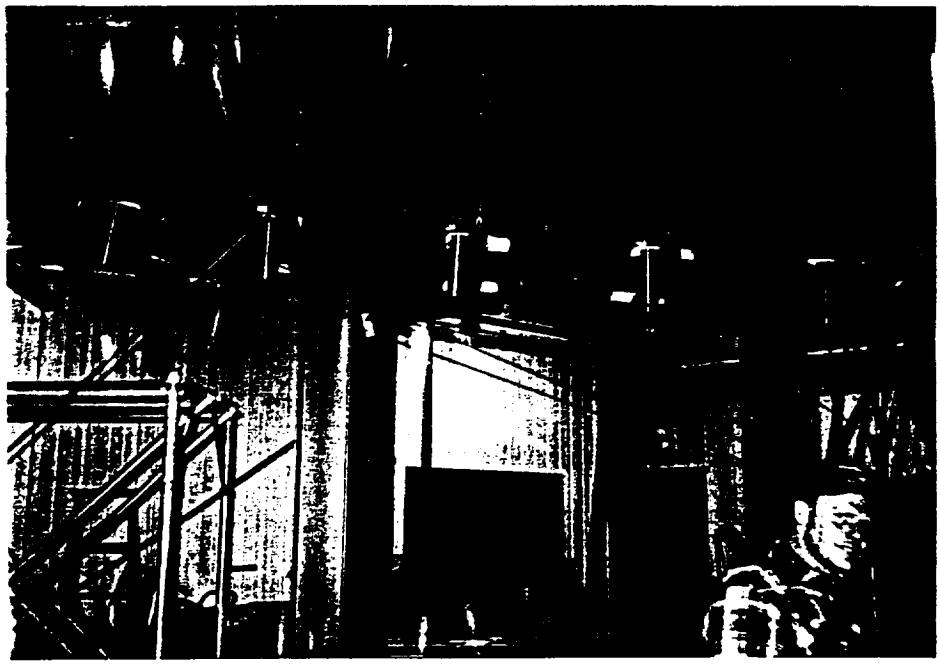

THE ULTRA-LIGHT WITH WEIGHTS HUNG

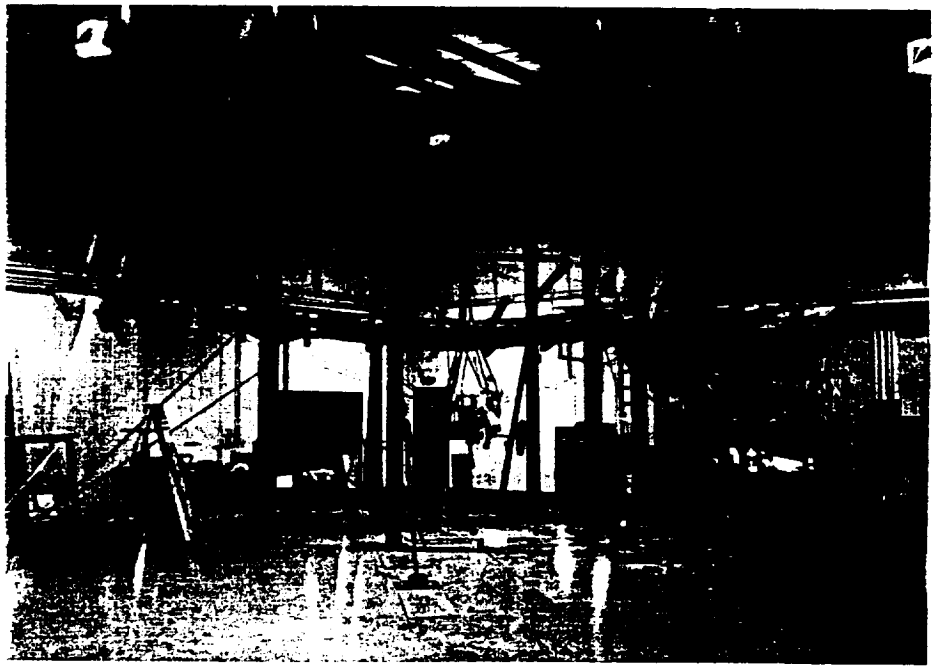

LEVELING THE ULTRALIGHT IN THE WHIFFLE-TREES

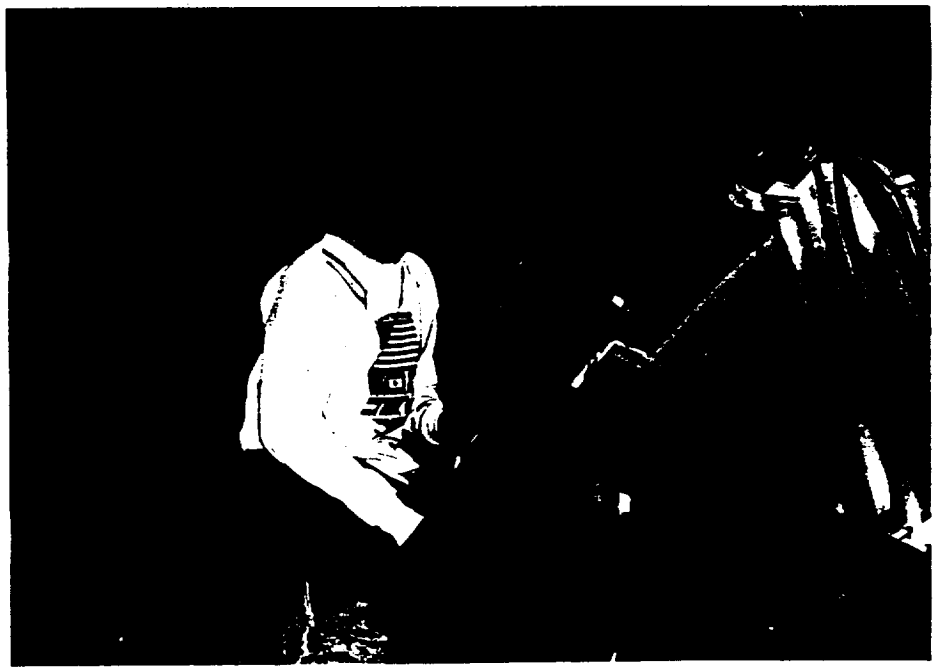

ORIGINAL PAGE
BLACK AND WHITE PHOTOGRAPH

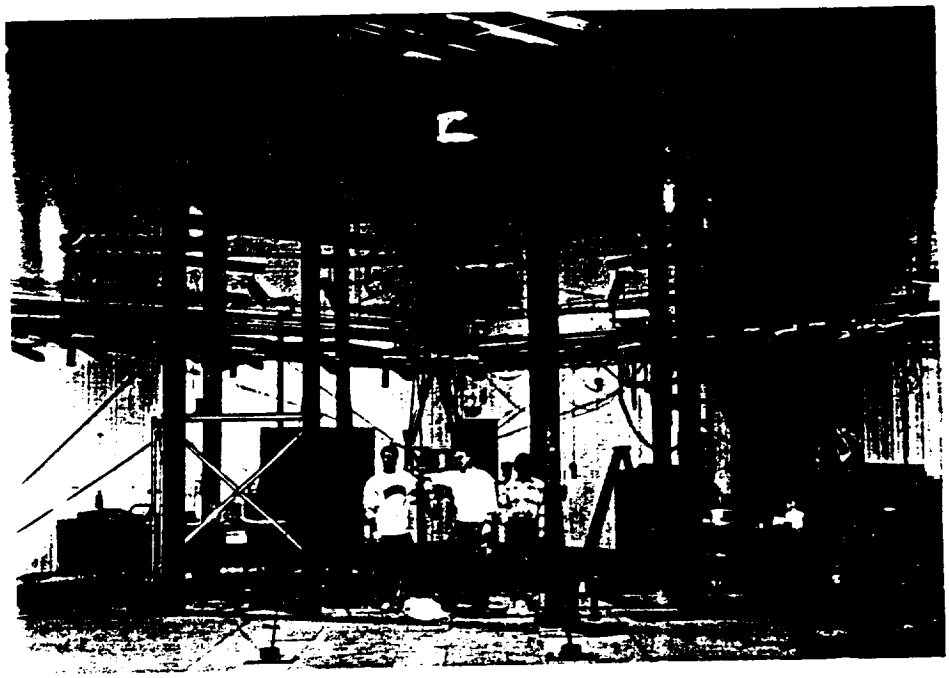

LEVELING THE ULTRALIGHT IN THE WHIFFLE-TREES

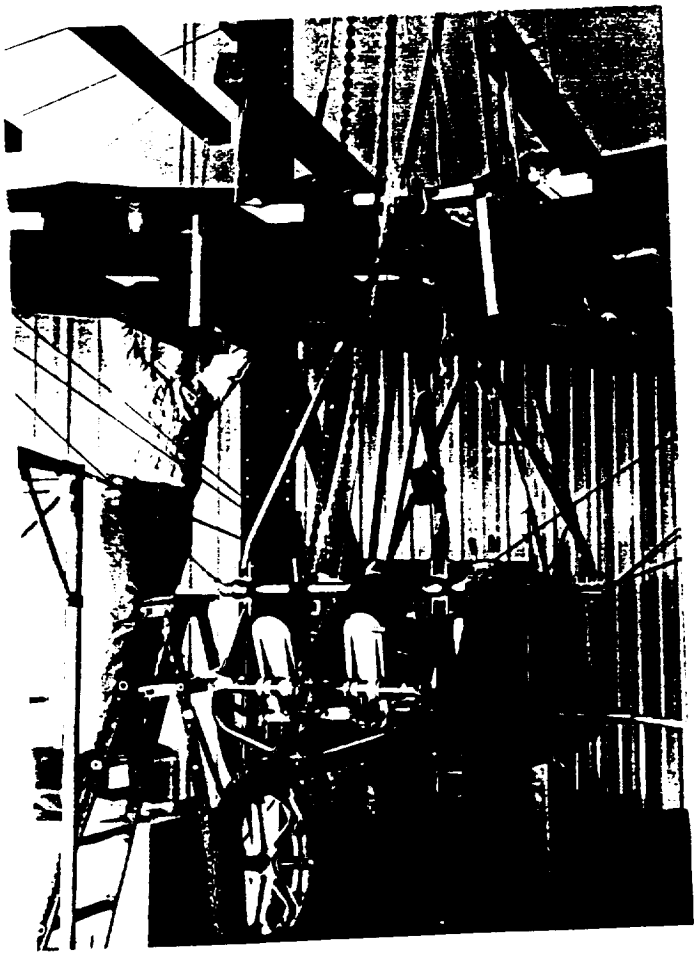

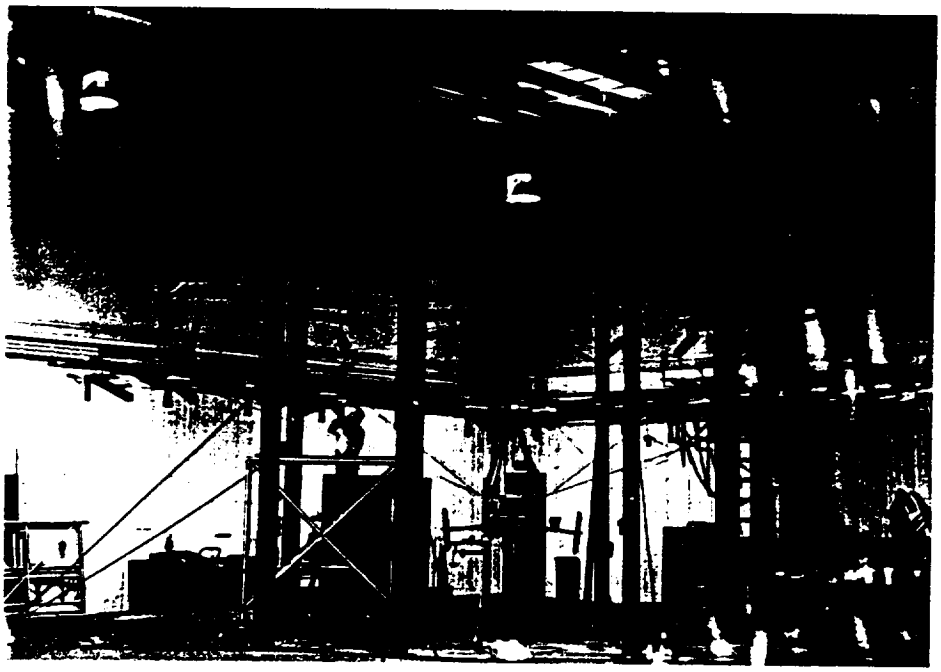

LEVELING THE ULTRALIGHT IN THE WHIFFLE-TREES

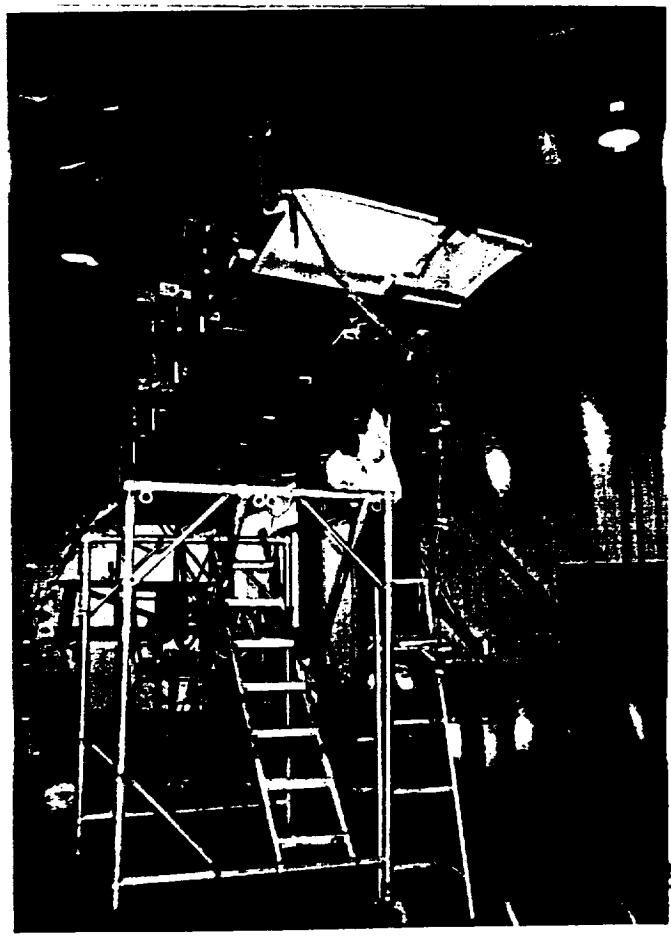

LEVELING THE ULTRALIGHT IN THE WHIFFLE-TREES

CUTTING THE TURNBUCKLES TO
TIGHTEN THE WHIFFLE-TREES

GRINDING THE THREADS ON AN EYE-BOLT

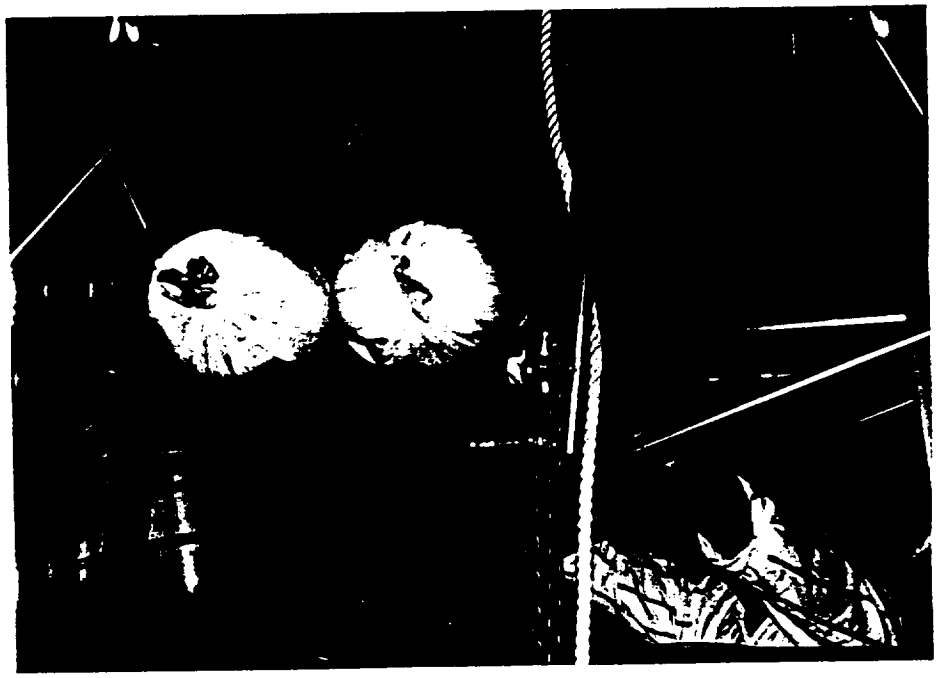

OUR ANTHROPOMORPHIC DUMMY

MEASURING THE LOAD CELL
AND ACTUATOR

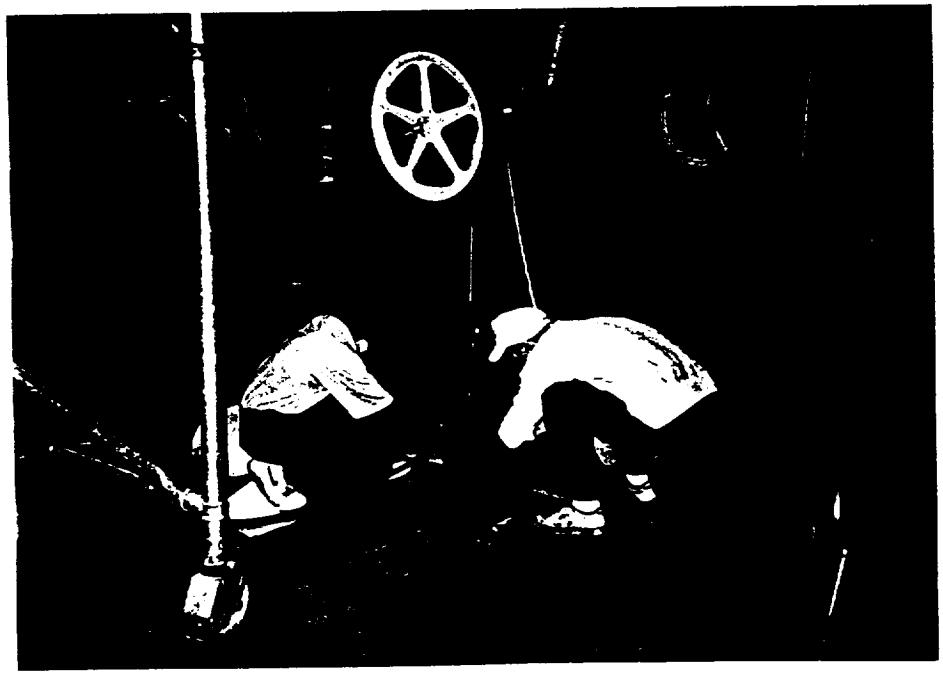

REMANUFACTURING THE ACTUATOR ASSEMBLY

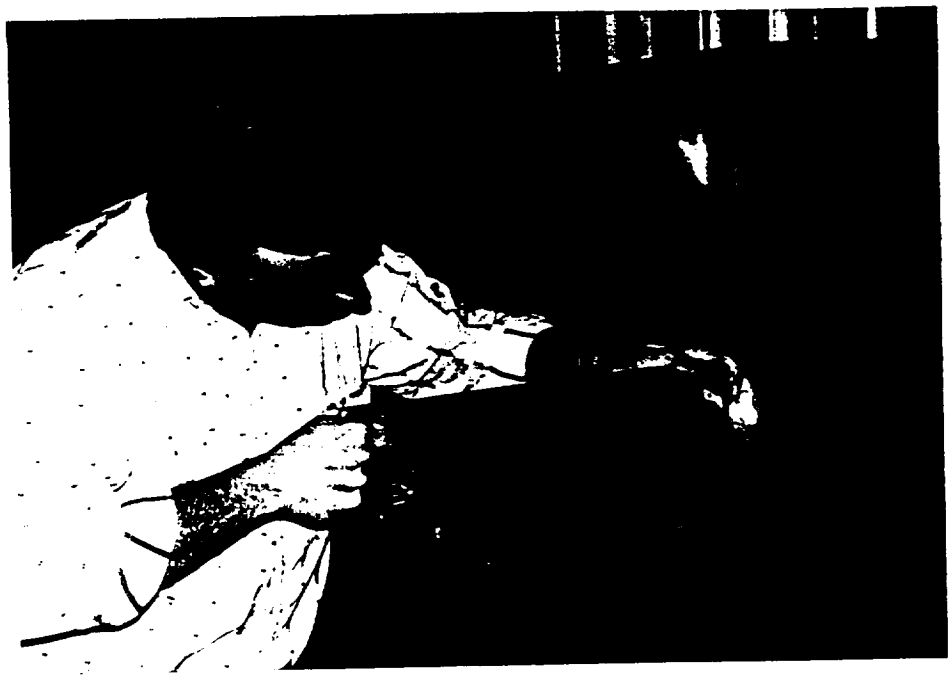

REMANUFACTURING THE ACTUATOR ASSEMBLY

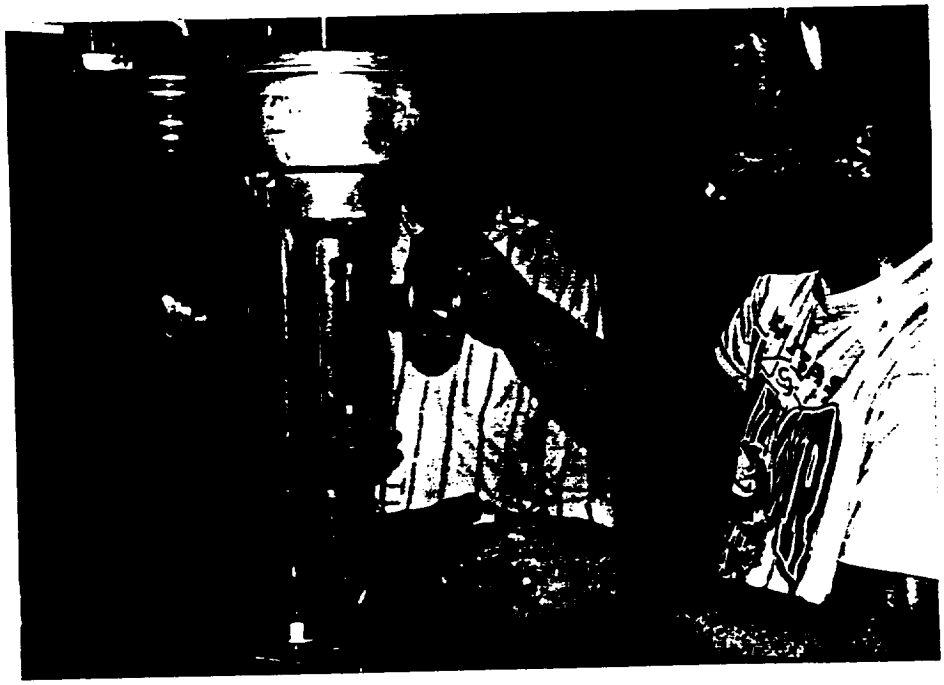

ASSEMBLING THE ACTUATOR ASSEMBLY

RE-SOLDERING THE STRAIN GAUGES

ORIGINAL PAGE
BLACK AND WHITE PHOTOGRAPH

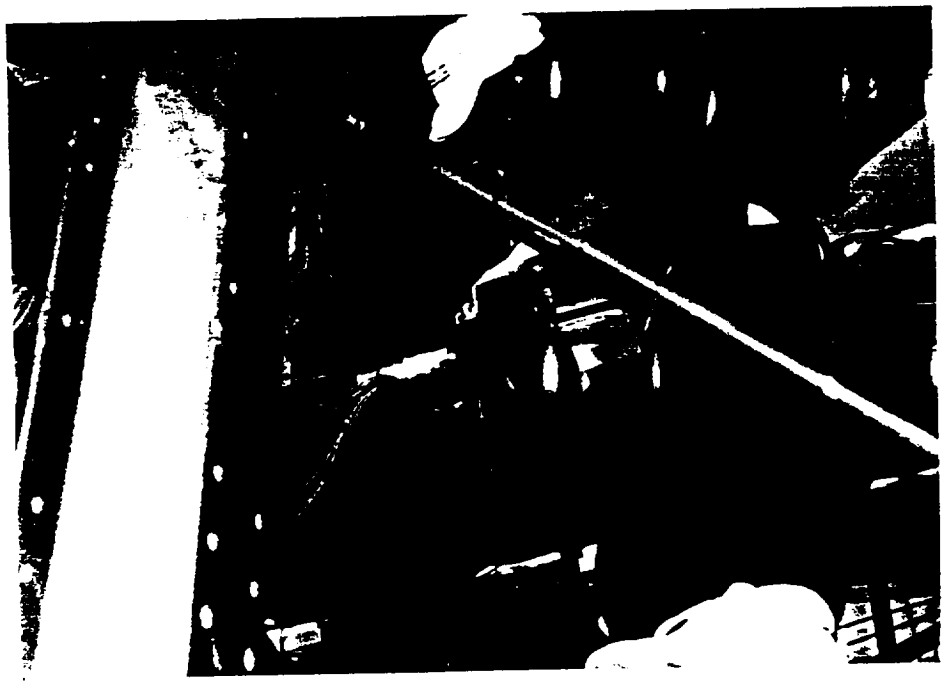

ORIGINAL PAGE
BLACK AND WHITE PHOTOGRAPH

RE-SOLDERING THE STRAIN GAUGES

RE-SOLDERING THE STRAIN GAUGES

TESTING THE STRAIN GAUGES

TESTING THE STRAIN GAUGES

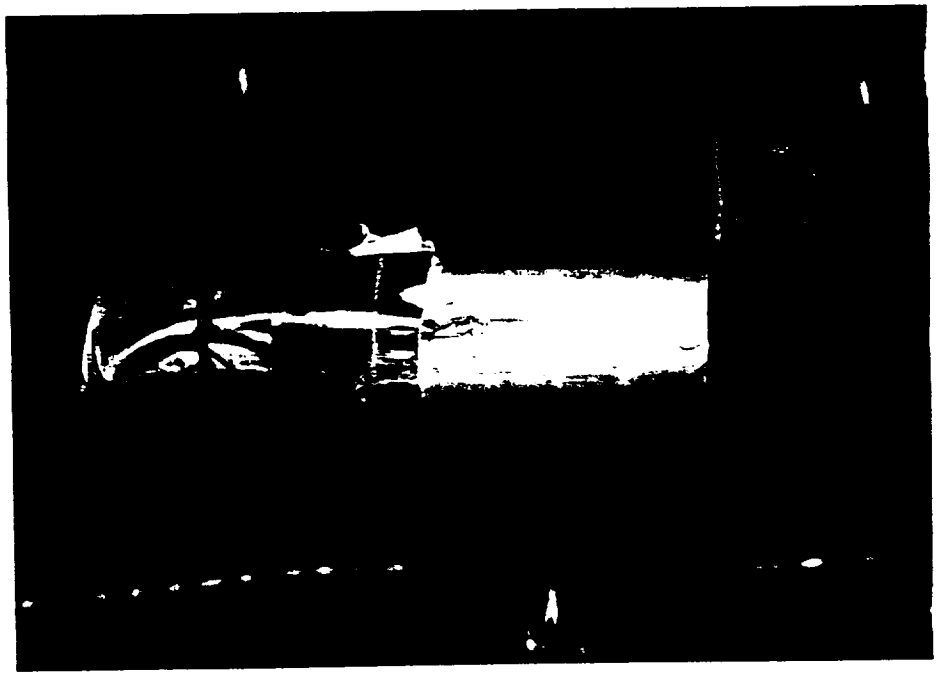

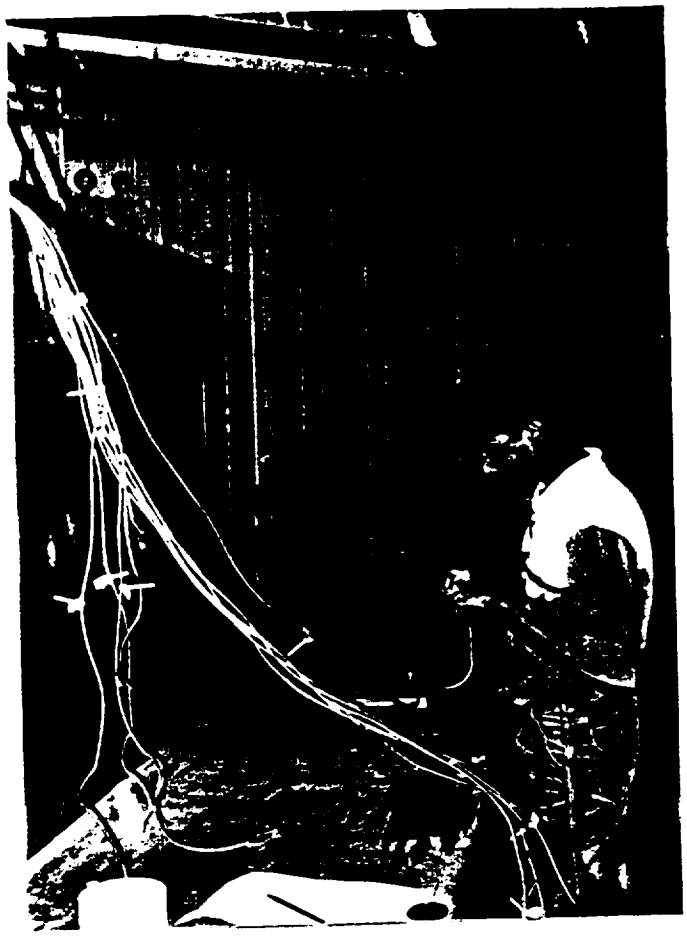

SETTING UP THE TEST EQUIPMENT
(WITH HELP FROM JERRY HANSON)

JERRY HANSON SETTING UP TEST EQUIPMENT

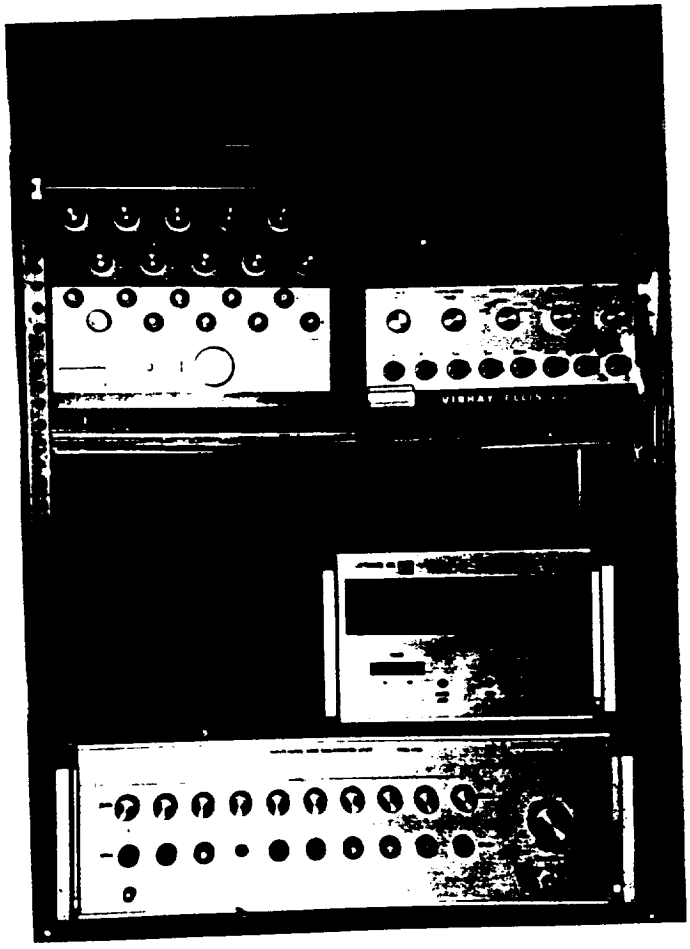

ASSEMBLING WHEATSTONE BRIDGES

SORTING STRAIN GAUGE LEADS

THE AIRCRAFT BEFORE THE FINAL TEST

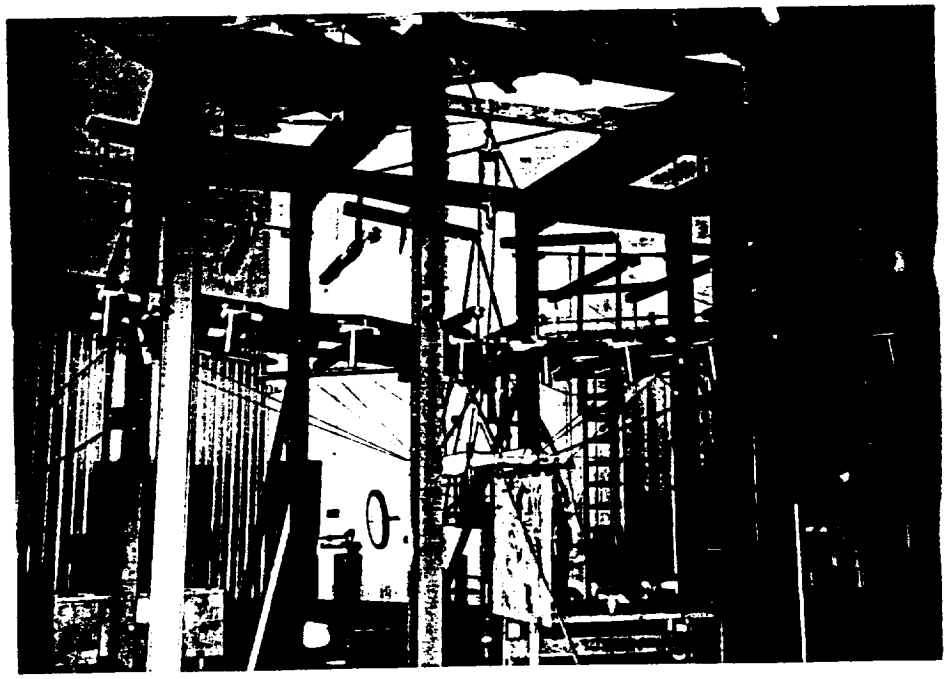

ORIGINAL PAGE
BLACK AND WHITE PHOTOGRAPH

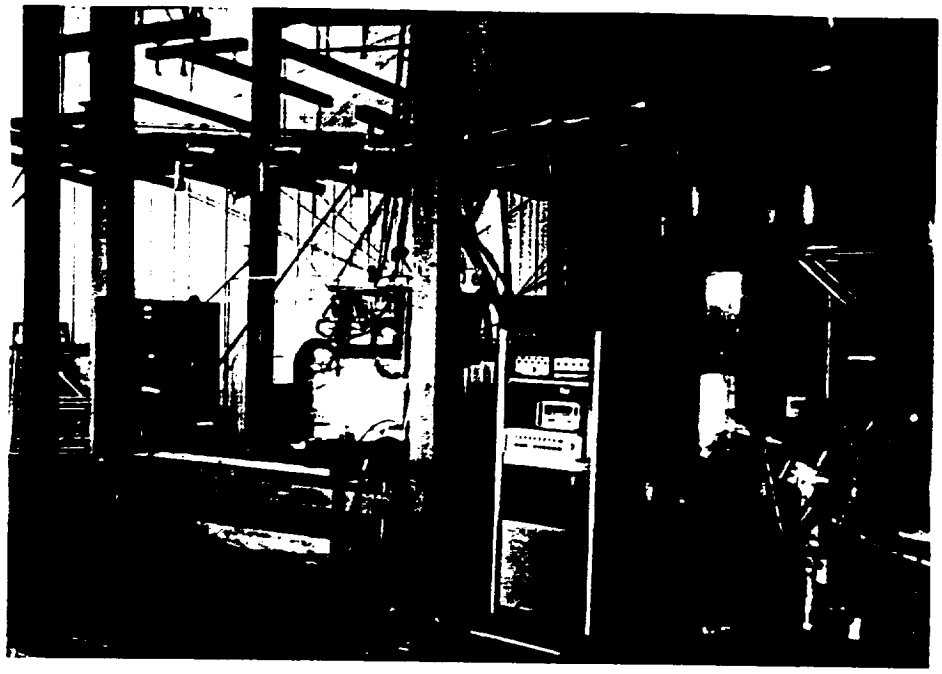

THE AIRCRAFT BEFORE THE FINAL TEST

ORIGINAL PAGE
BLACK AND WHITE PHOTOGRAPH

THE AIRCRAFT BEFORE THE FINAL TEST

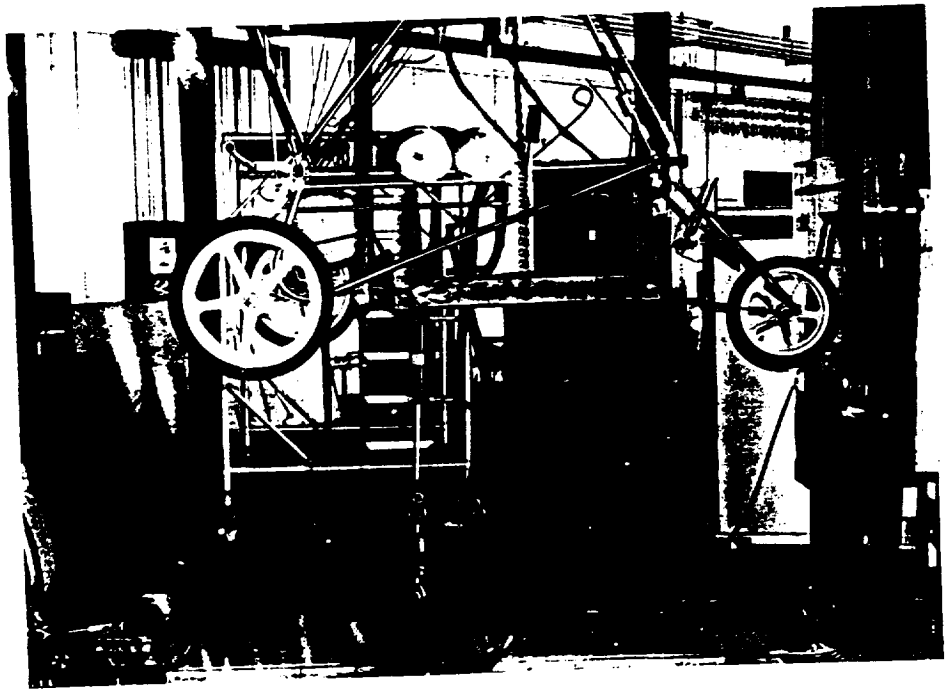

THE AIRCRAFT BEFORE THE FINAL TEST

THE AE 592 CREW (NOTICE 3 OF THE
5 PEOPLE ASLEEP IN THE FINAL PICTURE)

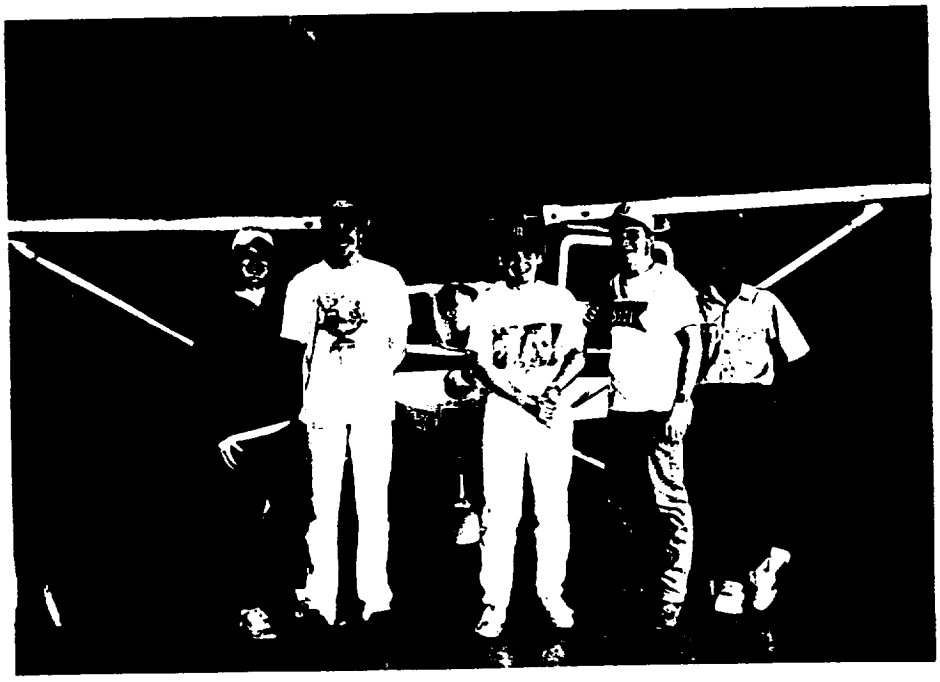

III. NASTRAN ANALYSIS FOR THE AIRMASS SUNBURST MODEL "C" ULTRALIGHT AIRCRAFT

John Verbestel
Graduate Student

Howard W. Smith
Professor
Department of Aerospace Engineering
University of Kansas

October 1991

Partially supported by
NASA Langley Research Center
Grant #NAG 1-345

1. PREFACE

This report was submitted to the aerospace engineering department of the University of Kansas. This report is to satisfy one credit hour in the course AE 592, special projects in aerospace engineering. The present research is a subset of project KU-FRL-6135 conducted under the supervision of professor Howard W.Smith.

TABLE OF CONTENTS

APPENDIX E (*): 2-D NASTRAN RESULTS

APPENDIX F(*): 3-D NASTRAN RESULTS

* APPENDIX E AND F ARE COMPUTER OUTPUT DATA WHICH ARE ATTACHED SEPARATELY.

LIST OF SYMBOLS

Symbol	Definition	Dimension
E	Modulus of Elasticity	ksi
Ec	Compression modulus of Elasticity	ksi
G	Modulus of Rigidity	ksi
Fcy	Compression Yield Strength	ksi
Fsy	Shear Yield Strength	ksi
Fty	Tensile Yield Strength	ksi
Ftu	Tensile Ultimate Strength	ksi

Acronyms	Definition
MAT	Material
NASTRAN	NASA Structural Program

Greek Symbols	Definition
ν	Poisson's Ratio
ρ	Density (lb/ft^3)

1. INTRODUCTION

The purpose of this report is to create a three dimensional NASTRAN model of the Airmass Sunburst Ultralight comparable to one made for finite element analysis. A two dimensional sample problem will be calculated by hand and by NASTRAN to make sure that NASTRAN finds the similar results. A three dimensional model, similar to the one analyzed by the finite element program, will be run on NASTRAN. A comparison will be done between the NASTRAN results and the finite element program results. This study will deal mainly with the aerodynamic loads on the wing and surrounding support structure at an angle attack of 10 degrees.

2. 2-DIMENSIONAL MODEL

The purpose of this chapter is to create a two dimensional truss model similar to the Sunburst Ultralight front spar and the three flying wires. The static loads to be used are calculated from the aerodynamic loads at an angle of attack of 10 deg. The resultant element forces will be calculated manually and by use of NASTRAN. From these results, a comparative study will be made between the NASTRAN results the results achieved by manual calculation.

2.1 MODEL DESCRIPTION

The purpose of this section is to describe the major assumptions used to create the 2-dimensional model of the Sunburst Ultralight. It is assumed for this analysis that the root beam and the two wire nodes are fixed. The resulting model will be essentially a fixed cantilever beam attached to three truss elements in tension. The following Nodes will be fixed:

Node 1, Front Spar and Root Beam connection
Node 9, Cable end
Node 12, Cable end

Figures 2.1.1 and 2.1.2 show the dimensioned truss and the nodal data for the 2-dimensional model. The following subsections contain the information required for the NASTRAN program to be completed. The Sub-sections contain the following:

Node and Constraint identification
Element Description
Material Description
Wing Loading Calculations

With this information, the resulting NASTRAN program can be run on the University of Kansas VAX system.

SCALE 1" = 30"

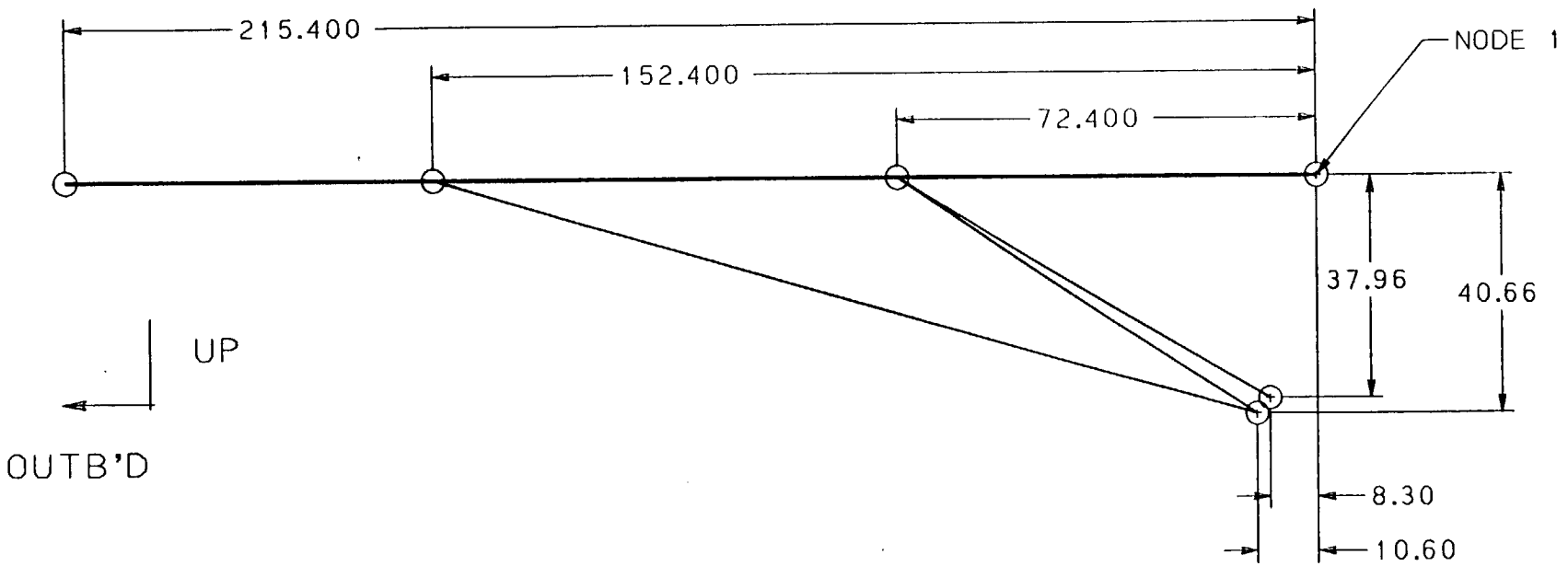

FIGURE 2.1.1: DIMENSIONED TRUSS MODEL

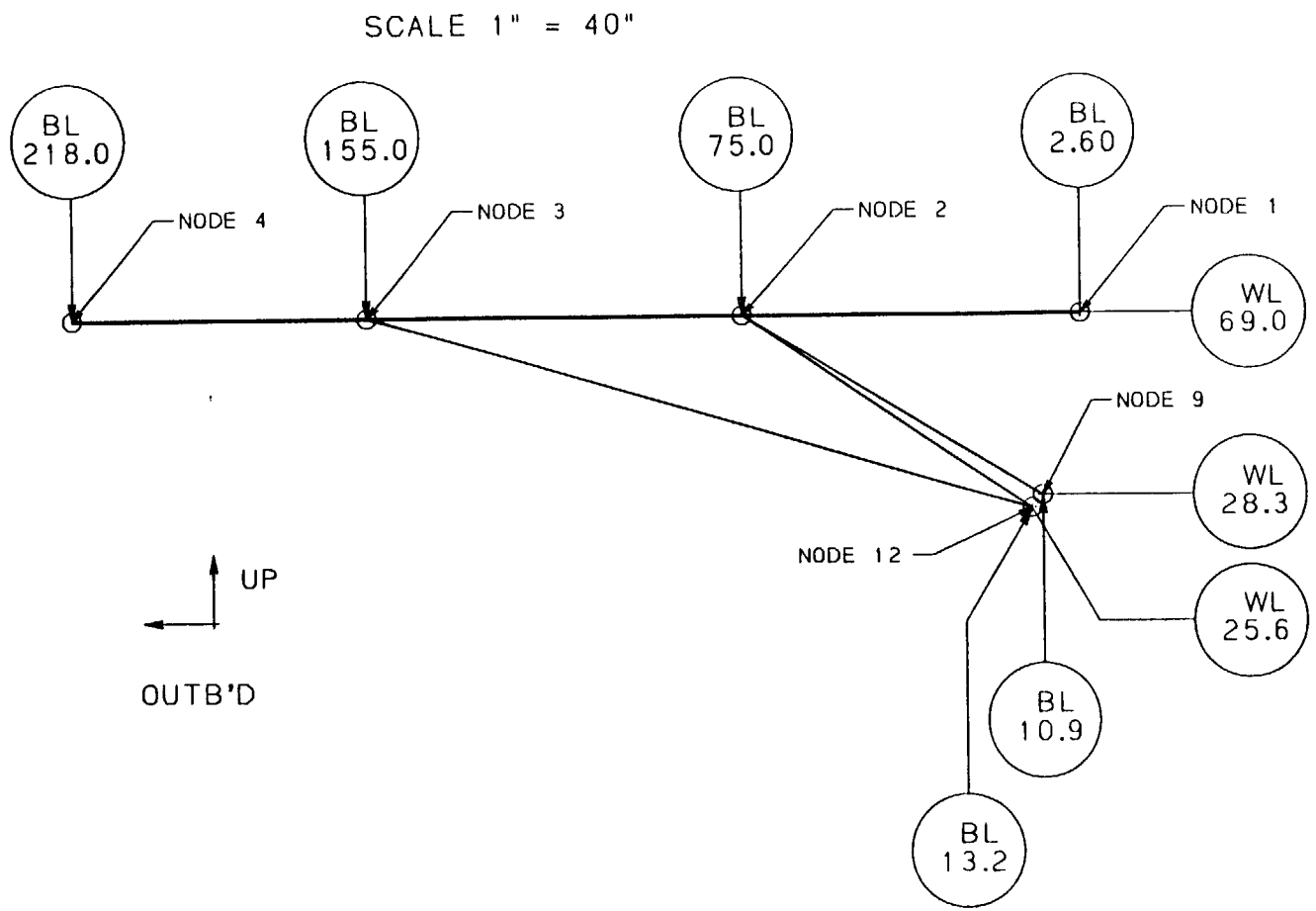

FIGURE 2.1.2: NODAL DATA FOR 2-D TRUSS

2.1.1 NODE POINT AND CONSTRAINT DEFINITIONS

The purpose of this section is to identify the grid points used and the constraint at each point. The constraints used by NASTRAN are as follows:

1 = Linearly constrained in the X-direction
2 = Linearly constrained in the Y-direction
3 = Linearly constrained in the Z-direction
4 = Constrained about the X-axis; Ox = 0 deg.
5 = Constrained about the Y-axis; Oy = 0 deg.
6 = Constrained about the Z-axis; Oz = 0 deg.

The following table contains the GRID cards used in the NASTRAN program for the 2-D model. Table 2.1.1 also includes the single point constraints for each point and the GRIDSET card for the default constraints.

Table 2.1.1: GRID and GRIDSET Cards used in NASTRAN

NASTRAN CARD	X (AFT) (IN)	Y (OUTB'D) (IN)	Z (UP) (IN)	CONSTR-AINT
GRIDSET				1,4,5,6
GRID #1	0.0	2.6	66.3	123456
" #2	0.0	75.0	66.3	
" #3	0.0	155.0	66.3	
" #9	0.0	10.9	28.3	123456
" #12	0.0	13.2	25.6	123456

2.1.2 ELEMENT IDENTIFICATION

The purpose of this section is to identify the elements used in the 3-dimensional NASTRAN model. The following table shows the elements used and their descriptions.

Table 2.1.2: Element Descriptions

ELEMENT NUMBERS (EID)	DESCRIPTION
1,2,3 (Fig.2.1)	Wing Spars; 1.75" Diameter Tubes, t = 0.049"
4,5,6 (Fig.2.1)	Flying Wires; (4) Diameter = 3/32" (5,6) Diameter = 1/8"

2.1.3 ELEMENT MATERIAL IDENTIFICATION

The purpose of this section is identify the materials used for each element of the ultralight model. The tube information is referenced from the ultralight model handbook. The cable information is experimental data taken from the analysis performed by students under the supervision of Dr. Howard W. Smith. The following are the material identifications for each element in the 3-dimensional model and pertinent material information:

Material ID = 1; EID = 1,2,3
6061-T6 Tube,
Spec = WW-T-700/6
Ftu = 42. ksi
Fcy = 34. ksi
Fsy = 27. ksi
E = 9.9+3 ksi
Ec = 10.1+3 ksi
μ = 0.33
ρ = 0.098 lb/in^3
(Ref. 3, Table 3.6.1.0(b))

Material ID = 2; EID = 4,5
Alloy steel cables,
Experimental Data
Ftu = 864. psi
E = 29.0 +3 Ksi
μ = 0.33
ρ = 0.283 lb/in^3

The materials used are assumed to be linear, temperature independent, isotropic materials. Therefore, MAT1 cards will be used in the NASTRAN program.

2.1.4 WING LOADING AND FORCE CALCULATIONS

The purpose of this section is to determine the forces on the wing nodes which must be equivalent to the wing loading. The wing loading was taken from test data in Reference 1, Table 3.3.2. The table and the calculations used to obtain the forces on the nodes can be found in Appendix A. The following are the results of these calculations:

Node 1, F1 = 56.1 lbs
Node 2, F2 = 55.6 lbs
Node 3, F3 = 30.2 lbs

These forces are considered static and thus Force cards will be used in the NASTRAN program. The forces are considered to act in the vertical, (z) direction.

2.2 MANUAL CALCULATION OF RESULTING FORCES AND MOMENTS

The purpose of this section is to calculate the resulting forces at each node for the 2-d model with the static loads. Manual calculations for the 2-dimensional truss model can be found in Appendix B. The following are the resulting element forces and stresses:

ELEMENT AXIAL FORCES AND STRESSES (APPENDIX B);

ELEMENT	AXIAL FORCE (lbs)	AXIAL STRESS (psi)
1-(TUBE)	-186.	710. (COMP.)
2-(TUBE)	-89.2	430. (COMP.)
4-(CABLE)	+94.2	13600. (TENSION)
5-(CABLE)	+0.70	101. (")
6-(CABLE)	+103.	8370. (")

2.3 NASTRAN CALCULATION OF RESULTING FORCES AND MOMENTS

The purpose of this section is to use the NASTRAN program to calculate the forces at each node for the 2-D model with the static loads. Appendix C contains the NASRTAN program for two dimensional model to be analyzed. The program was run and the resulting output from NASTRAN can be found in Appendix C, attached separately. The following are the nodal displacements and the element forces calculated by NASTRAN:

NODAL DISPLACEMENTS (APPENDIX E);

GRID POINT	X (in)	Y (in)	Z (in)
1,9,12	0.0	0.0	0.0
2	0.0	-.00504	+.0314
3	0.0	-.00809	+.173

ELEMENT AXIAL FORCES AND STRESSES (APPENDIX E);

ELEMENT	FORCE (lbs)	AXIAL STRESS	SAFETY MARGIN
1-(TUBE)	-180.5	-689. (COMP.)	4.8
2-(TUBE)	-98.7	-377. (COMP.)	8.9
4-(CABLE)	103.2	8390. (TENSION)	-0.90
5-(CABLE)	65.8	5350. (")	-0.84
6-(CABLE)	33.2	4807. (")	-0.82

The displacements of the nodes 2,3 which are wing nodes are physically displacing in the correct direction. The wing, under the wing loading, will move in the up and inboard direction as if it were rotating about the root beam. It can be seen that for the experimentally calculated failure stress of the wire (Ftu = 842. psi) that all the safety margins are negative, as calculated by NASTRAN. This means that the wires are loaded beyond the experimental failure stress.

2.4 CONCLUSIONS AND RECOMMENDATIONS

The purpose of this section is to comment on the results of the previous section and give some recommendations on the results.

2.4.1 Conclusions

The purpose of this section is to provide a summary of the previous chapter. The following are the element forces calculated manually:

ELEMENT AXIAL FORCES AND STRESSES (APPENDIX B);

ELEMENT	AXIAL FORCE (lbs)	AXIAL STRESS (psi)
1-(TUBE)	-186.	710. (COMP.)
2-(TUBE)	-89.2	430. (COMP.)
4-(CABLE)	+94.2	13600. (TENSION)
5-(CABLE)	+0.70	101. (")
6-(CABLE)	+103.	8370. (")

The following are the forces calculated by use of the NASTRAN program:

ELEMENT AXIAL FORCES AND STRESSES (APPENDIX E);

ELEMENT	FORCE (lbs)	AXIAL STRESS	SAFETY MARGIN
1-(TUBE)	-180.5	-689. (COMP.)	4.8
2-(TUBE)	-98.7	-377. (COMP.)	8.9
4-(CABLE)	103.2	8390. (TENSION)	-0.90
5-(CABLE)	65.8	5350. (")	-0.84
6-(CABLE)	33.2	4807. (")	-0.82

It can be seen that the results of the NASTRAN program and the manual calculations are compatible except for the values calculated for Element 5 and 6. The difference that does exist is due to NASTRAN taking into account the displacements of the wing root (Grid Points 2,3,4). It can be seen that the sum of the forces of elements 5 and 6 almost equals the sum of the same elements calculated by NASTRAN. The manually calculated values for element 5 and 6 must be off by a fraction of each. It is concluded that the NASTRAN program will produce correct results for the 3-dimensional model to be analyzed in Chapter 3.

2.4.2 Recommendations

The purpose of this section is to give recommendations on the results of the chapter. It is recommended that the nodal displacements be included in the hand calculations to compare with the NASTRAN output.

3. 3-DIMENSIONAL ULTRALIGHT MODEL

The purpose of this chapter is to create a 3-dimensional ultralight model of the wing and surrounding structure to be used by the NASTRAN program. The forces, moments, and displacements of each node and the element stresses will be calculated by the NASTRAN program. These results are to be compared with those obtained by the finite element method calculated in Reference 1.

3.1 MODEL DESCRIPTION

The purpose of this section is to describe the major assumptions used to create the model. It is assumed for this analysis that the root beam is fixed. Therefore, the following nodes will be fixed:

Node 1; Front Spar and Root beam connection
Node 8; Rear Spar and Root beam connection
Node 10; Forward truss attachment point
Node 11; Aft truss attachment point

Nodes 1 and 2, however, are hinge attachments in which the front and rear spar are free to rotate about the Z-axis. This will be dealt with in the single point constraint for nodes 1 and 3. Figure 3.1 to 3.3 show the top views of the model with the Nodes and Elements identified. The figures show the wing internal cables (Fig.3.1), wing flying wires (Fig.3.2), and the truss members (Fig.3.3). Figure 3.4 shows an isometric of the complete model for visual purposes.

The following subsections contain the information required for the NASTRAN program to be completed. The Sub-sections contain the following:

Node and Constraint identification
Element Description
Material Description
Wing Loading Calculations

With the information calculated and identified in these sub-sections the NASTRAN program can be written.

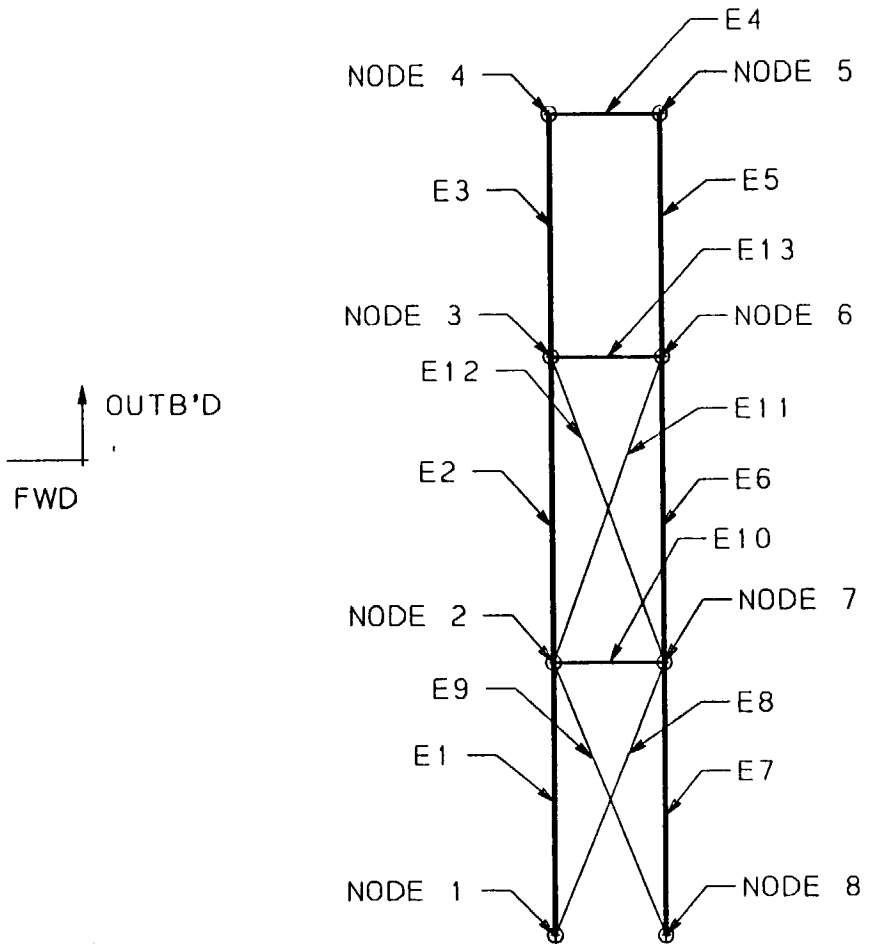

SCALE 1"=50"

FIGURE 3.1: 3-DIMENSIONAL MODEL OF WING AND INTERNAL WING CABLES

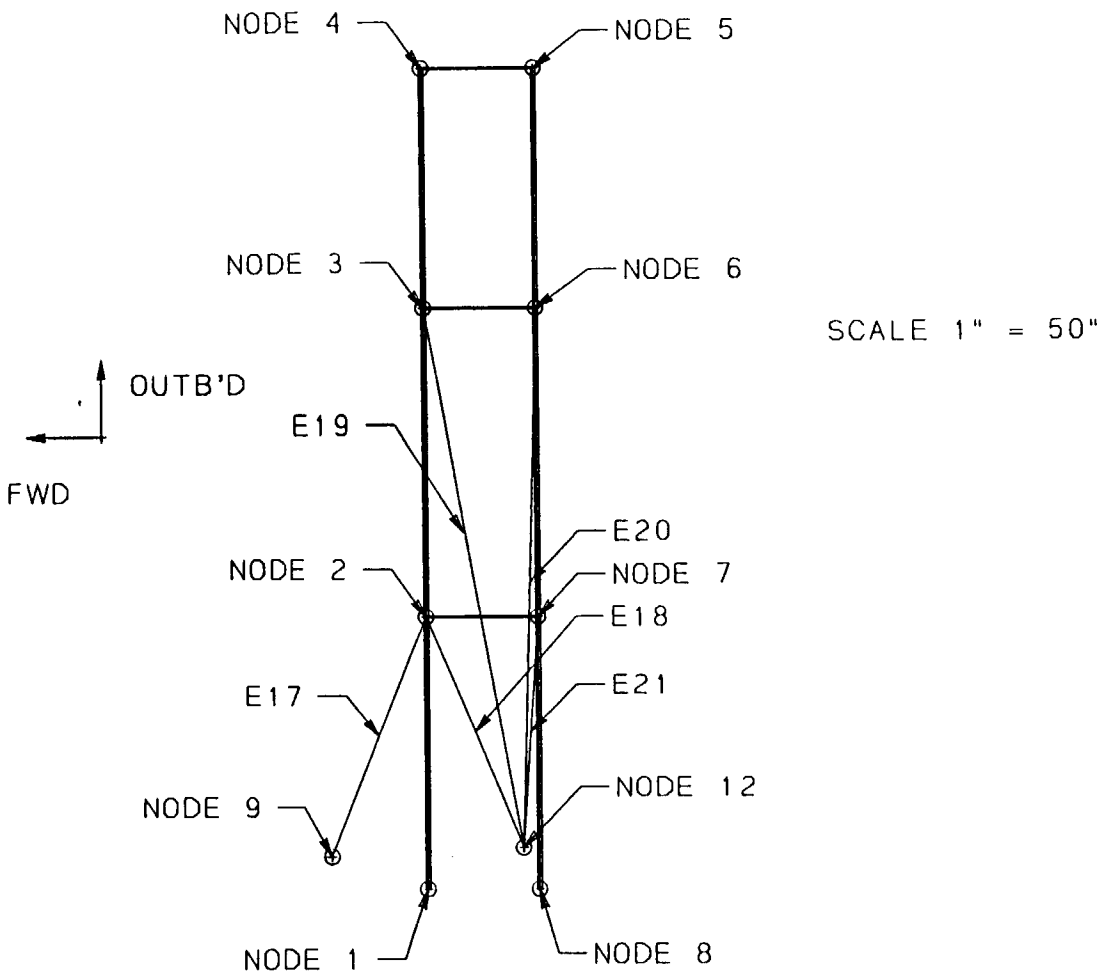

FIGURE 3.2: 3-DIMENSIONAL MODEL OF THE ULTRALIGHT WING FLYING WIRES; TOP VIEW

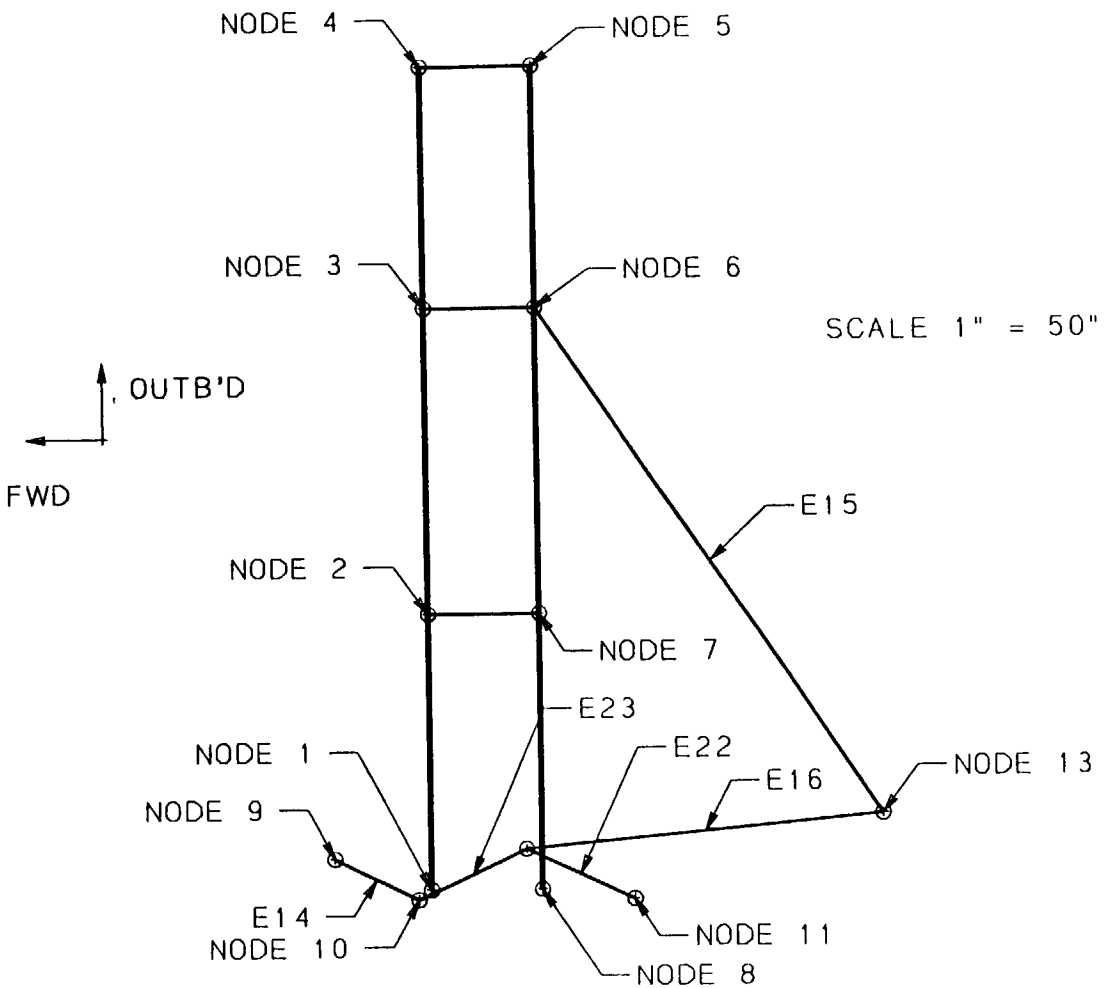

FIGURE 3.3: 3-DIMENSIONAL MODEL OF WING AND SURROUNDING STRUCTURE; TOP VIEW

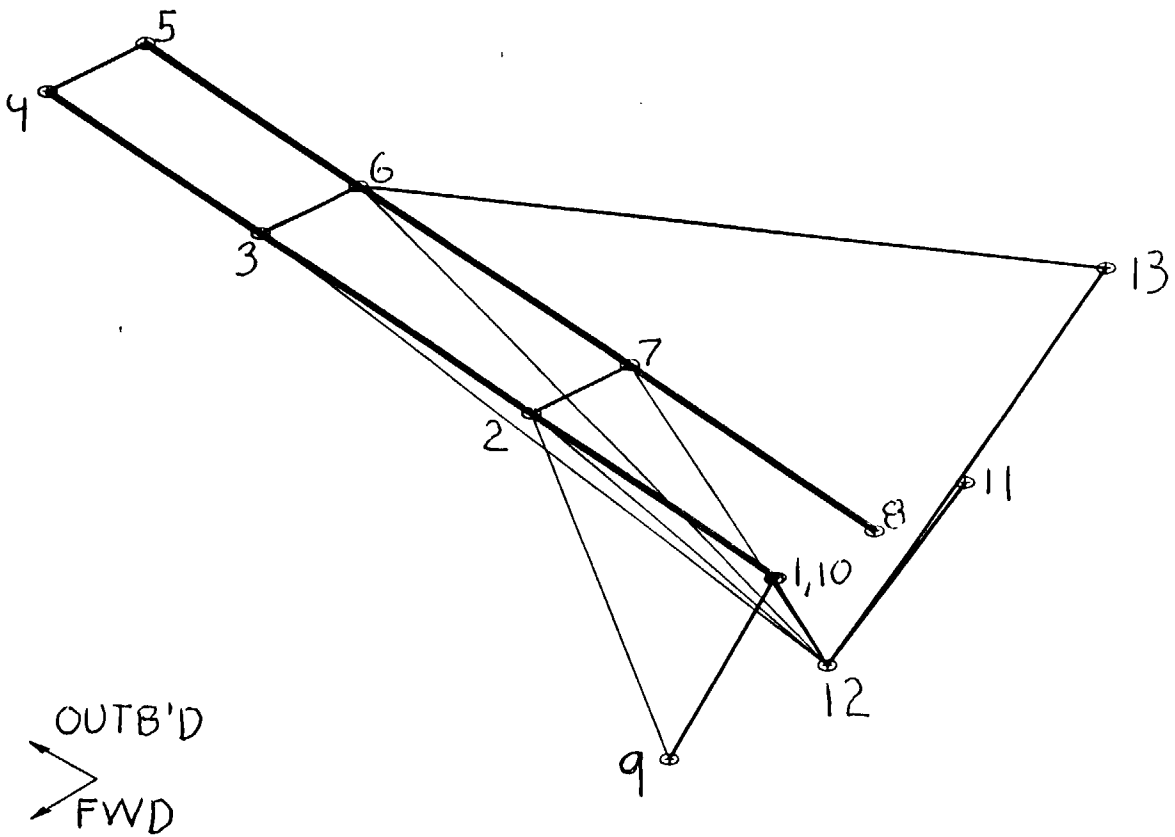

Figure 3.4; Isometric View of 3-D Model

3.1.1 NODE POINT AND CONSTRAINT DEFINITIONS

The purpose of this section is to identify the grid points used and the constraint at each point. The constraints used by NASTRAN are as follows:

1 = Linearly constrained in the X-direction
2 = Linearly constrained in the Y-direction
3 = Linearly constrained in the Z-direction
4 = Constrained about the X-axis; Ox = 0 deg.
5 = Constrained about the Y-axis; Oy = 0 deg.
6 = Constrained about the Z-axis; Oz = 0 deg.

The following table contains the GRID cards used in the NASTRAN program for the 3-D model. The table also includes the single point constraints for each point and the GRIDSET card for the default constraints.

Table 3.1.1: GRID and GRIDSET Cards used in NASTRAN

NASTRAN CARD	X (AFT) (IN)	Y (OUTB'D) (IN)	Z (UP) (IN)	CONSTR-AINT
GRIDSET				4,5,6
GRID #1	85.49	2.6	66.3	12345
" #2	85.49	75.0	73.2	
" #3	85.49	155.0	80.9	
" #4	85.49	218.0	87.0	
" #5	115.0	218.0	84.0	
" #6	115.0	155.0	77.9	
" #7	115.0	75.0	70.2	
" #8	115.0	2.6	63.0	12345
" #9	60.39	10.9	28.3	
" #10	82.09	0.0	69.0	123456
" #11	139.6	0.0	64.0	123456
" #12	110.8	13.2	25.6	2456
" #13	205.5	22.0	74.1	2456

3.1.2 ELEMENT IDENTIFICATION

The purpose of this section is to identify the elements used in the 3-dimensional NASTRAN model. The following table shows the elements used and their descriptions.

Table 3.1.2: Element Descriptions

ELEMENT NUMBERS (EID)	DESCRIPTION
1,2,3,5,6,7 (Fig.3.1)	Wing Spars; 1.75" Diameter Tubes, t = 0.049"
4,10,13 (Fig.3.1)	Wing Ribs; 1.00" Diameter Tubes, t = 0.035
8,9,11,12 (Fig.3.1)	Wing Internal Cables; 1/8" Diameter
14 (Fig.3.3)	Forward Root Tube Attachment Truss; 1.00" Diameter, t = 0.075"
15,16 (Fig.3.3)	Tail Attachment Truss Tubes; 1.125" Diameter, t = 0.065"
17,18,19,20,21 (Fig.3.2)	Flying Wires; (17) Diameter = 3/32" (18-21) Diameter = 1/8"
22,23 (Fig.3.3)	Aft Root Tube Attachment Truss; 1.00" Diameter t = 0.049"

3.1.3 ELEMENT MATERIAL IDENTIFICATION

The purpose of this section is identify the materials used for each element of the ultralight model. The tube information is referenced from the ultralight model handbook. The cable information is experimental data taken from the analysis performed by students under the supervision of Dr. Howard W. Smith. The following are the material identifications for each element in the 3-dimensional model and pertinent material information:

Material ID = 1; EID = 1-7,10,13,14,15,16,22,23
6061-T6 Tube,
Spec = WW-T-700/6
Ftu = 42. ksi

Fcy = 34. ksi
Fsy = 27. ksi
E = 9.9+3 ksi
Ec = 10.1+3 ksi
μ = 0.33
ω = 0.098 lb/in^3
(Ref. 3, Table 3.6.1.0(b))

Material ID = 2; EID = 8,9,11,12,17-21
Alloy steel cables,
Experimental Data (Ftu)
Ftu = 864. psi
E = 29.+6 psi (Ref. 3)
μ = 0.33 (")
ω = 0.283 lb/in^3 (")

The materials used are assumed to be linear, temperature independent, isotropic materials. Therefore, MAT1 cards will be used in the NASTRAN program.

3.1.4 WING LOADING AND FORCE CALCULATIONS

The purpose of this section is to determine the forces on the wing nodes which must be equivalent to the wing loading. The wing loading was taken from test data in Reference 1, Table 3.3.2. The table and the calculations used to obtain the forces on the nodes can be found in Appendix A. The following are the results of these calculations:

Node 1, F1 = 56.1 lbs
Node 2, F2 = 55.6 lbs
Node 3, F3 = 30.2 lbs
Node 6, F6 = 20.0 lbs
Node 7, F7 = 36.5 lbs
Node 8, F8 = 32.4 lbs

The forces calculated appear to be low. Since these forces are from the information from Reference 1, the results should still be consistent. These forces are considered static and thus Force cards will be used in the NASTRAN program. The forces are considered to act in the vertical, (z) direction.

3.2 PROGRAM DESCRIPTION

The purpose of this section is to describe the NASTRAN program created for analyzing the Sunburst Ultralight. The program was written with all the information identified in Section 3.1. The NASTRAN program output can be found in Appendix D.

The program is split up into three sections. The first section is the Executive Control Deck. This deck contains the user identification and administrative information. The second deck is the Case Control Deck. In this deck the codes identifying what type of analysis is to be performed is included. This lets NASTRAN identify what the program wants it to do. The final deck is the Bulk Data Deck. This deck contains all the model information identified in Section 3.1. The program is ready to be submitted at this point.

3.3 NASTRAN RESULTS

The purpose of this section is to document the NASTRAN program results. Appendix F contains the NASRTAN program results for the three dimensional NASTRAN model, attached separately. The reader is advised to look at Figure 3.1-2 to help locate visually the grid points and elements. The following are the nodal displacements and the element forces calculated by NASTRAN for the wing and flying wires:

NODAL DISPLACEMENTS;

GRID POINT	X (in)	Y (in)	Z (in)
1,8,10,11	0.0	0.0	0.0
2	0.0192	-0.00747	0.0440
3	0.0654	-0.0281	0.232
6	0.0564	-0.0236	0.146
7	0.0196	-0.0114	0.0462
9	-0.00184	0.0	0.0
12	-0.00196	0.0	0.00404
13	0.0722	0.0	-0.137

ELEMENT AXIAL FORCES;

ELEMENT	AXIAL FORCE (lbs)	AXIAL STRESS (psi)		SAFETY MARGIN
1 (F.S.)	-114.	-436.	(COMP.)	77.
2 (")	-72.2	-276.	(")	120.
6 (R.S.)	-81.8	-312.	(")	110.
7 (")	-175.	-668.	(")	50.
10 (RIB)	+8.21	+77.4	(TENSION)	540.
13 (RIB)	-7.06	-66.5	(COMP.)	510.
14 (TUBE)	-38.3	-176.	(")	190.
15 (")	0.0	0.0		N/A
16 (")	0.0	0.0		N/A
22 (")	-57.7	-394.	(COMP)	85.
23 (")	+124.	-844.	(")	39.

CABLES;

8 (Internal	SLACK			
9 wing)	SLACK			
11	+14.5	1179.	(TENSION)	-.28
12	SLACK			
17 (Flying	+58.6	8486.	(TENSION)	-0.90
18 wires)	+51.8	5350.	(")	-0.80
19	+112.	9125.	(")	-0.91
20	+72.8	5921.	(")	-0.86
21	+81.2	6603.	(")	-0.87

The displacements of the nodes 2,3,6,7 which are wing nodes are physically displacing in the correct direction. The wing, under the wing loading, will move in the up and inboard direction as if it were rotating about the root beam. It can be seen that for the experimentally calculated failure stress of the wires (Ftu = 842. psi) that all the wire safety margins are negative, as calculated by NASTRAN. This means that the Ultralight flying wires, if this model is any indication, will fail in the 10 degree angle attack flight condition, if not before.

It can be seen that the highest cable stress is on Cable Element 19. This cable is the critical cable which will fail first. The cable runs from Node 12 to Node 3 (On Front spar). This can be seen on Figure 3.2. The reason for the high stress level for this wire is the angle at which the cable makes relative to the front spar in the X=0 plane. The force at node three must be countered by a very large cable load for the small angle.

3.4 COMPARISON BETWEEN FINITE ELEMENT METHOD RESULTS AND NASTRAN RESULTS

The purpose if this section is to compare the results obtained by the NASTRAN model used in this analysis and those achieved by the use of the Finite Element Method (Ref.1). Due to the different nodes and loading method used, only the cable axial stresses will be compared. The following are the resulting axial stresses for the flying wires calculated by each method:

NASTRAN (3.3)			FINITE ELEMENT (Ref. 1)		
ELEMENT	AXIAL FORCE (lbs)	AXIAL STRESS (psi)	ELEMENT	AXIAL FORCE (lbs)	AXIAL STRESS (psi)
17	+58.6	8486.	34	+76.7	10396.
18	+51.8	5350.	35	+44.3	3610.
19	+112.	9125.	37	+222.	18110.
20	+72.8	5921.	38	+145.	11818.
21	+81.2	6603.	36	+65.4	5336.

It can be seen that the values calculated by the finite element method are not very close to those by NASTRAN. This is due to the difference in models and loading scenarios used. The values, however, are comparable in that they follow the same trend. The critical wire is still Element 19 (NASTRAN) or Element 37 (Finite Element).

3.5 CONCLUSIONS AND RECOMMENDATIONS

The purpose of this section is to comment on the results of the previous sections and give some recommendations on either the procedures used or the values assumed.

3.5.1 Conclusions

The purpose of this section is to provide a summary of the results calculated in this chapter.

It was found that the critical element in the structure is Element 19. This is the flying wire which runs from the pilot cage (Node 12) to the outboard location on the front spar (Node 3). The large force was primarily due to the very low angle that the cable makes relative to the front spar. The axial stress on the cable was much greater than the tested maximum stress of 842. psi (Experimental data from students under Howard W. Smith). From the comparison between the NASTRAN results the Finite Element Program results (Ref. 1), it was shown that Element 19 was critical in both. The values were not the same between both program results, but the calculated values did have common trends.

3.5.2 Recommendations

The purpose of this section is to present recommendations on the results obtained in this chapter. It is recommended that the 3-dimensional model be redone using more nodes so that a better idea of the actual stresses in all the elements can be found. A more enhanced model could use quadrilateral elements for the wing with the actual calculated wing loading. This would get much closer results than the concentrated static loads used in this analysis.

4. CONCLUSIONS AND RECOMMENDATIONS

The purpose of this chapter is to comment on the results of the major parameters in this report that were to be calculated. Recommendations will also be written about the values obtained and the methodologies used.

4.1 Conclusions

The purpose of this section is comment on the results of this report. It was concluded in Chapter 2 that the results of the NASTRAN program and the manual calculations were comparable. The difference that did exist is due to NASTRAN taking into account the displacements of the wing root (Grid Points 2,3,4). It was concluded that the NASTRAN program will produce correct results.

The following are the resulting forces and displacements calculated in Chapter 3 for the 3-dimensional Ultralight Model:

NODAL DISPLACEMENTS;

GRID POINT	X (in)	Y (in)	Z (in)
1,8,10,11	0.0	0.0	0.0
2	0.0192	-0.00747	0.0440
3	0.0654	-0.0281	0.232
6	0.0564	-0.0236	0.146
7	0.0196	-0.0114	0.0462
9	-0.00184	0.0	0.0
12	-0.00196	0.0	0.00404
13	0.0722	0.0	-0.137

ELEMENT AXIAL FORCES;

ELEMENT	AXIAL FORCE (lbs)	AXIAL STRESS (psi)		SAFETY MARGIN
1 (F.S.)	-114.	-436.	(COMP.)	77.
2 (")	-72.2	-276.	(")	120.
6 (R.S.)	-81.8	-312.	(")	110.
7 (")	-175.	-668.	(")	50.
10 (RIB)	+8.21	+77.4	(TENSION)	540.
13 (RIB)	-7.06	-66.5	(COMP.)	510.
14 (TUBE)	-38.3	-176.	(")	190.
15 (")	0.0	0.0		N/A
16 (")	0.0	0.0		N/A
22 (")	-57.7	-394.	(COMP)	85.
23 (")	+124.	-844.	(")	39.

CABLES;

8	(Internal		SLACK		
9	wing)		SLACK		
11		+14.5	1179.	(TENSION)	-.28
12			SLACK		
17	(Flying	+58.6	8486.	(TENSION)	-0.90
18	wires)	+51.8	5350.	(")	-0.80
19		+112.	9125.	(")	-0.91
20		+72.8	5921.	(")	-0.86
21		+81.2	6603.	(")	-0.87

It was found that the critical element in the structure is Element 19. This is the flying wire which runs from the pilot cage (Node 12) to the outboard location on the front spar (Node 3). The large force was primarily due to the very low angle that the cable makes relative to the front spar. The axial stress on the cable was much larger than the tested maximum stress of 842. psi (Experimental data from students under Howard W. Smith).

From the comparison between the NASTRAN results the Finite Element Program results (Ref. 1), it was found that Element 19 was critical in both. The cable stress values were not the same between the two program results, but the calculated values had common trends.

As a result of the analysis performed in this report it is concluded that the Ultralight Airmass Sunburst is unsafe. The outboard flying wire (Element 19) will fail due to the critically low angle it makes with the front spar.

4.2 Recommendations

The purpose of this section is to present recommendations on the results of this report. It is recommended that the nodal displacements be included in the hand calculations to obtain the same results. It is recommended that the 3-dimensional model be reworked using quadrilateral elements for the wing with the actual calculated wing loadings used. This would get much closer results than the concentrated static loads used in this analysis.

5. REFERENCES

1.) Muller de Almeida, Sergio F., Aerodynamic and Structural Analysis of an Ultralight Aircraft, May 6,1986.

2.) Smith, Howard W., Aerospace Structures: Matrix Analysis, The University of Kansas, December 1983.

3.) Smith, Howard W. Phd., Aerospace Materials and Processes, The University of Kansas, January 1978.

4.) MCS/NASTRAN, Version 6.6.

5.) MCS/NASTRAN, Handbook of Linear Analysis.

IV. CONSTRUCTION, WIND TUNNEL TESTING AND DATA ANALYSIS FOR A 1/5 SCALE ULTRA-LIGHT WING MODEL

Michael D. James
Graduate Student

Howard W. Smith
Professor
Department of Aerospace Engineering
University of Kansas

December 1988

Partially supported by
NASA Langley Research Center
Grant #NAG 1-345

SUMMARY

This report documents the construction, wind tunnel testing and the data analysis of a 1/5 scale ultra-light wing section. The original ultra-light this wing model is scaled after is Dr. Howard W. Smith's structural test ultra-light located at the Lawrence airport.

Wind tunnel testing provided accurate and meaningful lift, drag and pitching moment data. This data was processed and graphically presented as:

C_L vs. α

C_D vs. α

C_M vs. α

C_L vs. C_D

The wing fabric flexure was found to be significant and its possible effects on aerodynamic data was discussed. The fabric flexure is directly related to wing angle of attack and airspeed. Different wing section shapes created by fabric flexure are presented with explanations of the types of pressures acting on the wing surface.

This report provides conclusive aerodynamic data about ultra-light wing. This topic is well worthwhile for continuing studies.

TABLE OF CONTENTS

1. INTRODUCTION

This special project was performed to study the basic aerodynamic characteristics of an ultra-light wing. Few known wind tunnel tests have been performed of ultra-light wings since they are designed to be very inexpensive. Thus, aerodynamic data such as the variation angle of attack with lift coefficient, drag coefficient, or pitching moment coefficient is relatively unknown. Another specialty about ultra-light wings is that aerodynamic data becomes a function of wing fabric flexure, which itself is function of airspeed and angle of attack.

To perform these wind tunnel tests, a one-fifth scale wing model of Howard Smith's experimental test ultra-light was constructed. Particular attention was paid to keeping the wing model true-to-scale so that hopefully scale aerodynamic characteristics could be studied.

This wing was sized to fit in the small subsonic wind tunnel in the basement of Learned Hall. The two column support rod was used for the test mount. the aerodynamic forces were read by a balance table and displayed on a scale. This data was processed and displayed as standard Cl, Cd and Cm vs. alpha data.

2. WING CONSTRUCTION

The wing construction consisted of five phases:

1) scaling the wing
2) plotting the airfoil coordinates
3) sizing the wing
4) selecting materials
5) construction

Phase 1. Scaling the wing

The wing was primarily scaled down by measuring the chord and thickness of Dr. Smith's test ultra-light wing at the Lawrence airport and applying various scales to determine sizing. Scales of 1:10, 1:5 and 1:4 were considered. The scale of 1:5 was selected since it would size a model with a maximum thickness of 1.3 inches and chord of 10.2 inches; ideal size for the small subsonic wind tunnel.

Phase 2. Plotting the airfoil coordinates:

In order to perform this step, I visited the Lawrence airport where Dr. Smith's ultra-light is currently hoisted and being prepared for structural testing. To plot the airfoil coordinates, two methods were used:

1) plotting points measured on the wing surface
2) plotting points measured inside the wing

By plotting both sets of coordinates, erroneous data points could be eliminated and the airfoil surface could be developed. An airfoil section is shown in Figure 2.1. Note the flat bottom of the airfoil and the constant slope in the upper camber between half chord and the trailing edge. Figure 2.1 also shows the location and attitude of the mounting block in the wing. The mounting block is situated so that an angle of attack range of +20 to -10 degrees can be achieved.

Phase 3. Sizing the wing:

The wing was sized to create approximately 25 pounds of lift at maximum angle of attack at an airspeed of 75 feet per second. A maximum lift coefficient of 1.6 was assumed. It was figured that a wing area of 2.3 square feet feet was needed. The wing span was incremented by a scale rib spacing until the size was either 2.3 square feet or until the span was too large for the tunnel. A wing with four rib spacings was calculated to have an area of 2.0 square feet and a span of 2.35 feet. Perfect! the area requirement is close and it fits in the tunnel (with an inch on each wing tip to spare).

Phase 4. Selecting materials:

Since "scale" materials were too hard to find and were usually to expensive or hard to work with, substitute materials were used. A list of the materials and their uses is:

Material	Size	Purpose
1) Birch dowels	3/8" 1/2"	front spar (leading edge) rear spar
2) Birch plywood	3/32" 5-ply	wing ribs
3) Oak block	1" thck	mounting attachment
4) Music wire	1/32" 1/16	trailing edge stiffeners lower surface fabric supports, wing chord trailing edge supports
5) Nylon fabric	---	wing fabric
6) Two ton epoxy	---	used for wood-metal bonds
7) Wood glue	---	used for wood-wood and wood-fabric bonds

Phase 5. Construction:

Construction started by preparing the the wing ribs. First the plywood sheet was cut, mounted together and bonded lightly. Wing rib templates were laid out and holes for the front spar and rear spar were drilled. Next the wing ribs were cut out by a ban saw which insured that each rib would be the same size and shape. They were separated, sanded and bonded together in pairs. A 2.5 inch section of music wire was epoxied into a groove cut in to the trailing edge to simulate the trailing edge shape of the airfoil. The wing ribs were glued onto the front and rear spars maintaining a 1/5 scale distance between each wing rib and a 1 inch spacing between the two center ribs for mounting block.

Once the main wing structure was bonded together, the trailing edge music wire was added. The music wire in the model performs the function of the cables in the ultra-light. The music wire was soldered and glued to the trailing edge of the plywood wing ribs and the music wire extensions. Solder and epoxy lumps were files out to keep the trailing edge to a minimum thickness. 1/16" music wire supports were added in a criss-cross fashion between the leading edge and the main spar of the wing lower surface. These act as cables do in the ultra-light to provide fabric support. At this point, before the covering, the mounting

block was glued into place. Figure 2.2 shows two photographs of the uncovered wing frame.

The wing was finally covered with the nylon fabric. Wood glue was used since it binds between the fabric filaments. The fabric covering was stretched tight in the gluing process simulating that of the ultra light. An abundance of glue was used to provide a good rib-fabric bond since the fabric must carry the entire wing loading.

Overall, the model is an excellent 1/5 scale representative of the full size ultra-light wing.

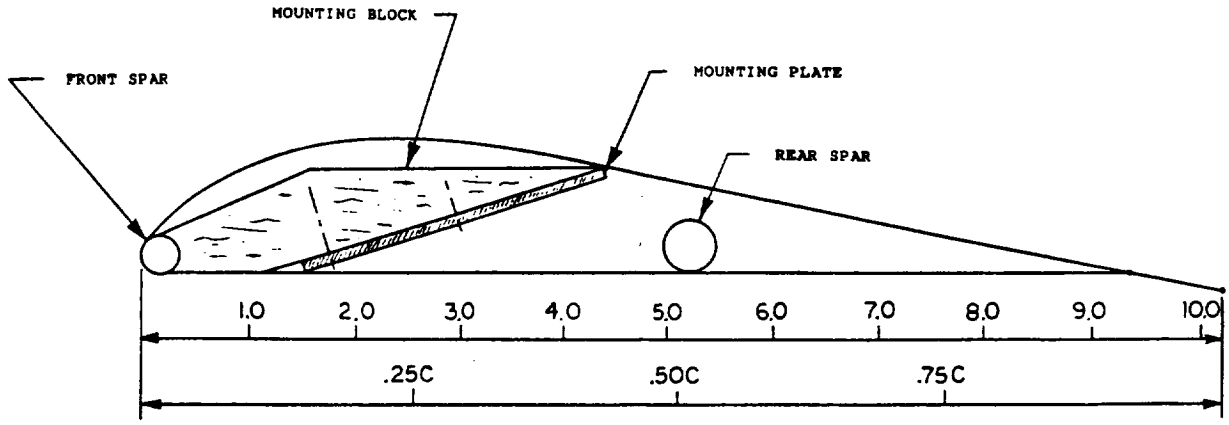

FIGURE 2.1 WING CROSS SECTION

C-2

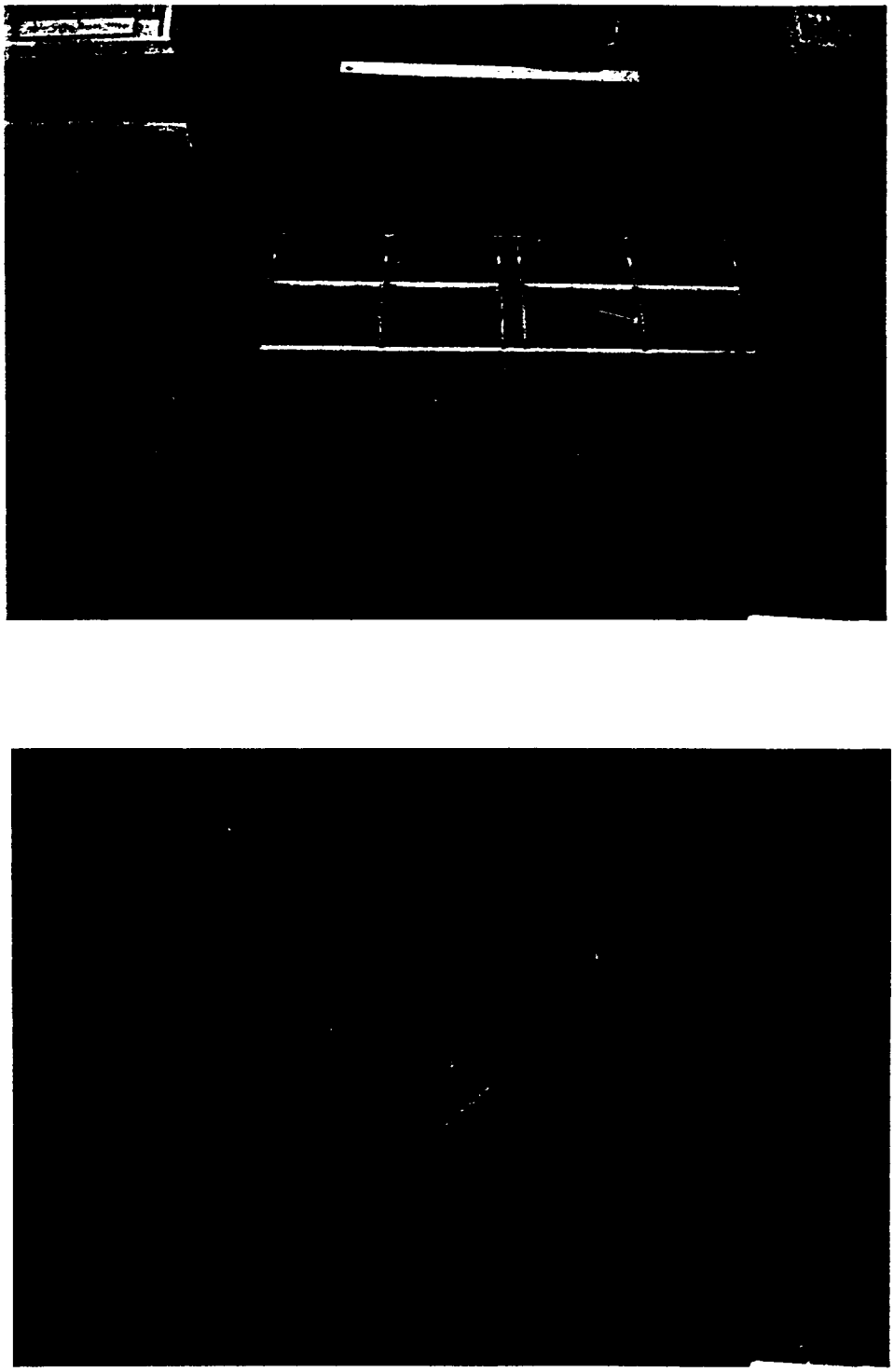

FIGURE 2.2 UNCOVERED WING FRAME

3. WIND TUNNEL TESTING METHOD

Once construction of the 1/5 scale ultra-light wing was finished, the wing was mounted in the small subsonic wind tunnel in the basement of Learned hall. Figure 3.1 shows a 3/4 view of the wing in the test section. Figure 3.2 shows a front view of the wing in the test section from inside the wind tunnel.

Raw data from the tunnel testing appears in Appendix A. The following data is included in the upper portion of these data sheets:

* Wind tunnel static pressure: P_S

* Wind tunnel total pressure: P_T

* Ambient temperature

* Atmospheric pressure

Once the tunnel is up to testing velocity lift, drag, and pitching moment were read off of a percent of range scale and recorded for a range of attack angles. The wing angle of attack is varied during the test run.

The basic purpose of the testing was to determine the aerodynamic data of the wing and compare it with regular airfoil data. During the testing it became apparent that the airfoil section shape, and thus aerodynamic data, depends highly on the fabric flexure. The fabric flexure is in turn determined by the airspeed and angle of attack of the wing. These compounding factors cannot be completely assessed individually but they are considered in explaining the aerodynamic data. Wing sections will be shown at varying angles of attack.

Eight individual tunnel test runs were performed for the ultra-light wing model. Tunnel speeds range in between 47 and 121 feet per second. Extreme caution was used in making certain that the wing would not receive loadings large enough to cause structural failure. This model is not designed to sustain lift or drag loadings over thirty pounds because of its light construction. This limit maximum limit loading on the model wing is, by the way, equivalent to fifteen pounds per square foot--the loading normally sustained by light all metal aircraft!

The aerodynamic forces carried through the wing are sensed by a force table beneath the test section of the wind tunnel. Strain gauges in the force table translate lift drag and pitching moment forces into electrical voltages through a Wheatstone bridge circuit. The data is finally displayed on a control panel which has selector knobs for lift, drag, pitching moment and scale factor and a percent of range scale for voltage reading. The scale factor knob

has magnitude selections of 50, 100, 200, 500, 1000 and 2000. The scale factor is read in percent of range which varies between -.5 and +.5. The scale factor and voltage are read for lift, drag and pitching moment for each angle of attack tested per trial.

Test runs #1 and #2 are considered inconclusive evidence. It was discovered through these tests that varying the scale factor caused significant error because only one scale factor can be zeroed to at a time. For the remaining tests the percent of range scale was zeroed to a certain scale factor, which was used for the entire test.

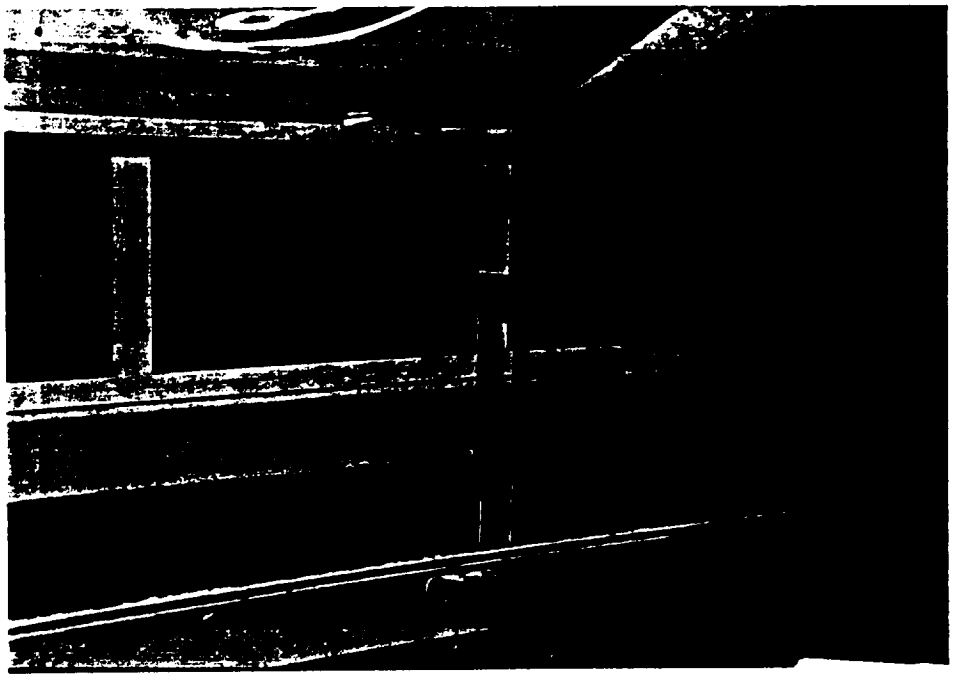

FIGURE 3.1 WING MOUNTED IN THE TEST SECTION: 3/4 VIEW

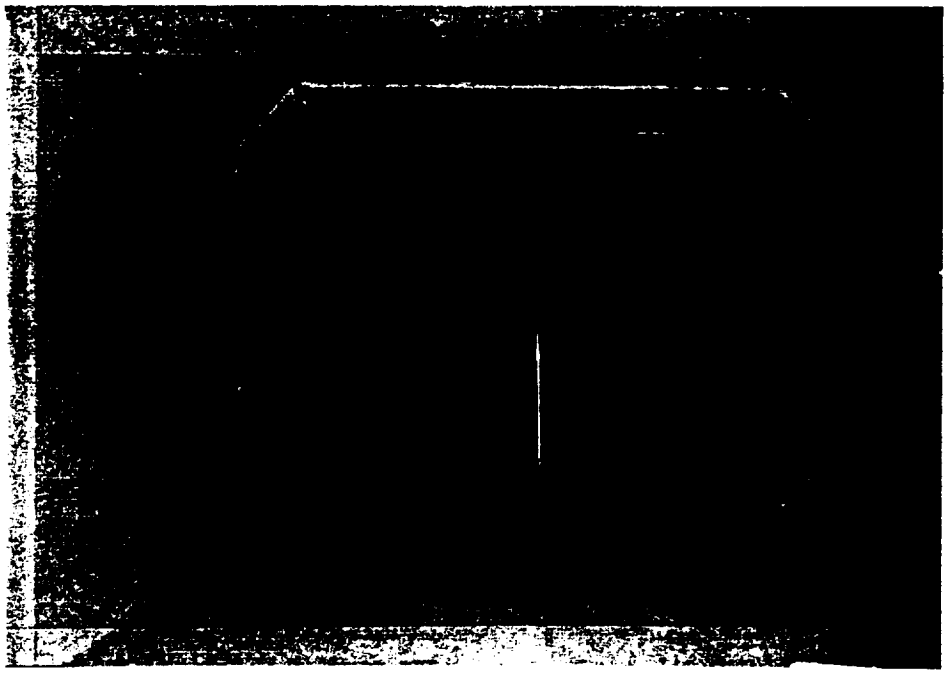

FIGURE 3.2 WING MOUNTED IN THE WIND TUNNEL FRONT VIEW

4. TEST TRIALS

Eight different testing runs were recorded. Trial numbers 1 and 2 are inconclusive but served to demonstrate a more accurate method of testing; picking one scale factor and using it for the entire test run. The remaining tests all provide meaningful data. These tests were run at different wind tunnel velocities, which were selected as to maintain a useful range of data.

Test #3: The scale factor of this particular test was set at 2000. The tunnel velocity was incremented until the maximum drag reading (at 20 degrees angle of attack) read the maximum of .5 on the scale. The wing angle of attack was varied from +20 degrees to -12 degrees by increments of 2 degrees. Lift and drag data was recorded for this trial. Noted are that buffeting occurred at -12 degrees and beyond +8 degrees. This was seen to be the case for the remaining trials.

Test #4: This test was run to obtain a complete record of lift, drag and pitching moment data. With the scale factor set at 2000, the tunnel velocity was stabilized so that the maximum pitching moment reading was -.5. This tunnel velocity is the maximum limit for complete lift drag and pitching moment data. This also means that the wing is oversized: the aerodynamic forces that the wing capable of are larger than those that can be supported by the balance table. This test was performed for an angle of attack range of +20 degrees to -12 degrees.

Test #5: This test is the first 'high speed' trial of the wing model. 'High speed' for this model is considered to be greater than 100 feet per second, which is the approximate tunnel velocity of this trial. The angle of attack range selected is +12 to -12 degrees. Again, structural constraints limited the maximum wing angle of attack. Lift and drag data only were recorded.

Test #6: This test is the second 'high speed' trial. This test is very similar to test #5 except a larger wind tunnel velocity was used; approximately 122 feet per second. This is the maximum recommended tunnel velocity to be used for this wing. Because of the high speed, the variation of angle of attack was maintained between +8 and -8 degrees. The main purpose of this test is to compare the lift and drag data of high speed trials to lower speed trials.

Test #7: This test is a duplication of test #4. The same approximate tunnel speeds were used and the same angle of attack range was used. The purpose of this test is to determine the the test replicability of this testing procedure by attempting to duplicate the results.

Test #8: This test is the 'low speed' trial. The scale factor used for this test was 1000. Again, the pitching moment reading was the limiting factor: the tunnel velocity was set such that the maximum pitching moment registered -.5 on the percent of scale range. Angle of attack for this trial was varied between 20 and -12 degrees.

5. DATA ANALYSIS

Of the eight wind tunnel test runs performed, six trials had meaningful data. These data for these six wind tunnel tests was processed and they are displayed in this chapter in the following figures:

Figure 5.1: Section Lift Characteristics for the 1/5 Scale Ultra-Light Wing Model
Figure 5.2: Section Drag Characteristics for the 1/5 Scale Ultra-Light Wing Model
Figure 5.3: Section Pitching Moment Characteristics for the 1/5 Scale Ultra-Light Wing Model
Figure 5.4: Drag Polar Characteristics for the 1/5 Scale Ultra-Light Wing Model

The raw wind tunnel data is listed in Appendix A. The equations which relate percent of range and scale factor readings into actual lift, drag and pitching moment forces were obtained from an AE 245 laboratory exercise. These equations and along with lift, drag and pitching moment equations were written into a basic program to speed up the data analysis program. The final output of this program gives the tunnel speed, Reynold's number and the wing lift coefficient, drag coefficient and pitching moment coefficient. The output listing for runs 3-8 are in Appendix A.

The lift coefficient-angle of attack curve is seen in Figure 5.1. Data from trials number 6 and 7 were plotted. Although these two trials were performed at 122 and 67 feet per second respectively, the data compares very well. The lift coefficients at higher angles of attack for the high speed case lies below those for the low speed case. This most likely indicates that wing section deformation at higher speeds lowers the wing's lift producing efficiency. An unusual characteristic of this lift curve is that there appears to be two different and distinct lift curve slopes. Between -4 and +2 degrees angle of attack the lift curve slope is roughly 7.6 per radian. Between +6 and 16 degrees angle of attack the lift curve slope drastically drops to 1.8 per radian. This indicates that this wing section does not generate much incremental lift coefficient at high angles of attack. Also evident is that lift coefficient is very sensitive to angle of attack change at small angles of attack. Another interesting characteristic of this wing section is the high lift at zero angle of attack. The angle of zero lift is approximately -5 degrees. Obviously this wing section generates a relatively large margin of positive lift at small negative angles of attack.

The drag coefficient-angle of attack curve is seen in Figure 5.2. Data for this plot was taken from test run #3. Minimum drag for this wing section occurs between -4 and -2 degrees angle of attack. It should be clarified that this drag is for the entire model and support mount! No tare

runs were performed due to time restrictions. Since most of the data runs were taken at low speeds and since the model is relatively large this wont create a significant error. The drag bucket in this curve also seems fairly symmetrical between -12 and +8 degrees angle of attack. One interesting characteristic of this curve is the intense amplification of drag at large angles of attack. The drag reading at 20 degrees is a factor of 24 times larger than the drag reading at -2 degrees. This "amplification factor" in ordinary wings is usually not as large. This is perhaps caused by the wing fabric pocketing at high angles of attack and further destroying the air flow. Another possible theory is derived from the fact that the wing frontal area to tunnel test section area ratio is small at large angles of attack. The airflow is constrained to this area, and normal flow probably cannot be achieved, and the air pressure is probably increased, thus the drag is increased. A third possibility of excess drag at high angles of attack could be due to the model flutter at these angles. The model was seen to flutter at -12 degrees and above +8 degrees angle of attack. Drag is known to increase with flutter.

The pitching moment-angle of attack curve is seen in Figure 5.3. Data for this plot was taken from test rum #7. It should be reminded that this pitching moment data is about the main model support mount which is located at .18c of the wing. Pitching moment data is usually referenced at .25c or the aerodynamic center. A simple transformation can be performed to shift the pitching moment coefficient to this point but time constraints limited this process. Never the less, the slope and shape of the pitching moment curve is accurate and can be commented on. The slope of a pitching moment-angle of attack curve should ideally be a straight line. The pitching moment curve plotted indicates three different upwardly sloping "troughs". The angle of attack breaks between the three troughs are 0 degrees and 14 degrees. It is uncertain what causes these distinct breaks, but again it is assumed to be the fabric flexure. Apparently fabric flexure change at 0 and 14 degrees angle of attack is very critical to pitching moment characteristics of the wing.

The lift coefficient-drag coefficient curve is seen in Figure 5.4. Data for the two curves were taken from test runs #6 and #8, the high speed and low speed trials, respectively. The slope of this curve indicates the maximum lift to drag ratio of the model. For the low speed case (run #8) the maximum lift to drag ratio is 12. The maximum lift to drag ratio for the high speed case (run #6) is 7. This indicates that the lift to drag ratio is reduced at higher speeds. This is probably because the fabric flexure at higher speeds is more warped and less conducive to lift.

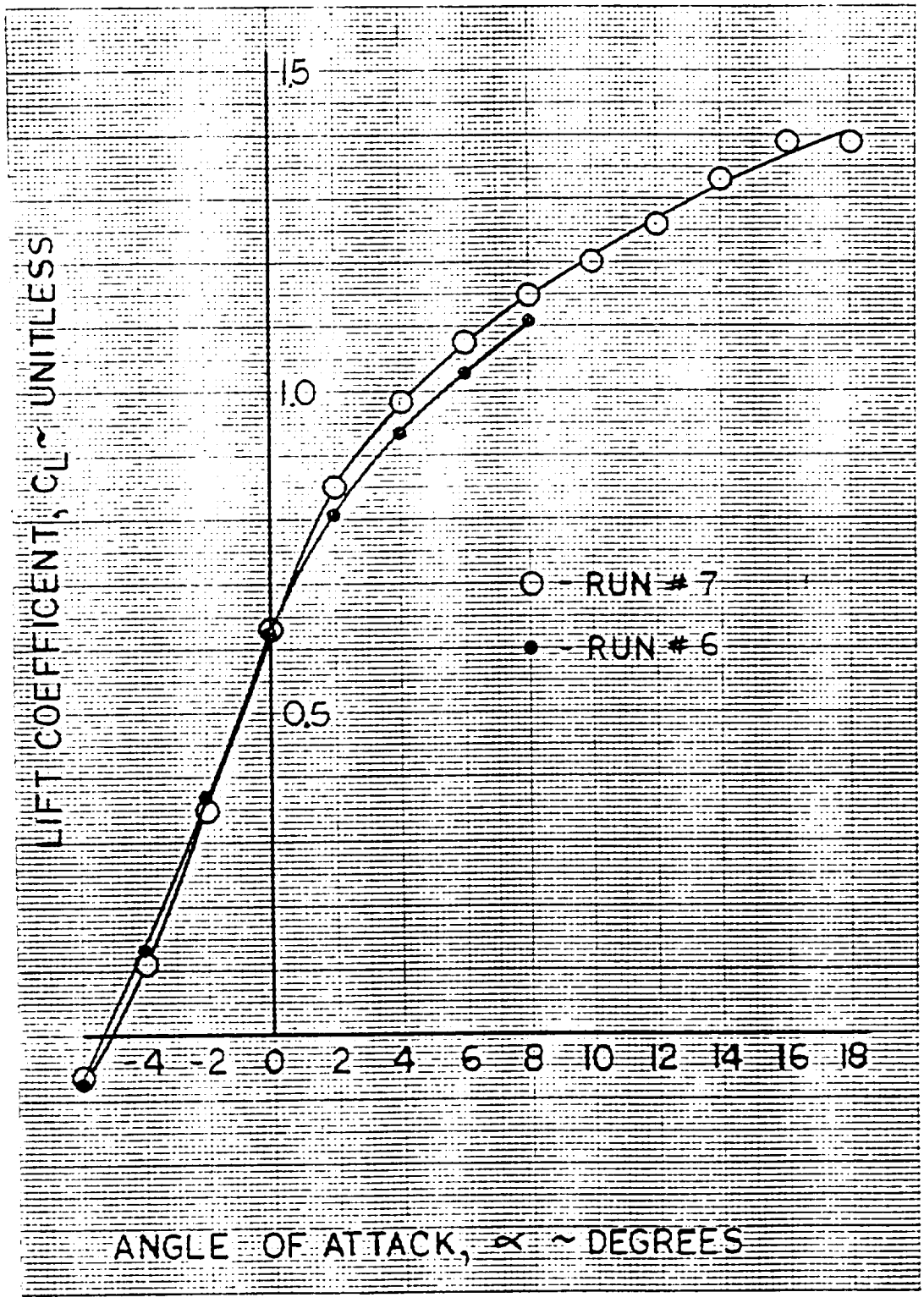

CALC	M. James		REVISED	DATE
CHECK				
APPD				
APPD				

FIGURE 5.1 SECTION LIFT CHARACTERISTICS FOR THE 1/5 SCALE ULTRA-LIGHT WING MODEL

AE 592

UNIVERSITY OF KANSAS

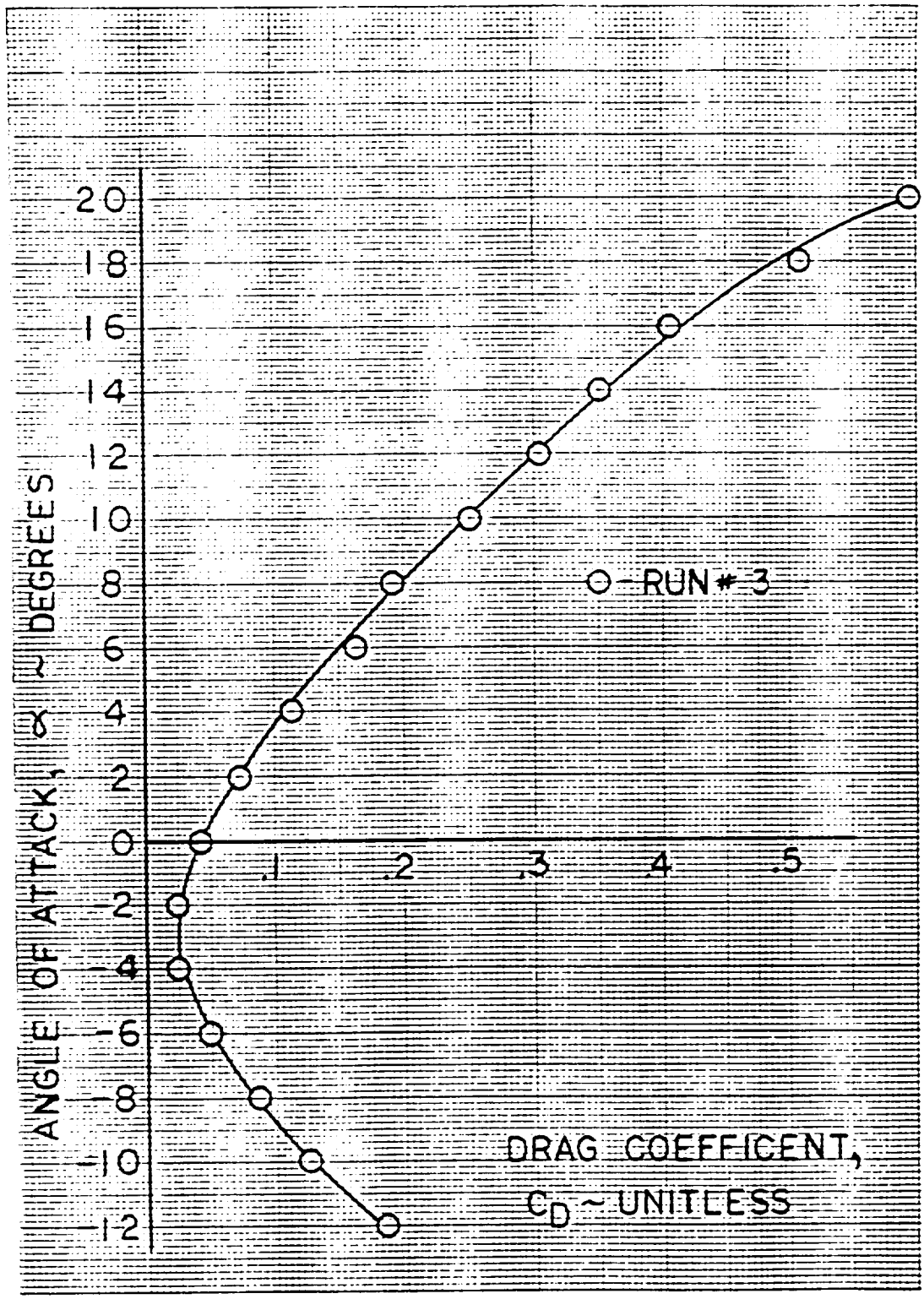

CALC	M. James		REVISED	DATE	FIGURE 5.2 SECTION DRAG CHARACTERISTICS FOR THE 1/5 SCALE ULTRA-LIGHT WING MODEL
CHECK					
APPD					
APPD					

AE 592

UNIVERSITY OF KANSAS

PAGE 15

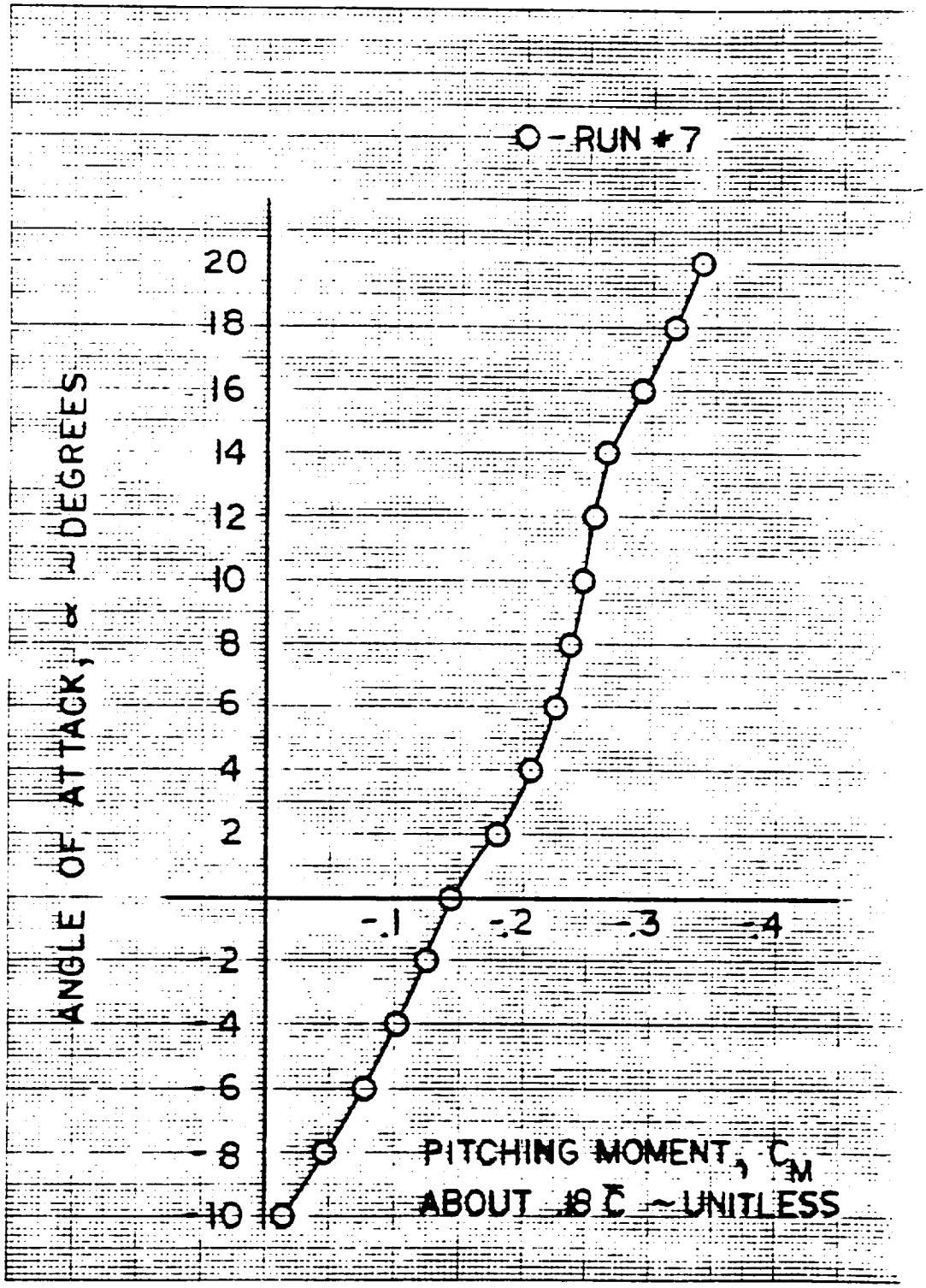

CALC	M. James		REVISED	DATE	FIGURE 5.3 SECTION PITCHING MOMENT CHARACTERISTICS FOR THE 1/5 SCALE ULTRA-LIGHT WING MODEL
CHECK					
APPD					
APPD					
					UNIVERSITY OF KANSAS

AE 592

PAGE 16

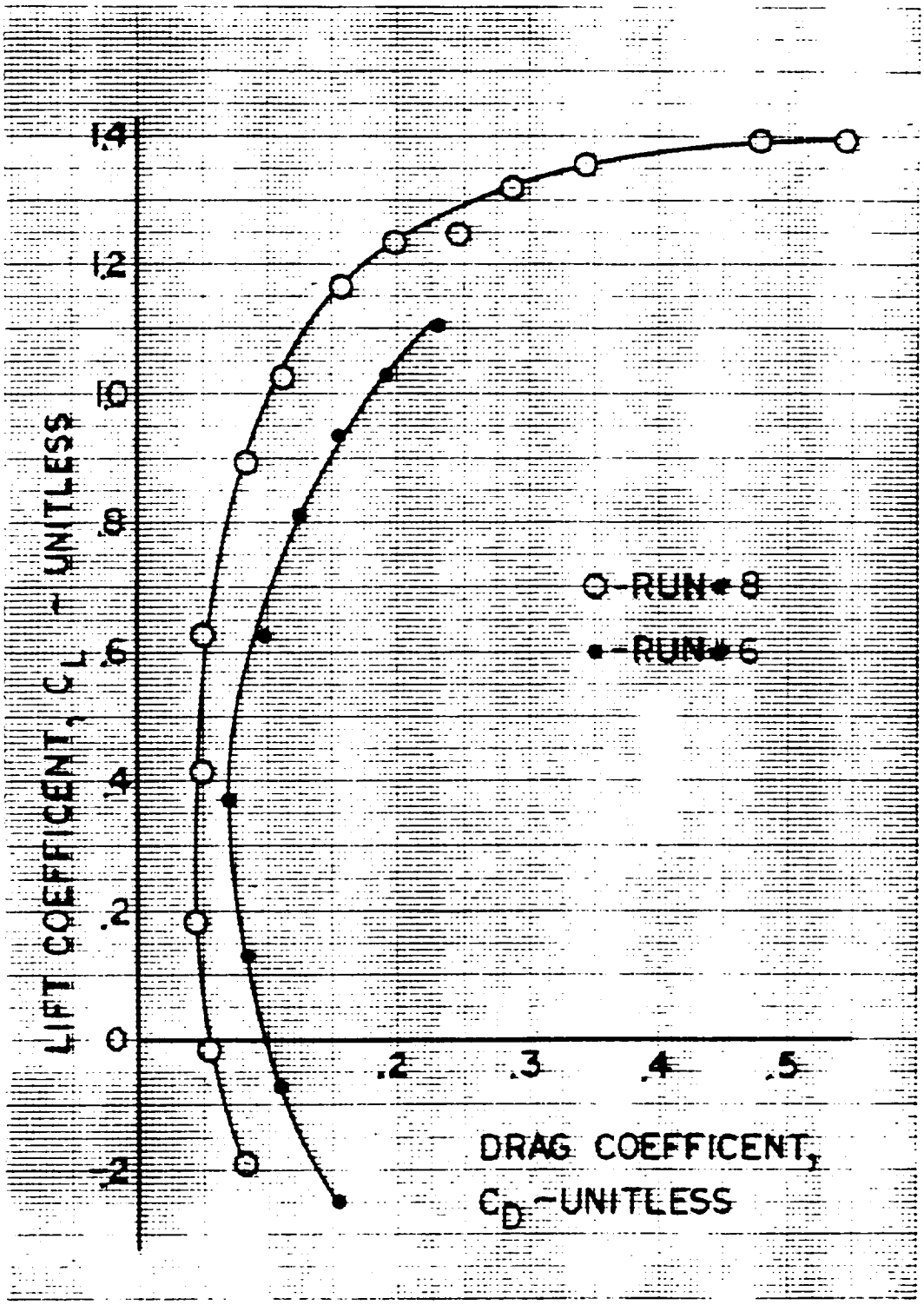

CALC	M. James		REVISED	DATE	FIGURE 5.4 DRAG POLAR CHARACTERISTICS FOR THE 1/5 SCALE ULTRA-LIGHT WING MODEL
CHECK					
APPD					
APPD					
					UNIVERSITY OF KANSAS

AE 592

PAGE 17

6. WING FABRIC FLEXURE

The topic of wing fabric flexure was mentioned often in the previous chapter. The section shape of an ultra-light wing is highly variant to airspeed and angle of attack. Airspeed tends to vary the magnitude of the fabric flexure. Angle of attack varies the location and direction (inwards or outwards) of fabric flexure. The fabric flexure for five different angle of attack settings were sketched in Figures 6.1 to 6.5. The many different (and odd !) airfoil shapes should be noticed for the range of attack angle settings. These figures show generalized airfoil shapes. The wing model was constructed with wire cross braces on the lower surface between the leading edge and main spar for fabric support (as stated in the construction chapter) which obviously are reflected in the lower surface fabric flexure shape. These helped to limit the fabric deflection in that particular area, but the exact shape they create is not determined in the figures.

-10 degrees angle of attack: This setting is shown in Figure 6.1. The upper surface leading edge and trailing edge are indented signifying a pressure force exerted downward on the wing. The entire lower surface is bubbled outwards, again displaying a downwards pressure force. There is a very interesting bubble in the fabric on the upper surface of the wing at about .25c. This perhaps is the only upwards pressure force on the wing, and serves to form a very unusual airfoil surface.

-6 degrees angle of attack: This setting is shown in Figure 6.2. The upper surface leading edge and trailing edge are indented, and so is the lower surface trailing edge. These indented surfaces are all handling inward pressure forces. The surfaces bubbling outward (experiencing outward pressure forces) lie on the middle upper surface and the lower leading surface of the wing.

0 degrees angle of attack: This setting is shown in Figure 6.3. The upper surface leading edge and entire lower surface of the wing are experiencing inward pressure forces. The remaining upper surface is bubbled outward and is experiencing lift.

6 degrees angle of attack: This setting is shown in Figure 6.4. It is virtually identical to the setting of zero degrees in Figure X.4. The only difference is that the upper surface fabric bubbling is more marked.

20 degrees angle of attack: This setting is shown in Figure 6.5. This is quite similar to the previous two settings (0 and 6 degrees), however the upper surface leading edge and lower surface fabric deflection is more marked, and the upper surface bubble is shifted more aft.

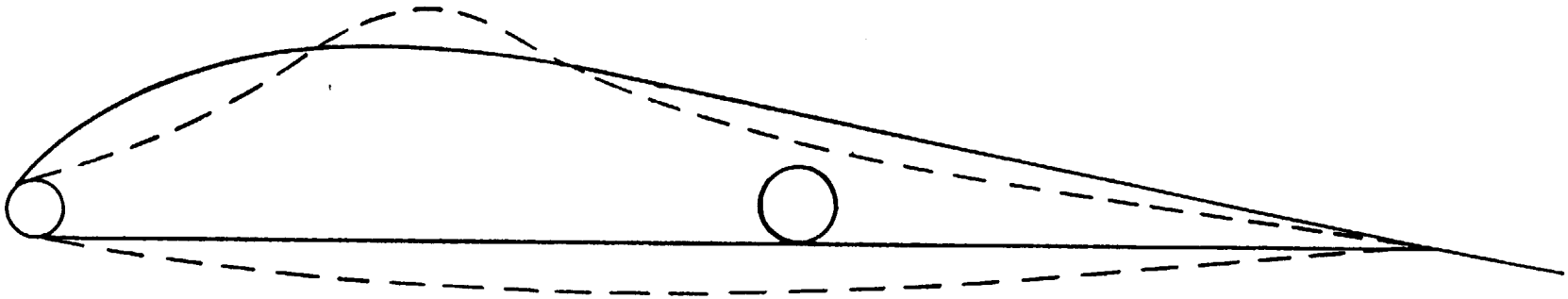

FIGURE 6.1 WING SECTION SHAPE DUE TO FABRIC FLEXURE
AT -10 DEGREES ANGLE OF ATTACK

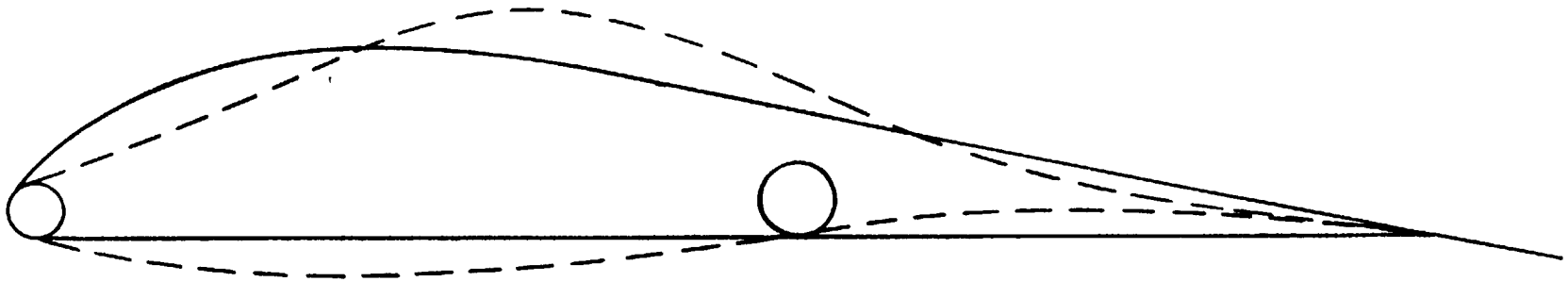

FIGURE 6.2 WING SECTION SHAPE DUE TO FABRIC FLEXURE
AT -6 DEGREES ANGLE OF ATTACK

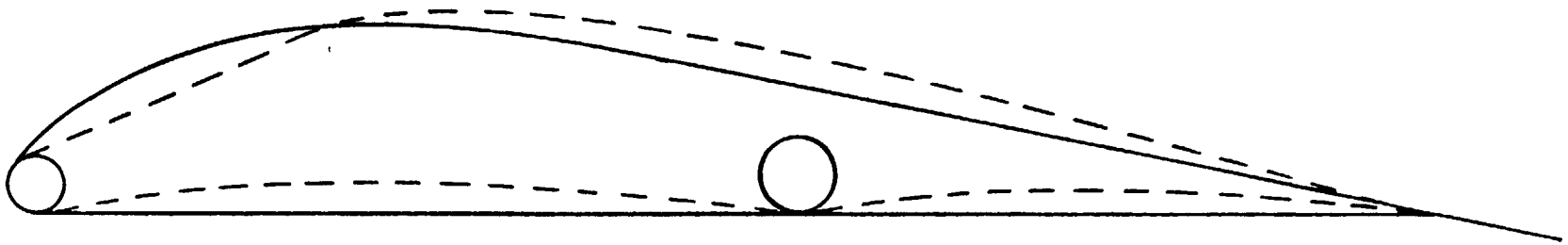

FIGURE 6.3 WING SECTION SHAPE DUE TO FABRIC FLEXURE
AT 0 DEGREES ANGLE OF ATTACK

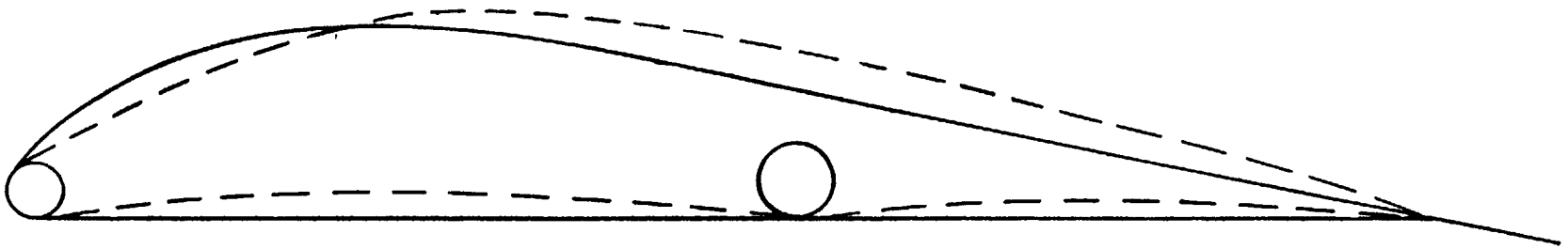

FIGURE 6.4 WING SECTION SHAPE DUE TO FABRIC FLEXURE
AT +6 DEGREES ANGLE OF ATTACK

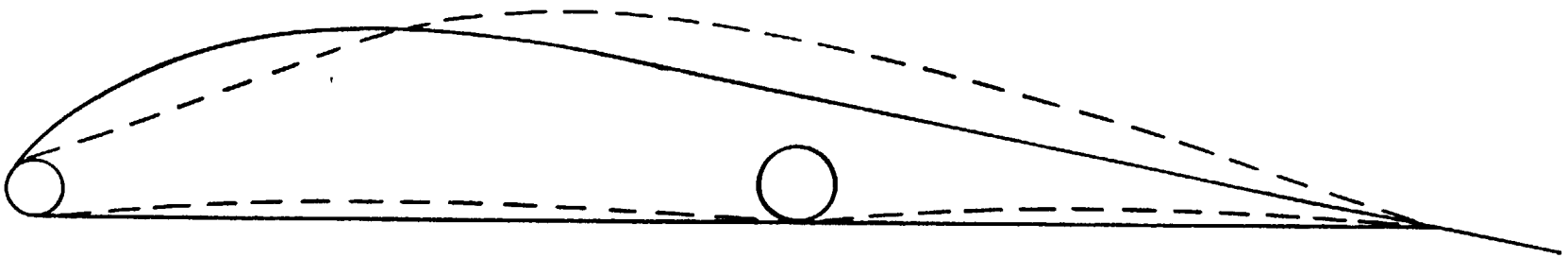

FIGURE 6.5 WING SECTION SHAPE DUE TO FABRIC FLEXURE
AT +20 DEGREES ANGLE OF ATTACK

7. RECOMMENDATIONS AND CONCLUSIONS

This project is an initial attempt to provide aerodynamic data for an ultra-light wing. Conclusive and fairly accurate lift, drag and pitching moment data were recorded and analyzed for the wing model. Some of the important findings are:

1) The lift coefficient-angle of attack curve indicated the presence of two entirely different lift curve slopes at different angles of attack.

2) The change in drag between small and large angles of attack is quite marked.

3) There occur two distinct break points on the pitching moment coefficient-angle if attack curve, indicating a particular sensitivity at these two angles of attack.

4) Lift to drag ratios for this model are 12 at low speeds and 7 at high speeds.

5) Aerodynamic data for an ultra-light wing is a function of the fabric flexure, which in turn is directly related to angle of attack and airspeed.

There are range of other tests that could be performed with this wing model. Hopefully a structural failure test will not be one of them. Ideas for future experiments with this wing may include:

1) Building a rigid model of the ultra-light wing to provide base data so that a more accurate study of the effects of fabric flexure can be studied.

2) Re-doing the drag data and taking drag tare data.

3) Calculating the pitching moment about a more useful reference point such as 0.25c.

4) Performing this testing in a different wind tunnel that can register the maximum forces endured by the wing.

Overall this was a very enjoyable project and it is encouraged that other students use this wing in individual or group testing--such as an AE 245 laboratory exercise.

Appendix A: Data Analysis

AE 592 SPECIAL PROJECT:

1/5 SCALE ULTRA-LITE WING

FOR DR. H. W. SMITH

BY MIKE JAMES

DATE: 12/16/88

TEMP = 73.8°F

P_{ATM} = 29.26 ↑

P_S = TUBE # 39 = 39.49

P_T = TUBE # 40 = 25.38

TEST NUMBER: 1

ZERO SCALE: (Y) N

	α	LIFT		DRAG		PITCHING MOMENT	
		S.F.	READING	S.F.	READING	S.F.	READING
99928	-12°	500	-33.3	1000	24.0	500	+ 34.5
99948	-10°	500	-25.5	500	38.5	200	- 21.0
99968	-8°	200	-27.5	500	29.0	500	- 38.0
99988	-6°	100	+29.0	500	20.8	1000	- 33.0
00008	-4°	500	+19.8	500	16.5	1000	- 47.0
00028	-2°	500	37.8	500	17.0	2000	- 30.0
00048	0°	1000	23.3	500	20.8	2000	- 35.3
00068	+2°	1000	30.5	500	30.8	2000	- 43.0
(BUFFETING) 00088	+4°	1000	34.5	500	40.8	2000	-47.8
00108	+6°	1000	38.0	1000	22.2	2000	-51.5
00128	+8°	1000	40.0	1000	27.2		PEGGED
00148	+10°	1000	44.0	1000	32.0		
00168	+12°	1000	46.0	1000	39.0		
00188	+14°	1000	48.0	1000	46.0		
00208	+16°	1000	49.0	2000	23.5		
00228	+18°	1000	49.5	2000	30.2		
00248	+20°	1000	51.0	2000	36.0		

AE 592 SPECIAL PROJECT :

1/5 SCALE ULTRA-LITE WING

FOR DR. H. W. SMITH

BY MIKE JAMES

DATE : 12/16/88

TEMP = 73.8°F

P_{ATM} = 29.26

P_S = TUBE # 39 = 28.50

P_T = TUBE # 40 = 25.12

TEST NUMBER : 2

ZERO SCALE: (Y) N
CALIBRATED TO 500

	α	LIFT		DRAG		PITCHING MOMENT	
		S. F.	READING	S. F.	READING	S. F.	READING
00248	+20°	1000	33.0	2000	20.8	2000	-50.0
	+18°	1000	31.5	1000	44.5	2000	-49.0
	+16°	1000	31.8	1000	33.0	2000	-45.0
	+14°	1000	30.8	1000	27.5	2000	-40.0
	+12°	1000	29.5	1000	23.3	2000	-38.5
	+10°	1000	27.8	1000	19.0	2000	-37.5
	+8°	1000	26.0	500	39.8	2000	-36.3
	+6°	1000	25.5	500	32.0	2000	-35.0
	+4°	1000	22.8	500	24.3	2000	-32.3
	+2°	500	48.0	500	17.5	2000	-28.7
	0°	500	36.0	200	43.5	1000	-38.5
	-2°	500	23.3	200	39.8	1000	-32.8
	-4°	200	39.5	200	40.0	1000	-28.0
	-6°	100	34.0	200	46.0	500	-38.5
	-8°	50	-28.5	500	20.3	200	-35.0
	-10°	200	-34.0	500	28.8	50	+38.0
	-12°	200	-47.5	500	40.0	500	+27.5

AE 592 SPECIAL PROJECT :

1/5 SCALE ULTRA-LITE WING

FOR DR. H. W. SMITH

BY MIKE JAMES

DATE : 12/16/88 @ 2300

TEMP = 76.0

P_{ATM} = 29.27

P_S = TUBE # 39 = 30.82

P_T = TUBE # 40 = 25.59

TEST NUMBER : 3

ZERO SCALE: (Y) N TO 1000

α	LIFT		DRAG		PITCHING MOMENT	
	S.F.	READING	S.F.	READING	S.F.	READING
+20°	2000	.320	2000	50.0		
+18°	2000	.320	2000	42.8		
+16°	2000	.320	2000	34.0		
+14°	2000	.303	2000	29.5		
+12°	2000	.298	2000	25.5		
+10°	2000	.280	1000 2000	50.0 21.0		
+8° (AFFTING STOPPED)	2000	.253	1000 2000	42.3 15.3		
+6°	2000	.238	1000 2000	35.0 13.5		
+4°	2000	.215	1000 2000	24.8 9.5		
+2°	2000	.183	1000 2000	20.0 6.0		
0°	2000	.125	1000 2000	14.5 3.5		
-2°	2000	.070	1000 2000	12.0 2.0		
-4°	2000	.010	1000 2000	12.0 2.0		
-6°	2000	-.050	1000 2000	16.0 4.0		
-8°	2000	-.085	1000 2000	22.3 7.0		
-10°	2000	-.110	1000 2000	29.5 10.5		
-12° (BUFFET)	2000	-.125	1000 2000	39.5 15.5		

AE 592 SPECIAL PROJECT :

1/5 SCALE ULTRA-LITE WING

FOR DR. H. W. SMITH

BY MIKE JAMES [SET TO MAX PITCHING MOMENT]

DATE : 12/16/88 @ 2345

TEMP = 76.2° F

P_{ATM} = 29.30

P_S = TUBE # 39 = 27.83

P_T = TUBE # 40 = 25.19

TEST NUMBER : 4

NOTE : APPARENT ERROR WHEN USING MULTIPLE SCALE FACTORS : WILL STICK TO 1 SCALE FACTOR.

ZERO SCALE : (Y) N TO 2000

α	LIFT		DRAG		PITCHING MOMENT	
	S. F.	READING	S. F.	READING	S. F.	READING
+ 20°	2000	21.5	2000	32.9	2000	-50.0
+ 18°		20.3		27.0		- 46.3
+ 16°		20.3		23.5		- 43.0
+ 14°		20.0		18.5		-39.0
+ 12°		19.0		16.0		- 37.3
+ 10°		18.0		13.8		- 36.0
+ 8°		17.0		11.8		- 35.0
+ 6°		16.3		9.5		-33.0
+ 4°		14.8		8.3		- 30.0
+ 2°		13.0		5.3		-26.0
0°		10.0		3.8		-20.5
-2°		6.2		3.3		-17.3
-4°		2.8		3.3		- 14.5
-6°		0.2		4.0		-11.0
-8°		-1.2		5.8		- 5.8
-10°		-4.0		8.0		- 1.0
-12°		-5.8		12.0		+ 8.5

AE 592 SPECIAL PROJECT :

1/5 SCALE ULTRA-LITE WING

FOR DR. H. W. SMITH

BY MIKE JAMES

DATE : 12/17/83 @ 0030

TEMP = 76.2

P_{ATM} = 29.30"

P_S = TUBE # 39 = 33.58

P_T = TUBE # 40 = 25.94

TEST NUMBER : 5

ZERO SCALE : Y (N)
LAST SET ON 2000

α	LIFT		DRAG		PITCHING MOMENT	
	S. F.	READING	S. F.	READING	S. F.	READING
+12°	2000	45.0	2000	41.0		
+10°		43.0		34.5		
+8°		38.8		29.3		
+6°		35.8		24.3		
+4°		32.5		18.8		
+2°		29.0		14.8		
0°		21.3		11.0		
-2°		13.5		9.3		
-4°		6.2		9.0		
-6°		-1.5		12.0		
-8°		-5.5		16.0		
-10°		-8.3		20.0		
-12°		-10.3		26.5		

AE 592 SPECIAL PROJECT :

1/5 SCALE ULTRA-LITE WING

FOR DR. H. W. SMITH

BY MIKE JAMES

DATE : 12/17/88

@ 0050

TEMP = 76.2

P_{ATM} = 29.30"

*NOTE: RECORD #39 & #40 AT ZERO ANGLE OF ATTACK.

P_S = TUBE # 39 = 36.78

P_T = TUBE # 40 = 26.38

TEST NUMBER : 6

ZERO SCALE: Y (N)
LAST ZEROED ON 2000

α	LIFT		DRAG		PITCHING MOMENT	
	S. F.	READING	S. F.	READING	S. F.	READING
8°	2000	50.0	2000	38.8		
6°		46.5		32.2		
4°		42.3		26.0		
2°		36.5		20.8		
0°		28.3		16.3		
-2°		16.7		11.5		
-4°		6.0		13.9		
-6°		-3.3		18.0		
-8°		-11.3		25.8		

AE 592 SPECIAL PROJECT :

1/5 SCALE ULTRA-LITE WING

FOR DR. H. W. SMITH

BY MIKE JAMES

DATE : 12/17/88

@ 0100

TEMP = 76.0

P_{ATM} = 29.31

DO :
- READ OF MAX C_M AT 2000
- ST. DRAG AT 1000
- C_A at 1000

P_S = TUBE # 39 = 28.38

P_T = TUBE # 40 = 25.27

TEST NUMBER : 7

ZERO SCALE : (Y) N

α	LIFT		DRAG		PITCHING MOMENT	
	S.F.	READING	S.F.	READING	S.F.	READING
+ 20°	2000	20.0	2000	31.8	2000	- 50.0
+ 18°		18.8		27.0		- 47.0
+ 16°		18.8		22.0		- 43.0
+ 14°		18.0		17.9		- 39.0
+ 12°		17.0		15.3		- 37.5
+ 10°		16.2		12.8		- 36.3
+ 8°		15.5		11.3		- 35.0
+ 6°		14.5		8.8		- 33.3
+ 4°		13.3		6.8		- 30.3
+ 2°		11.5		4.7		- 26.5
0°		8.5		3.4		- 21.0
- 2°		4.7		2.6		- 17.8
- 4°		1.5		1.6		- 14.9
- 6°		- 0.9		3.7		- 11.3
- 8°		- 1.5		5.4		- 6.6
- 10°		- 4.7		7.8		- 2.0
- 12°		- 6.1		10.9		+ 6.3

AE 592 SPECIAL PROJECT :

1/5 SCALE ULTRA-LITE WING

FOR DR. H. W. SMITH

BY MIKE JAMES

DATE : 12/17/99

@ 0130

TEMP = 76.0

P_{ATM} = 29.31

P_S = TUBE # 39 = 26.58

P_T = TUBE # 40 = 25.01

TEST NUMBER : 8

ZERO SCALE : (Y) N

ZEROED TO 1000

α	LIFT		DRAG		PITCHING MOMENT	
	S.F.	READING	S.F.	READING	S.F.	READING
+20°	1000	20.5	1000	33.5	1000	-50.0
+18°		19.0		27.5		-45.5
+16°		19.0		24.0		-44.0
+14°		18.5		17.3		-35.5
+12°		18.0		14.5		-34.0
+10°		17.0		12.4		-33.0
+8°		16.8		10.0		-32.0
+6°		15.9		8.0		-30.0
+4°		14.0		5.7		-26.7
+2°		12.2		3.9		-21.8
0°		8.5		2.5		-17.5
-2°		5.7		2.5		-14.5
-4°		2.5		2.2		-12.2
-6°		-0.2		2.7		-9.7
-8°		-2.6		4.2		-5.5
-10°		-5.0		7.4		-1.0
-12°		-6.5		11.0		+8.0

Equations:

1. Lift Calculation: $L = \frac{(\text{Reading} \times \text{Scale Factor})}{27}$

2. Drag Calculation $D = \frac{(\text{Reading})(\text{Scale Factor})}{100}$

3. Pitching Moment Calculation: $PM = \frac{(\text{Reading})(\text{Scale Factor})}{29 \times 12}$

4. Calculation of Tunnel Speed:

$$V = \sqrt{\frac{(P_T - P_S)(3.2174)}{\rho}} \quad ; \quad \rho = \frac{P}{1716\,T}$$

5. Calculation of Reynold's Number:

$$R_N = \frac{\rho V \bar{c}}{\mu} \quad ; \quad \mu = 3.408 \times 10^{-7} + 5.48 \times 10^{-10}\, T(^\circ F)$$

6. Calculation of C_L:

$$C_L = \frac{L}{\bar{q} S} \quad ; \quad \bar{q} = \frac{1}{2} \rho V^2$$

7. Calculation of C_D:

$$C_D = \frac{D}{\bar{q} S}$$

8. Calculation of C_M:

$$C_M = \frac{PM}{\bar{q} S \bar{c}}$$

```
 10 RHO=0
 20 L=0
 30 D=0
 40 TEMP=0
 50 PRESS=0
 60 PM=0
 70 MU=0
 80 V=0
 90 CDTARE = 0
100 INPUT "TRIAL RUN NUMBER =";NUM
110 INPUT "STATIC PRESSURE =";PS
120 INPUT "TOTAL PRESSURE =";PT
130 INPUT "PRESSURE IN INCHES HG =";P
140 INPUT "TEMPERATURE IN DEGREES FARENHEIT =";T
150 INPUT "WING CHORD IN FEET =";C
160 INPUT "WING SPAN IN FEET =";B
170 S = B*C
175 PRINT "WING AREA =";S
180 PRESS = P*70.722
185 PRINT "PRESSURE =";PRESS
188 PRINT "PRESSURE ="PRESS
190 TEMP = T+459.6
195 PRINT "TEMPERATURE =";TEMP
200 RHO = PRESS/(1716*TEMP)
210 V = ((PS-PT)*3.2174/RHO)^.5
220 Q = .5*RHO*(V^2)
225 PRINT "DYNAMIC PRESSURE =";Q
230 MU = ((5.48*10^-10)*T)+(3.408*10^-7)
235 PRINT "VISCOSITY =";MU
240 RN = RHO*V*C/MU
250 LPRINT "WIND TUNNEL RUN NUMBER ";NUM
260 LPRINT "TUNNEL VELOCITY IN FT/S =";V
270 LPRINT "REYNOLDS NUMBER =";RN
280 LPRINT "    ALPHA    |      CL      |      CD      |      CM    "
290 LPRINT "-------------------------------------------------------"
300 INPUT "SCALE FACTOR =";SF
305 INPUT "ANGLE OF ATTACK =";ALPHA
310 INPUT "LIFT READING =";LREAD
320 L = LREAD*SF/27
330 CL = L/(Q*S)
340 INPUT "DRAG READING =";DREAD
350 D = DREAD*SF/100
360 CD = (D/(Q*S))-CDTARE
370 INPUT "PITCHING MOMENT READING =";PMREAD
380 PM = PMREAD*SF/348
390 CM = PM/(Q*S*C)
400 LPRINT TAB(4) ALPHA TAB(15) CL TAB(30) CD TAB(47) CM
410 GOTO 305
```

WIND TUNNEL RUN NUMBER 3
TUNNEL VELOCITY IN FT/S = 86.4358
REYNOLDS NUMBER = 432672.9

ALPHA	CL	CD	CM
20	1.410434	.5950268	0
18	1.410434	.5093429	0
16	1.410434	.4046182	0
14	1.335505	.3510658	0
12	1.313466	.3034637	0
10	1.234129	.2499112	0
8	1.115124	.1820782	0
6	1.04901	.1606572	0
4	.9476352	.1130551	0
2	.8065918	7.140321E-02	0
0	.5509507	4.165187E-02	0
-2	.3085324	2.380107E-02	0
-4	4.407606E-02	2.380107E-02	0
-6	-.2203803	4.760214E-02	0
-8	-.3746465	8.330375E-02	0
-10	-.4848367	.1249556	0
-12	-.5509507	.1844583	0

WIND TUNNEL RUN NUMBER 4
TUNNEL VELOCITY IN FT/S = 61.3908
REYNOLDS NUMBER = 307416.8

ALPHA	CL	CD	CM
20	1.877324	.7732828	-.3985074
18	1.772543	.6365438	-.3690178
16	1.772543	.5540288	-.3427163
14	1.746348	.4361504	-.3108358
12	1.65903	.3772112	-.2972865
10	1.571713	.3253446	-.2869253
8	1.484396	.2781932	-.2789551
6	1.423274	.2239691	-.2630149
4	1.292298	.1956783	-.2391044
2	1.135126	.1249512	-.2072238
0	.8731739	8.958764E-02	-.163388
-2	.5413678	.0777998	-.1378836
-4	.2444887	.0777998	-.1155671
-6	1.746348E-02	9.430279E-02	-8.767162E-02
-8	-.1047809	.136739	-4.622686E-02
-10	-.3492696	.1886056	-7.970147E-03
-12	-.5064409	.2829084	6.774625E-02

wIND TUNNEL RUN NUMBER 5
TUNNEL VELOCITY IN FT/S = 104.4355
REYNOLDS NUMBER = 522964.7

ALPHA	CL	CD	CM
12	1.357762	.3340095	0
10	1.297417	.2810568	0
8	1.170693	.2386946	0
6	1.080175	.1979617	0
4	.9806059	.1531556	0
2	.8750022	.1205693	0
0	.6426741	.0896123	0
-2	.4073286	7.576313E-02	0
-.4	.1870695	7.331915E-02	0
-6	-4.525874E-02	9.775888E-02	0
-8	-.1659487	.1303452	0
-10	-.2107767	.2158842	0
-10	-.2504317	.1629315	0
-12	-.3107767	.2158842	0

IND TUNNEL RUN NUMBER 6
TUNNEL VELOCITY IN FT/S = 121.8479
REYNOLDS NUMBER = 610158.1

ALPHA	CL	CD	CM
8	1.108258	.2322023	0
6	1.03068	.192704	0
4	.9375865	.1555995	0
2	.8090285	.1244796	0
0	.6272741	9.754889E-02	0
-2	.3701582	6.882284E-02	0
-4	1.32991	8.318586E-02	0
-4	.132991	8.318586E-02	0
-6	-7.314504E-02	.1077227	0
-8	-.2504664	.1544025	0

WIND TUNNEL RUN NUMBER 7
TUNNEL VELOCITY IN FT/S = 66.60797
REYNOLDS NUMBER = 333876

ALPHA	CL	CD	CM
20	1.482431	.6364076	-.3382829
18	1.393485	.5403461	-.3179859
16	1.393485	.440282	-.2909233
14	1.334188	.3582294	-.2638607
12	1.260066	.3061961	-.2537122
10	1.200769	.2561641	-.2455934
8	1.148884	.2261448	-.236798
6	1.074763	.1761128	-.2252964
4	.9858166	.1360872	-.2049994
2	.8523978	9.406024E-02	-.17929
0	.6300331	6.804358E-02	-.1420788
-2	.3483713	5.203333E-02	-.1204287
~~-4~~	~~.1111823~~	~~0~~	~~.1008083~~
-4	.1111823	3.202051E-02	-.1008083
-6	-.0667094	7.404743E-02	-7.645194E-02
-8	-.1111823	.1080692	-4.465334E-02
-10	-.3483713	.1561	-1.353132E-02
-12	-.4521415	.2181397	4.262365E-02

WIND TUNNEL RUN NUMBER 8
TUNNEL VELOCITY IN FT/S = 47.32559
REYNOLDS NUMBER = 237222.1

ALPHA	CL	CD	CM
20	1.504973	.6640236	-.3350507
18	1.394853	.545094	-.3048962
16	1.394853	.4757184	-.2948446
14	1.358147	.3429137	-.237886
12	1.32144	.2874132	-.2278345
10	1.248027	.2457879	-.2211335
8	1.233344	.198216	-.2144325
6	1.167272	.1585728	-.2010304
4	1.027787	.1129831	-.1789171
2	.8956426	7.730424E-02	-.1460821
0	.6240133	.049554	-.1172677
-2	.418456	.049554	-.0971647
-4	.1835333	4.360752E-02	-8.175237E-02
-6	-1.468267E-02	5.351832E-02	-.6499984
-8	-.1908747	8.325072E-02	-3.685558E-02
-10	-.3670667	.1466798	-6.701014E-03
-12	-.4771867	.2180376	5.360811E-02

V. STATIC TEST OF AN ULTRALIGHT AIRPLANE

Reprinted from *J. Aircraft*, Vol. 25, No. 1, January 1988

Howard W. Smith
Professor
Department of Aerospace Engineering
University of Kansas

Partially supported by
NASA Langley Research Center
Grant #NAG 1-345

Static Test of an Ultralight Airplane

Howard W. Smith*
University of Kansas, Lawrence, Kansas

This paper describes the work necessary to perform the static test of an ultralight airplane. A steel reaction gantry, loading whiffletrees, hydraulic actuation system, and instrumentation systems were designed. Load and stress analyses were performed on the airplane and on the newly designed gantry and whiffletrees. Load cell calibration and pressure indicator calibration procedures are described. A description of the strain and deflection measurement system is included. The engine, propeller, fuel, and pilot were removed and replaced with masses to fulfill center-of-gravity requirements prior to testing. Data obtained to date are compared to the analytical predictions.

Nomenclature

C_L = wing lift coefficient
d = displacement, mm
F_{cu} = ultimate compression stress, ksi
h = altitude, ft
M_x = wing bending moment, N·m
n = limit load factor
R_N = nose wheel reaction, lb
R_L = left main wheel reaction, lb
R_R = right main wheel reaction, lb
S = wing area, ft²
V = airplane speed, ft/s
W_0 = empty weight, lb
W_{BF} = basic flight design weight, lb

Introduction

As the service life of the fleet of ultralight vehicles increases, the number of fatal accidents is expected to increase as well. Several cases have been documented by the National Transportation Safety Board[1] in which the integrity of the structure was questioned. When similarities between cases occur, it is logical to formulate a plan to investigate the basic behavior of a typical vehicle.

The opportunity to formulate a plan presented itself in early 1985. Research on the aerodynamics and flight characteristics of an Airmass Sunburst "C" was drawing to a close and a master's thesis by Blacklock[2] was published. Consequently, a full-scale ultralight airplane was available for further research. A proposal was written and presented to the NASA Langley Research Center. The primary goal of this proposal was to perform a structural test to destruction of an ultralight airplane.

The structural floor and the ultralight airplane specimen are shown in Fig. 1. To perform a static test, a steel gantry and its sway bracing was designed.[3] Similarly, the upper and lower whiffletrees were designed and integrated with the loading device. Finally, the strain and deflection systems were designed. This paper describes the details of the work accomplished.

Presented as Paper 86-2600 at the AIAA General Aviation Technology Meeting, Anaheim, CA, Sept. 29–Oct. 1, 1986; received Oct. 28, 1986; revision received June 12, 1987.

*Professor, Aerospace Engineering. Associate Fellow AIAA.

Analysis

Design Criteria

In the early days, an airplane had to be able to carry the limit load without permanent deformation and the ultimate load for 3 s passing the static test sequence was a time of joy and celebration for the structures engineers. Nowadays, aircraft are governed by much more rigorous specifications. The static strength requirement has been retained, but is now only one element of a much larger array of specifications under a comprehensive umbrella known as the structural integrity program. Among the factors included are: corrosion, durability, damage tolerance, and flutter. Aircraft that are to be certified prior to use must meet or exceed specifications. These requirements are specified in either Federal Aviation Regulations or Military Specifications and the "meet or exceed" phrase is satisfied by analysis or by test or both.

A set of design guidelines for an utralight has been published by the Powered Ultralight Manufacturers Association (PUMA).[4] However, there are no specifications governing the structural integrity of an ultralight airplane. For this analysis, the ultralight was treated as though it were a normal category general aviation airplane governed by FAR-23. All related Mil-Specs and Mil-Standards were invoked as well.

It should be noted that student interest in this research project was very high. One student elected to write a report on a structural integrity program for ultralights,[5] probably the only one of its kind in existence.

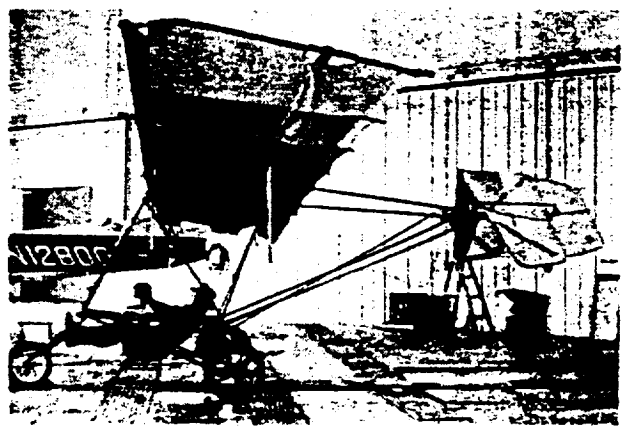

Fig. 1 Sunburst "C" ultralight.

Table 1 Lift distribution

Speed (maneuvering)	69 ft/s
Altitude h	1000 ft
Weight W_{BF}	468 lb
C_L (max)	1.48
S	150.9 ft^2
n (limit)	3.8

Lift Distribution

Ordinarily, a structural test engineer begins with air load distributions as "known" values. Both spanwise and chordwise pressure distributions must be given beforehand to allow determination of "patch" loads. For this ultralight, six spanwise and two chordwise stations were selected to simulate the subsonic pressure distribution. In reality, the airfoil behavior is unknown, since it is only sail cloth stretched over the front and rear spar tubes. During a maximum positive load factor condition, the airfoil is taut and has a particular set of ordinates. During any other flight condition, including inverted flight, the ordinates are variable.

Since an air load distribution was not available, one was calculated using a quasivortex lattice method. This work was done by a student who favored this method and the analysis was performed with ease.[6,7] With this knowledge, patch loads could be determined. Those data were incorporated in the upper whiffletree design. The design maneuvering speed at a limit load factor of 3.8 was 69.0 ft/s. (See Table 1.) The spanwise lift distribution is shown in Fig. 2. The spanwise drag distribution was assumed to be negligible.

Dead Weights

The weight breakdown for our test condition is given in Table 2. The engine, propeller, shaft, and mounts were removed and replaced with a mass whose magitude and center of mass were correctly located. The lower whiffletree mass was included to correct the 1g dead weight loads. Fuel was replaced with water of the correct weight.

Our ultralight pilot, named Bellerophon, was constructed of army coveralls, worn-out army boots, a cap, and a mask (Halloween) for cosmetic purposes. The cap was adorned with a NASA logo. Bellerophon's center of gravity was built up with concrete cylinders at the buttock and thigh locations. The remainder was constituted from plastic bags and Kaw River sand. Weighing and loading him into the aircraft required the assistance of four strong students.

Overall airplane weight and center-of-gravity location was checked and rechecked by actual weighings with three balance scales under the wheels. Results of the weighings were: $R_N = 11.49$ lb, $R_L = 127.0$ lb, $R_R = 133.2$ lb, for a total of 271.69 lb. (See Fig. 3.)

Point Load Calculations

With many scientific developments, the creators of the breakthrough cannot foresee the eventual applications of their work. Likewise, Joseph Fourier could not have known that his work with sines and cosines would be used to calculate air load pressures on an ultralight airplane nor could Fred Whipple have known that his method would be used to approximate that air load.

The upper whiffletrees are simple three-point beam pairs made from ordinary 2×4 and 2×6 pieces of lumber. There are five "tiers" of trees. The first is the highest and the fifth the lowest. The trees are connected with heavy-duty turnbuckles. Tier 1 is connected to the steel gantry with a single steel strap. Tier 5 is just below the wing and is in direct contact with the tubular spars. Plywood bearing plates are used to spread the load along the spars. Tiers 1-3 are the spanwise trees, while tiers 4 and 5 assure the chordwise center-of-pressure location. With no load in the actuator, the ultralight is suspended above the hangar floor in straight and level flight.

Table 2 Weight breakdown of test aircraft, lb

Structure	
Tube WG-1	5.31
Wing skins	16.25
Landing gear	
Wheel-nose	3.12
Main wheels and tires	10.90
Rear axle	7.01
Seat	8.71
Powerplant	
Engine and propeller	78.38
Muffler	5.70
Propeller shaft	8.88
Misc., each < 3 lb	Remainder
W_0 Weight empty	277.48
Fuel	15.52
Pilot ("Bellerophon")	175.00
W_{BF} Basic flight weight	468.00

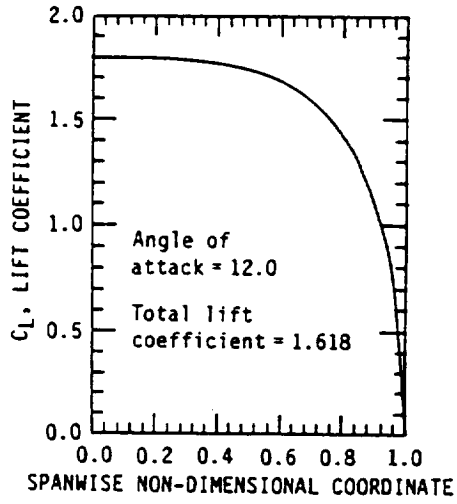

Fig. 2 Wing spanwise lift coefficient.

The upper whiffletree arrangement for the left-hand wing is shown in Fig. 4.

The lower whiffletree is a loading mechanism as well. A pair of steel straps connect at the engine mount holes and the U-straps bear directly on the fuselage cage tubes. These whiffletrees are commercial grade steel and are designated tiers 6 and 7. Tier 6 is adjacent to the fuselage and tier 7 (the lowest) connects to the 10,000 lb hydraulic actuator. A load cell is in series with the actuator. These linkages are bolted directly to a floor fitting where they are reacted. The floor fitting, called the "alligator," was specially designed for that purpose. It is located directly below the air load center-of-pressure vector P, shown in the lower whiffletree sketches (Figs. 5 and 6). All of the lower whiffletree members are made from standard AISC steel sections: rectangular tubing, tees, and flat straps.

Internal Loads Analysis

A stress analysis of the wing structure was performed using the air loads discussed above. Availability of the Polo finite-element method and its ease of use were the reasons for its selection.[8] Results are given in DeAlmeida's report.[6] The flying wire loads at the design limit load factor of $n = 3.8$ are:

Forward inboard 44 lb
Aft inboard 65 lb

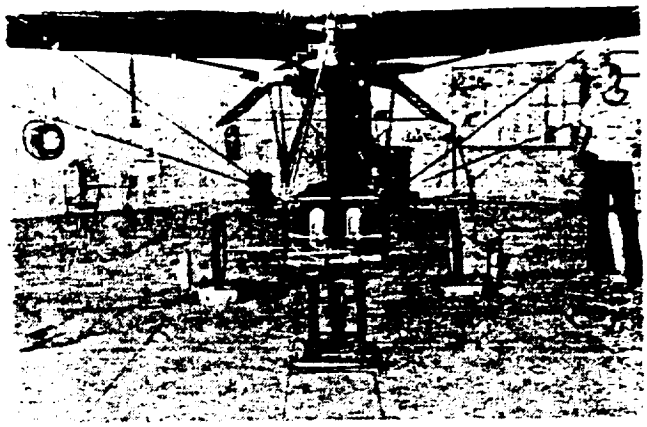

Fig. 3 Weight and center of gravity.

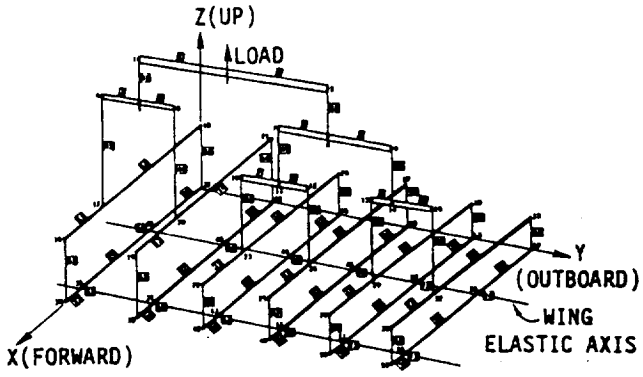

Fig. 4 Upper whiffletree.

Forward outboard 222 lb
Aft outboard 145 lb

Wing bending moments M_x and spar displacements d are shown in Figs. 7 and 8.

Systems Design

For this study, the test rig was divided into four independent systems. The design and assembly of each system is described below.

Hydraulic System

A 3000 psi hydraulic system was designed to apply the load. An Allis-Chalmers 10,000 lb, 8 in. stroke actuator and a Prince hand pump were purchased from a surplus machinery supplier. A pressure gage and short hydraulic lines were obtained from the same supplier. A schematic of the hydraulic system is shown in Fig. 9.

The Boeing Company supplied the hydraulic lines, a four-port Barksdale valve, and several hydraulic fittings. The 2 gal reservoir and hydraulic oil were purchased locally. These parts were assembled and the lines purged of air by two students. The system was tested during the two-by-four destruction test described below.

Load Cell System

A 5000 lb Baldwin-Lima-Hamilton load cell has been in the Aero Department for a number of years. A pair of load cell "eyes" had to be purchased to match the special internal threads. The eyes have 1 in. diameter self-aligning bearings. A pair of links connect to a smaller eye at each end. The smaller eye shaft could then be gripped in test machine jaws. Excellent linearity was achieved. A calibration constant was determined to be 82 lb per unit readout.[9]

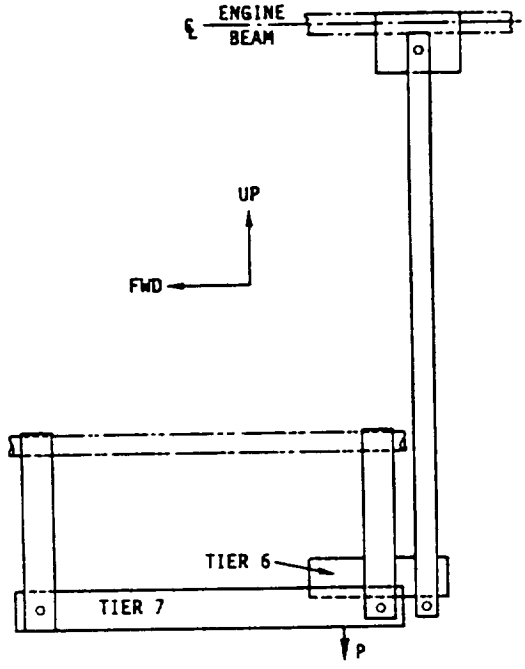

Fig. 5 Lower whiffletree, left side view.

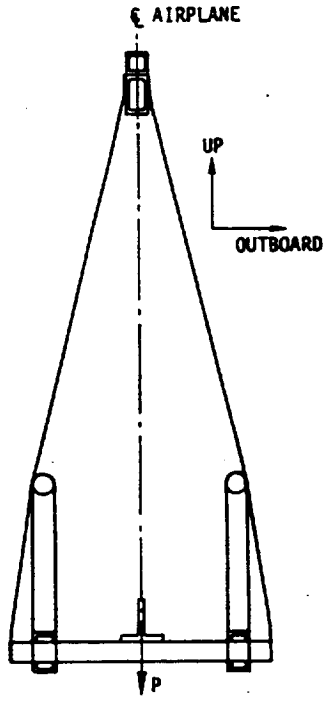

Fig. 6 Lower whiffletree, rear view.

Deflection Measurement System

Large deflections were measured with a sliding scale system. In hazardous situations, a telescope or transit was used. This was the case when cable failures were imminent. When deflections were small (less than 1 in.), a dial indicator was used. Tip deflections of 3.70 in. limit were expected. The sliding scale concept was proved during the wood bending destruction test, which was recorded on video tape.

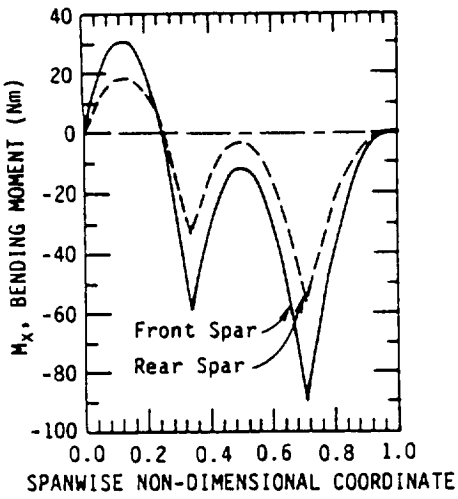

Fig. 7 Wing limit bending moments.

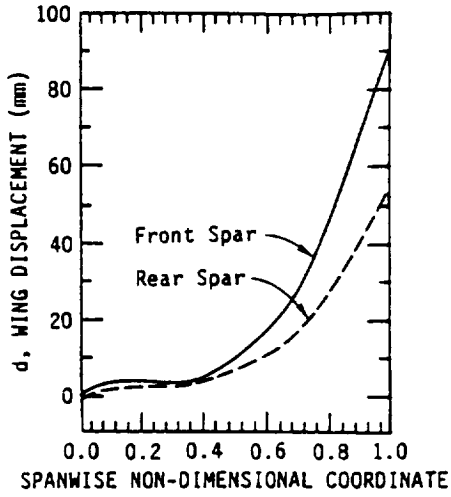

Fig. 8 Wing limit deflections.

Strain Measurements System

All strain gages were single-element foil gages from Micro Measurements. A 10 channel switch and balance unit and a strain readout unit were available from previous research. The strain gage terminal board was borrowed from the Aerospace Medical Research Laboratory. The resulting strain measurement system design was proved during the tube tension component tests described below. Data were taken with a Vishay-Ellis switch and balance unit and strain indicator.

Component Tests

Tube Compression

Compression tests of the 6061-T6 tubes were run to verify the heat treat level. The ultimate stress in compression was: F_{CU} (measured) = 47.8 ksi and F_{CU} (MIL-HDBK-5A) = 42.0 ksi.

Wood Bending

Wood bending tests were performed on a pair of medium-grade "S-P-F" lumber. The test simulated an upper whiffletree and was performed to spot check the modulus of rupture of "spruce-pine-fir," another unknown. Both the stress magnitude and the failure mode were missed. The modulus of rupture in bending, not to be confused with the civil engineering design value, was estimated to be 9600 psi. The wood beam ensemble failed in horizontal shear and "prying" near the point of maximum moment. The magnitude was 85% of the predicted ultimate load. For this test, the load-deflection curve was linear up to 50% of the failure load.

Cable Tension

Cable testing was very interesting and informative. Four assemblies of ⅛ in. diameter, 7 × 19 aircraft cables were designed to represent the "flying wires" on the ultralight. They were fitted with thimbles, grommets, tangs, and Nico-press clamps. Failure load for the cable is estimated to be 1740 lb. None of the cables carried more than 975 lb. All "failed" by the cable sliding out of the Nico-press fitting. Cable testing is incomplete at this time. All cables will be fitted with double clamps and retested in an attempt to rupture the cable strands. Special safety precautions have been taken to keep humans out of a 100 in. cable whipping lethal radius drawn with each cable end as an arc center.

Recommendations

1) Unscathed portions of the ultralight, such as the wing tip, can be sawn off and used in future wind-tunnel work. The two-dimensional lift and drag coefficients should be obtained from minimum to maximum C_L.

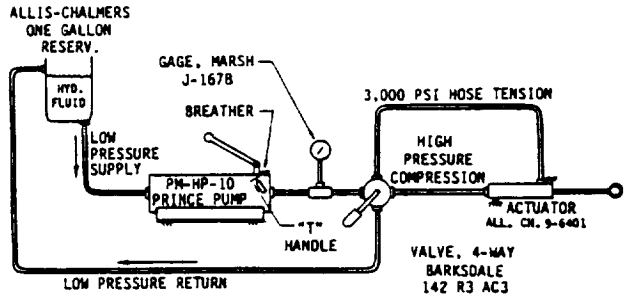

Fig. 9 Hydraulic system.

2) Almost nothing is known about the behavior of an ultralight structure under repeated loads. A durability and damage tolerance research program is highly recommended.

Acknowledgments

Many people freely volunteered to work on this project: Steve Waddell, Geoffrey Smith, Ron Schorr and Paul Oelschlaeger. Thanks to the Caroline Wire and Rope Company who supplied the cable and assembled the test specimens at no charge. This work was supported by NASA Langley Research Center under NASA Grant NAG 1-345 and the Aerospace Engineering Department of the University of Kansas.

References

[1]"Safety Study: Ultralight Vehicle Accidents," National Transportation Safety Board, Rept. NTSB/SS-85/01, Feb. 7, 1985.

[2]Blacklock, C. L. Jr., "Summary of the General Powerplant, Weight and Balance and Aerodynamic Characteristics of an Ultralight Aircraft," M.S. Thesis, University of Kansas, Lawrence, Aug. 1984.

[3]Smith, H.W., "Design of Static Reaction Gantry for an Ultralight Airplane Destruction Test," AIAA Paper 85-4022, Oct. 14, 1985.

[4]"Airworthiness Standards for Powered Ultralight Vehicles," Powered Ultralight Manufacturers Association, Annandale, VA, Dec. 9, 1983.

[5]Turnipseed, Michael E., "Aircraft Structural Integrity Program for Ultralights," University of Kansas, Lawrence, May 7, 1986.

[6]DeAlmeida, S.F.M., "Aerodynamic and Structural Analyses of an Ultralight Aircraft," University of Kansas, Lawrence, May 6, 1986.

[7]Lan, C.T., "A Quasi Vortex Lattice Method in Thin Wing Theory," *Journal of Aircraft*, Vol. 11, 1974, p. 518.

[8]Lopez, L.A. et al., "Polo-Finite," University of Illinois, Urbana, 1985.

[9]Page, L., "Cable Testing for Ultralight Airplanes," University of Kansas, Lawrence, May 6, 1986.

[10](All) Engineering Drawings, University of Kansas, Lawrence, (125 drawings total).

VI. SELECTION AND STATIC CALIBRATION OF THE MARSH J1678 PRESSURE GAUGE

Charles R. Oxendine
Graduate Student

Howard W. Smith
Professor
Department of Aerospace Engineering
University of Kansas

March 1986

Partially supported by
NASA Langley Research Center
Grant #NAG 1-345

TABLE OF CONTENT

LIST OF TABLES

LIST OF FIGURES

SUMMARY

During the experimental testing of the ultralight, it was determined that a pressure gauge would be required to monitor the simulated flight loads. After analyzing several factors, which are indicated in the discussion section of this report, the Marsh J1678 pressure gauge appeared to be the prominent candidate for the task. However, prior to the final selection the Marsh pressure gauge was calibrated twice, using two different techniques. As a result of the calibration, the Marsh gauge was selected as the appropriate measuring device during the structural testing of the ultralight.

Although, there are commerical pressure gauges available on the market that would have proven to be more efficient and accurate. However in order to obtain these characteristics in a gauge, one has to pay the price on the price tag, and this value is an exponential function of the degree of accuracy efficiency, precision, and many other features that may be designed into the gauge. After analyzing the extent of precision and accuracy that would be required, a more expensive gauge wouldn't have proven to be a financial benefit towards the outcome of the experiment.

INTRODUCTION

There are several manufactures that design and produce a large variety of measuring devices with specific capabilities that are predetermined for each instrument.

There are two primary objectives of this report. First, it will justify the logical deductions that lead to the selection of the Marsh J1678 pressure gauge as the measuring instrument to monitor the experimental loads that would be exerted on the structure of the ultralight at any given time. Second, it will indicate the two different techniques that were used to calibrate the Marsh pressure gauge, and the margin of error thats associated with each reading as a result of each calibration.

Also, this report was written in partial fulfillment of course requirements in A.E. 592. This report is rated with a worth of 3/4 of a semester hour out of the two hours of A.E. 592.

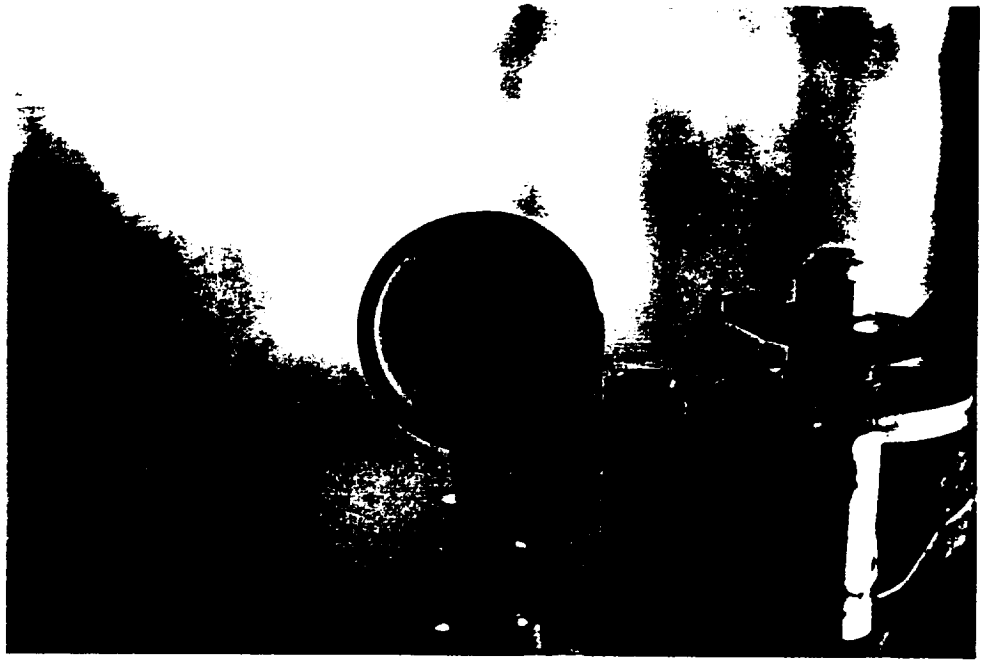

MARSH PRESSURE GAUGE
Figure 1

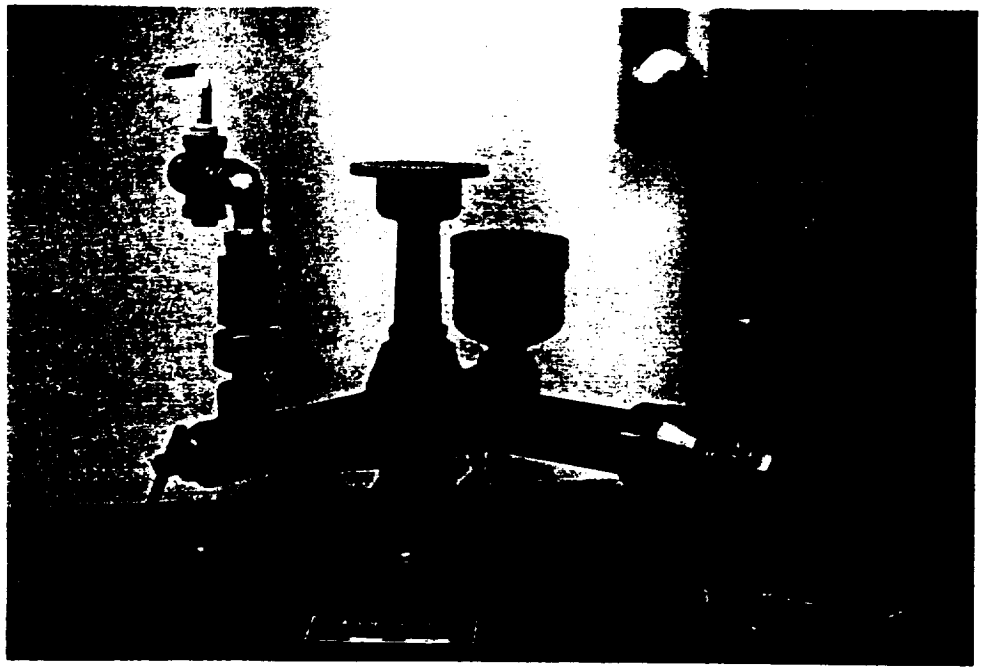

ASHCROFT TESTER
Figure 2

Calibration Process

There were two calibration tests performed on the Marsh J1678 pressure gauge prior to its acceptance as an experimental measuring device. The first test was completed with an Ashcroft dead weight tester (model no. 1300, and serial no. 1788).

The following procedures were used during the test process and are illustrated in Figure (5) in Appendix (B).

1 - The reservoir was filled with a light mineral oil.

2 - Value B was retracted, so that the compression cylinder could be filled with mineral oil from the resevoir.

3 - The Marsh pressure gauge was connected to the Ashcroft tester at point E.

4 - Value B was closed to prevent the mineral oil from escaping back into the reservoir.

5 - Value D was opened to expose the port of the pressure gauge to the mineral oil contained in the compression cylinder.

6 - Weights of desired increments were added to the platform of piston F.

7 - Value H was screwed until the piston floated freely approximately two inches above cylinder G.

8 - The platform was spun.

9 - A pressure reading was read from the pressure gauge.

After each incremental weight increase, the steps that followed the addition of weights were compiled. With the Ashcroft dead weight tester, the Marsh pressure gauge was calibrated up to 500 psi. Even though the tester had the capability of calibrating a gauge above 500 psi, the accessories that were required to continue the calibration process were not available. The calibration data can be observed in Table 1 and Figure 3.

ASHCROFT DEAD WEIGHT TEST LAB RESULTS

	CALIBRATED PRESSURE (PSI)	GAUGE READING (PSI)
1.	5	5
2.	205	200
3.	305	290
4.	405	390
5.	490	485

TABLE I

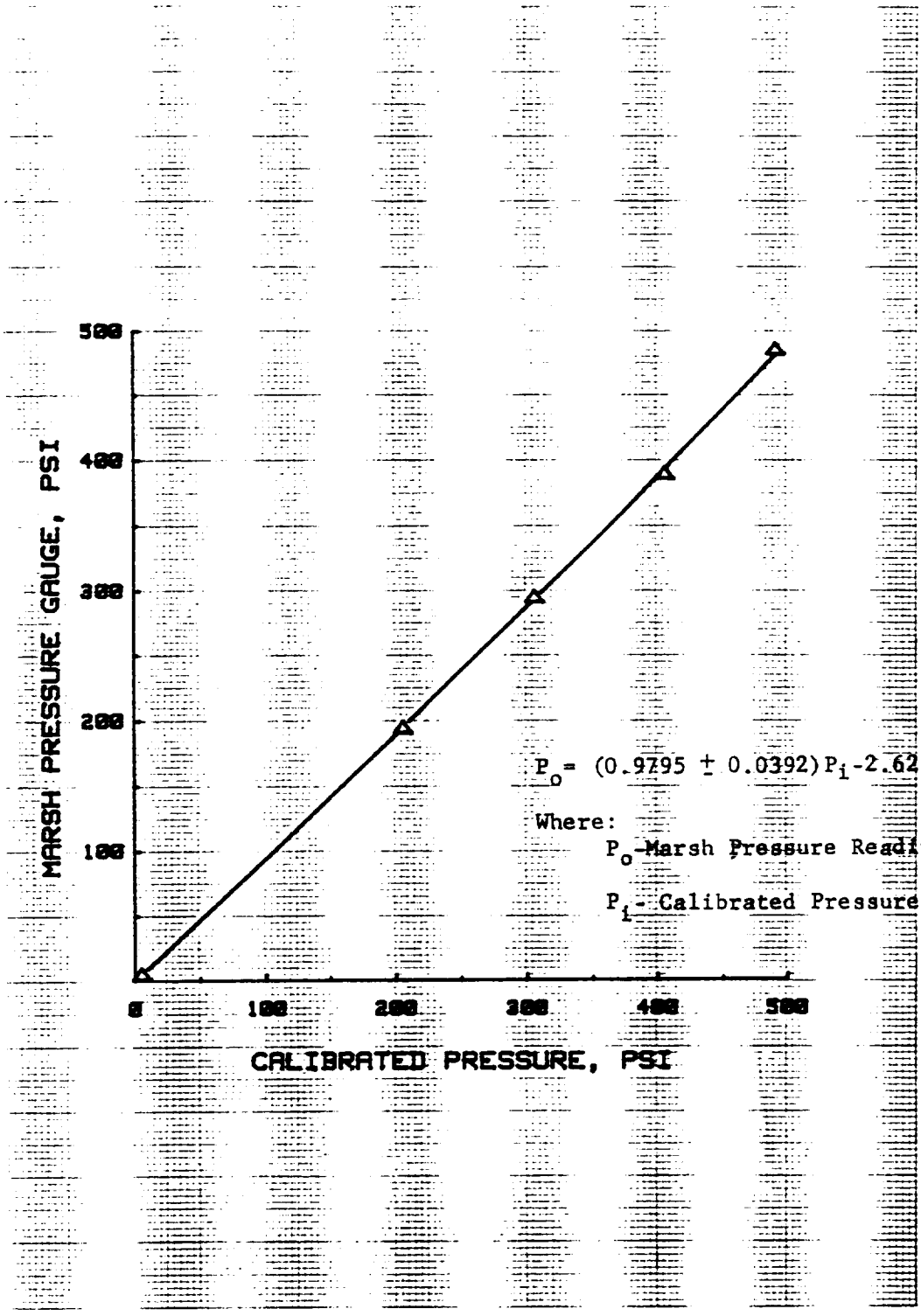

CALC	OXENDINE	03/86	REVISED	DATE	ASHCROFT DEAD WEIGHT TESTER CALIBRATION CURVE FOR THE MARSH PRESSURE GAUGE	A.E.592
CHECK						FIGURE 3
APPD						
APPD					UNIVERSITY OF KANSAS	PAGE 6

CALIBRATION PROCESS (CONTINUED)

The second calibration was accomplished by using the facilities at Richards-Gebaur Air Force Base in Missouri.

Initially the test equipment was prepared for testing. The steps that were involved in preparing the test equipment are outlined in appendix B. Once the equipment was ready, the calibration process was completed by using the following steps:

A) Isolate the gauge from the test stand system by closing the associated shut off valve.

B) Using an independent source of pressure connected to a master gauge of known accuracy, connect this pressure source to the test port of the gauge to be calibrated.

C) Remove the ring and glass from the gauge and use a screwdriver and adjust the position of the pointer by turning the self-locking worn adjustment screw

D) Then check the calibration of the pressure gauge at several different pressures, when the adjustment is satisfactory replace the glass and ring

However, when the Marsh pressure gauge was tested, the gauge didn't need to be adjusted, and this fact can be observed fron the data that was obtained during the calibration process at Richard Gebaur. This data can be observed in TABLE II, and the calibration curve can be observed in figure 4.

RICHARDS GEBAUR CALIBRATION RESULTS

	CALIBRATED PRESSURE (PSI)	INDICATED GAUGE PRESSURE (PSI)
1.	400	395
2.	500	495
3.	1000	1000
4.	1500	1500
5.	1800	1800
6.	2000	2000
7.	2100	2100
8.	2300	2300
9.	2500	2500
10.	2800	2800
11.	3000	3000

TABLE II

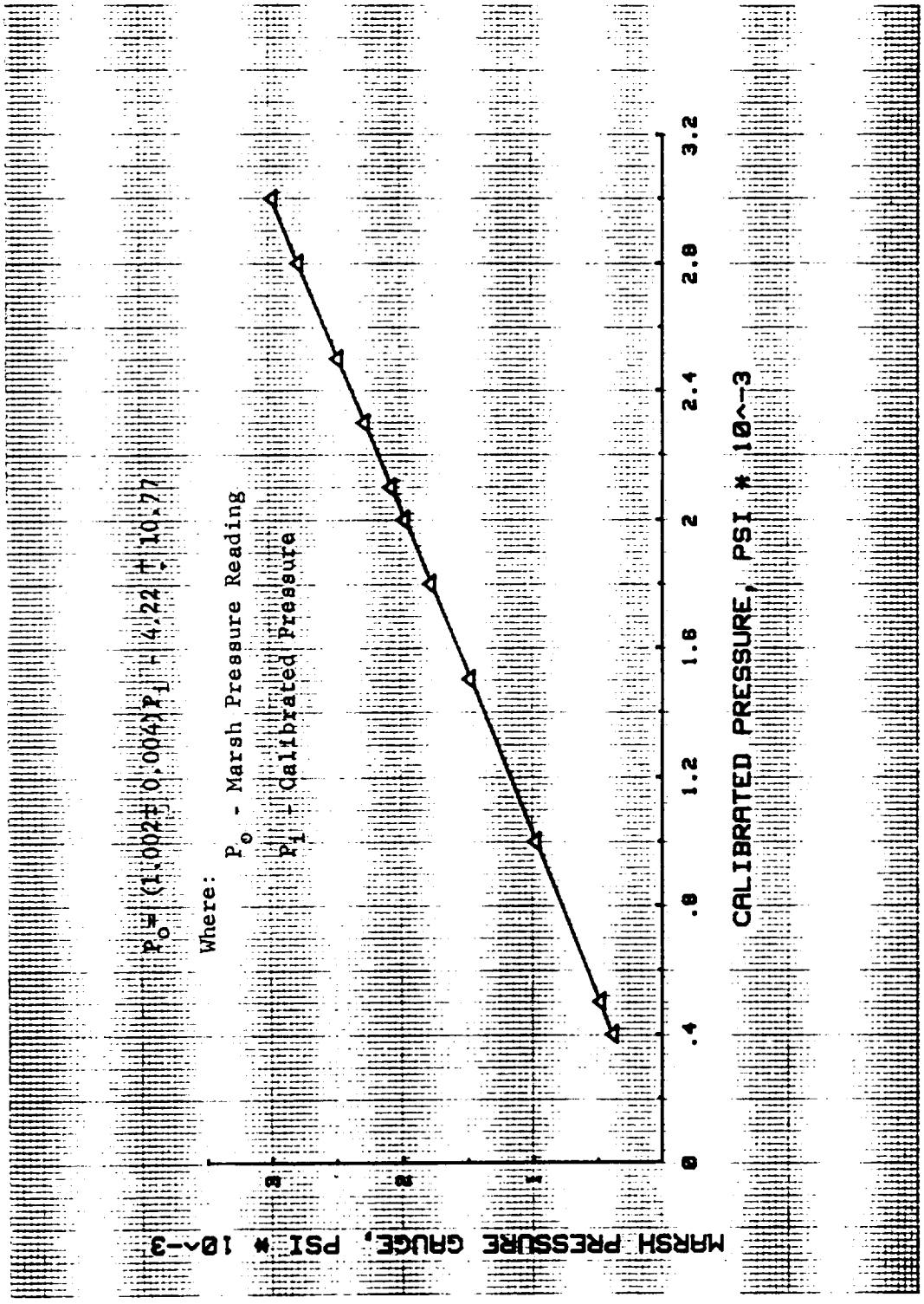

CALC	[illegible]	08/21/85	REVISED	DATE	CALIBRATION CURVE FOR MARSH PRESSURE GUAGE	A.E. 592
CHECK						FIGURE 4
APPD						
APPD					UNIVERSITY OF KANSAS	PAGE 9

DISCUSSION

When a pressure gauge or any other measuring device is being considered for a particular task, several factors have to be analyzed to ensure that the proper gauge has been selected for the job. Because, if the time is not taken to properly analyze these factors, complications as well as inaccuracies can result directly from an improper selection. From the available gauges, the Marsh J1678 pressure gauge was preferred over the other models and brands.

Our decision was based on several factors which included the gauges's operating environment, readability, accuracy, measuring range, recalibration capabilities and versitility for future usages.

Readability During experimental testing the scale on the measuring instrument should be highly visible and relitively easy to comprehend. On the Marsh pressure gauge the scale is marked with slashes in 100 psi increments. The face on the dial gauge has a white enamel background with slashes and numerical values painted in black enamel. The needle is also painted black which enhances the reader's ability to accurately interpret the correct pressure.

Accuracy In experimental testing the degree of accuracy in the laboratory data is an extremely important consideration. Therefore, methods should be developed and practiced in the lab to enhance the accuracy of experimental data, as long as the results of the experiment are more important than the cost. The Marsh company publishes a handbook on standard gauges. This book shows that the Marsh J1678 gauge has a margin of +/- 2% error for the middle half of the scale, and +/- 3% for the remaining half. From Appendix A, it is evident that the margin of error is much less than either 2 or 3 percent, except at pressures below 175 psi.

Measuring Range The measuring range is a factor that can be easily over looked when selecting the proper gauge. However, through a theoretical analysis, it was determined that the ultralight structure could withstand approxi-

mately up to four G's, which is equivalent to 600 psi, prior to catastrophic failure. With this information, the range of loads that are of interest can be determined and used in selecting the proper gauge. On the Marsh pressure gauge, the effective range is from approximately 750 psi to 2250 psi, which is the middle half of the gauge.

Recalibration When recalibrating a pressure gauge it is beneficial to have the ability to adjust the location of the pointer so that it can be re-adjusted to rest within the zero band when the pressure applied to the gauge is zero. The Marsh pressure gauge includes a zero band denoting that the pointer may fall anywhere within this band when the gauge is properly calibrated. In addition the gauge is designed in such a way that the needle can be adjusted within a limited range so that a seriously damaged instrument can not be falsely recalibrated.

Versitility When a gauge is selected for versitility a decision has to be made as to whether the gauge will be used for a specific task or for a variety of tasks. If the selection was based on a specific task then, gauge versitility can be limited. However, if the gauge was selected based on a variety of tasks, then the gauge will have to be versitile in order to be used efficiently. When the Marsh pressure gauge was selected, the selection was based mainly on precision and accuracy. Even though versitility was not a deciding factor, the manufacturer designed the gauge with versitility in mind. The universal design features of the Marsh pressure gauge can be observed in Table V.

CONCLUSION

From the limited selection of gauges that were readily available the Marsh J1678 pressure gauge was selected as the proper gauge for the task. However, there are gauges on the market that would have proven to be more efficient in accomplishing the same task. Also, it is evident from Figure 1 that accurate scale reading will be difficult to obtain. Although the margin error (inaccuracy) is not suspected to exceed +/- 10 psi. Although even with this error and after analyzing the extent of accuracy that is required during experimental testing, in conjunction with the capabilities of the Marsh pressure gauge, it was concluded that the Marsh gauge would be an acceptable measuring device.

In determining the accuracy and precision of the Marsh instrument, the Gaussian distribution method was used and the calculations are outlined in Appendix A.

The results of the Gaussian distribution for the +/- 3s approach are as follows:

FOR THE DEAD WEIGHT TESTER

$$P_o = (0.9795 \pm 0.0392)P_i - 2.62 \pm 12.78$$

FOR THE HYDRAULIC TESTER

$$P_o = (1.002 \pm 0.004)P_i - 4.22 \pm 10.77$$

Where: P_o - Marsh Pressure Reading (out-put)

P_i - Calibrated Pressure (in-put)

APPENDIX A

(CALIBRATION CALCULATIONS)

CALIBRATION CALCULATIONS

In the calibrating a pressure gauge the relationship between the calibrated input pressure and the output (Gauge Reading) pressure is ideally a straight line. However in reality nothing is perfect. Although the calibration curve is still considered to be a straight line. This line was determined through the least squares method. This method minimizes the sum of the squares of the vertical deviations of the data points from the fitted curve.

USING THE LEAST SQUARES METHOD

$$P_O = MP_i + B$$

Where:

P_o - Output Quantity

P_i - Input Quantity

M - Sole Of The Line

B - Intercept of the Line On the Vertical Axis

$$M = \frac{N\Sigma P_i P_o - (\Sigma P_i)(\Sigma P_o)}{N\Sigma P_i^2 - (\Sigma P_i)^2}$$

$$B = \frac{(\Sigma P_o)(\Sigma P_i)^2 - (\Sigma P_i P_o)(\Sigma P_i)}{N\Sigma P_i^2 - (\Sigma P_i)^2}$$

Where: N is the total number of data points.

STANDARD DEVIATION

$$s_m^2 = \frac{N\, S_{P_o}^2}{N\sum P_i^2 - (\sum P_i)^2}$$

$$s_b^2 = \frac{S_{P_o} \sum P_i^2}{N \sum P_i^2 - (\sum P_i)^2}$$

The numerical values of the mean and standard deviation were calculated for both calibration processes. The data that was substituted into the above equations were obtained from Table III and IV

Where:

$$S_{P_o}^2 = \frac{1}{N} (\sum M_{P_i} + B - P_o)^2$$

FOR THE ASHCROFT TEST

MEAN

$$M = \frac{(5)(5.25\text{X}10^{5}) - (1405)(1365)}{(5)(5.39\text{X}10^{5}) - (1405)^{2}}$$

$$= \frac{7.072\text{X}10^{5}}{7.219\text{X}10^{5}} = 0.9795$$

$$B = \frac{(1365)(5.39\text{X}10^{5}) - (5.25\text{X}10^{5})(1405)}{7.219\text{X}10^{5}}$$

$$= \frac{-1.89\text{X}10^{6}}{7.219\text{X}10^{5}} = -2.62$$

STANDARD DEVIATION

$$S_m = \left(\frac{(5)(123.66)}{7.219\text{X}10^{5}} \right)^{1/2} = 1.308\text{X}10^{-2}$$

FOR 3s, $S_m = \pm 3.92\ \text{X}10^{-2}$

$$S_b = \left(\frac{(123.66)^2 (5.39 \times 10^5)}{7.219 \times 10^5} \right)^{1/2} = 4.26$$

FOR 3s, $S_b = \pm 12.78$

FOR THE RICHARD[S] GEBAUR HYDRAULIC TEST

MEAN

$$M = \frac{(11)(4.368 \times 10^7) - (1.989 \times 10^4)(1.991 \times 10^4)}{(11)(4.369 \times 10^7) - (1.991 \times 10^4)^2}$$

$$= \frac{8.474 \times 10^7}{8.458 \times 10^7} = 1.002$$

$$B = \frac{(1.989 \times 10^4)(4.36 \times 10^7) - (4.368 \times 10^7)(1.991 \times 10^4)}{8.458 \times 10^7}$$

$$= \frac{-3.573 \times 10^8}{8.458 \times 10^7} = -4.22$$

STANDARD DEVIATION

$$S_m = \left(\frac{(11)(161.49)}{8.458 \times 10^7} \right)^{1/2} = 1.38 \times 10^{-3}$$

For 3s, $S_m = 4.14 \times 10^{-3}$

$$S_b = \left(\frac{(161.49)\ (4.369 \times 10^6)}{8.458 \times 10^7} \right)^{1/2}$$

$= 3.589$ For 3s, $S_m = 10.77$

CALCULATED DATD OF THE ASHCROFT TSET

	P_i	P_o	P_iP_o	P_i^2	P_o^2
	5	5	25.0	25.0	25.0
	205	200	4.1×10^4	4.2×10^4	4.0×10^4
	305	290	8.85×10^4	9.30×10^4	8.41×10^4
	405	390	1.58×10^4	1.64×10^4	1.52×10^5
	490	485	2.38×10^5	2.41×10^5	2.35×10^5
Σ	1405	1365	5.25×10^5	5.39×10^5	5.12×10^5

TABLE III

CALCULATED DATA OF RICHARD GEBAUR HYDRAULIC TEST

	P_i	P_o	P_iP_o	P_i^2	P_o^2
	400	395	1.58×10^5	1.61×10^5	1.56×10^5
	500	495	2.48×10^5	2.50×10^5	2.45×10^5
	1000	1000	1.00×10^6	1.00×10^6	1.00×10^6
	1500	1500	2.25×10^6	2.25×10^6	2.25×10^6
	1800	1800	3.24×10^6	3.24×10^6	3.24×10^6
	2000	2000	4.00×10^6	4.00×10^6	4.00×10^6
	2100	2100	4.41×10^6	4.41×10^6	4.41×10^6
	2300	2300	5.29×10^6	5.29×10^6	5.29×10^6
	2500	2500	6.25×10^6	6.25×10^6	6.25×10^6
	2800	2800	7.84×10^6	7.84×10^6	7.84×10^6
	3000	3000	9.00×10^6	9.00×10^6	9.00×10^6
Σ	1.99×10^4	1.989×10^4	4.369×10^7	4.369×10^7	4.368×10^7

TABLE IV

APPENDIX B

(CALIBRATION PROCEDURES)

ASHCROFT DEAD WEIGHT GAUGE TESTER

TYPE 1300

DIRECTIONS FOR USING

FILL RESERVOIR "A" WITH A LIGHT GRADE OF MINERAL O_ (ABOUT SAE 20), OR GLYCERINE. WATER SHOULD ONLY BE USED WHERE IT IS MANDATORY, SUCH AS TESTING OF OXYGEN GAUGES. TO FILL COMPRESSION CYLINDER "C", CLOSE VALVE "D", OPEN VALVE "B", AND BACK OUT COMPRESSION SCREW "H".

CONNECT GAUGE TO BE TESTED AT "E", CLOSE VALVE "B" AND OPEN VALVE "D". PLACE THE DESIRED WEIGHTS ON WEIGHT PLATFORM OF PISTON "F" AND SCREW IN "H" UNTIL PISTON "F" AND THE WEIGHTS ARE FLOATING FREELY ABOUT 2" ABOVE THE CYLINDER "G".

FOR TESTERS UP TO 500 LBS. CAPACITY THE PISTON AND WEIGHT PLATFORM ALONE PRODUCE THE FIRST 5 LBS. OF PRESSURE; THEREFORE, IF TWO 10 LB. WEIGHTS ARE PLACED ON THE PLATFORM, 25 LBS. PRESSURE IS PRODUCED.

FOR TESTERS ABOVE 500 LBS. CAPACITY, A SMALLER PISTON "F" IS USED, AND THE PISTON AND WEIGHT PLATFORM ALONE PRODUCE THE FIRST 10 LBS. OF PRESSURE.

WEIGHTS AND PISTONS MUST BE KEPT REVOLVING BY HAND DURING TESTS

BEFORE DISCONNECTING THE GAUGE, BACK OUT THE COMPRESSION SCREW "H", THUS RELEASING PRESSURE AND LOWERING WEIGHTS. TO INSURE THAT NO PRESSURE IS REMAINING, VALVE "B" MAY BE OPENED. CLOSE "B" BEFORE MAKING NEW TEST.

VALVE "D" IS ORDINARILY LEFT OPEN AFTER COMPRESSION CYLINDER "C" HAS BEEN ORIGINALLY FILLED IT IS ONLY CLOSED WHEN RE-PRIMING CYLINDER "C" AND IF GAUGE IS IN PLACE, WILL THUS RETAIN ANY PRELIMINARY PRESSURE WHICH HAS BEEN PRODUCED IN THE GAUGE.

SUITABLE WRENCHES, TOOLS, ETC. ACCOMPANY THE TESTER FOR CONNECTING GAUGE AND MAKING ADJUSTMENTS.

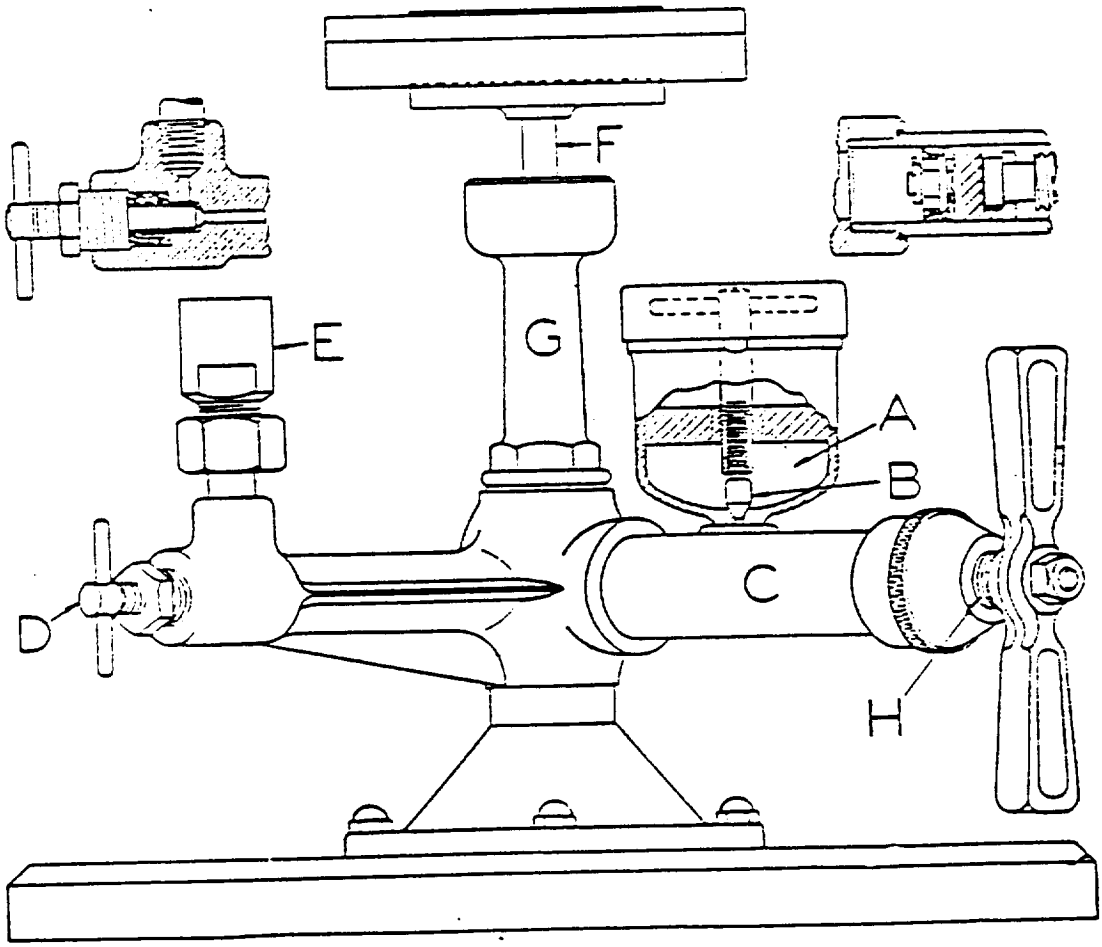

MADE ONLY BY

ASHCROFT GAUGE DIVISION

OF

MANNING, MAXWELL & MOORE INC.

BRIDGEPORT CONNECTICU

Figure V
page 22

SECTION VII
CALIBRATION

7-1. GENERAL.

7-2. A calibration check is required every 180 days, however, calibration of the complete test stand as a unit is not considered practical. Refer to paragraph 3-5 for the initial adjustments to be made before operation of the test stand.

7-3. FLUID TEMPERATURE CONTROLLER. (15, figure 4-2.)

7-4. To adjust the fluid temperature controller, proceed as follows:

CAUTION

The fluid temperature controller requires clean, dry, oil free air at 18 to 20 psi. A piece of hard paper (lint free) placed between the nozzle (10, figure 7-1) and the flapper (9) will show the presence of moisture, oil, or dirt. Add dryers or filters to the air supply line as required to obtain clean dry air before operating or calibrating the temperature controller. Be sure the flapper is lined up with the nozzle and makes a square contact.

a. Turn on air and drain filter (15, figure 4-7) through its drain valve. Adjust pressure regulator (6) to 20 psi supply pressure as shown on supply gage (15, figure 7-1). Set red index pointer (1) at 100°F by turning index setting knob (6).

b. Operate the test stand to pump oil past the sensing element of the temperature controller (refer to paragraph 4-5 and step j of paragraph 3-5 for this operating procedure).

c. Observe the operation of the temperature controller.

Note

Temperature control processes respond slowly (as compared with pressure). Be sure that the period of observation is of sufficient length for the controller to respond to changes in oil temperature. Also, the position of the sensing element in the hydraulic circuit will cause long delays in adjusting due to load changes.

d. If observation of the temperature controller shows that the controlled temperature cycles too much, proceed as follows:

(1) Turn proportional band adjustment (12, figure 7-1) with a screwdriver to increase (widen) the proportional band in steps until the controller is just stable.

(2) Then increase the setting by half for a margin of stability.

e. If observation of the temperature controller shows that the controlled temperature is sluggish or wandering, proceed as follows:

(1) Turn proportional band adjustment (12) with a screwdriver to decrease the proportional band in steps until measurement is jittery or just cycles a bit.

(2) Increase proportional band until control is stable.

(3) Then increase the setting by half for a margin of stability.

Note

An attempt to secure a fine operating adjustment which is just stable under the operating conditions of the moment is not advised since slightly changed operating conditions will probably result in instability and cycling.

f. Normal adjustment of the temperature controller should not require excessive adjustment. If the process being controlled is subject to extreme temperature changes or frequent shut-downs and start-ups the temperature controller should be observed through the period of upset to make certain that it remains stable.

g. If continued adjustment does not bring the process under control, refer to the trouble shooting table in Section VI and check for erratic behavior in the hydraulic system, water system, and temperature controller. To determine if the controller or the process is at fault, operate the controller manually as follows:

(1) Set red index pointer (1) well above black indicating pointer (2) and above the desired temperature of the hydraulic fluid.

(2) Adjust the air supply pressure regulator valve to vary the pressure on the controller diaphragm and thus manually regulate the action of the controller.

(3) When temperature stabilizes at desired value, record the pressure on the output gage (5).

(4) Move the red index pointer (1) back toward the desired temperature until the pressure on the output gage (5) just drops. Restore the air supply pressure to 20 psi. Adjust the red index pointer to be sure the pressure on the output gage is brought to the exact value recorded in step (3) above.

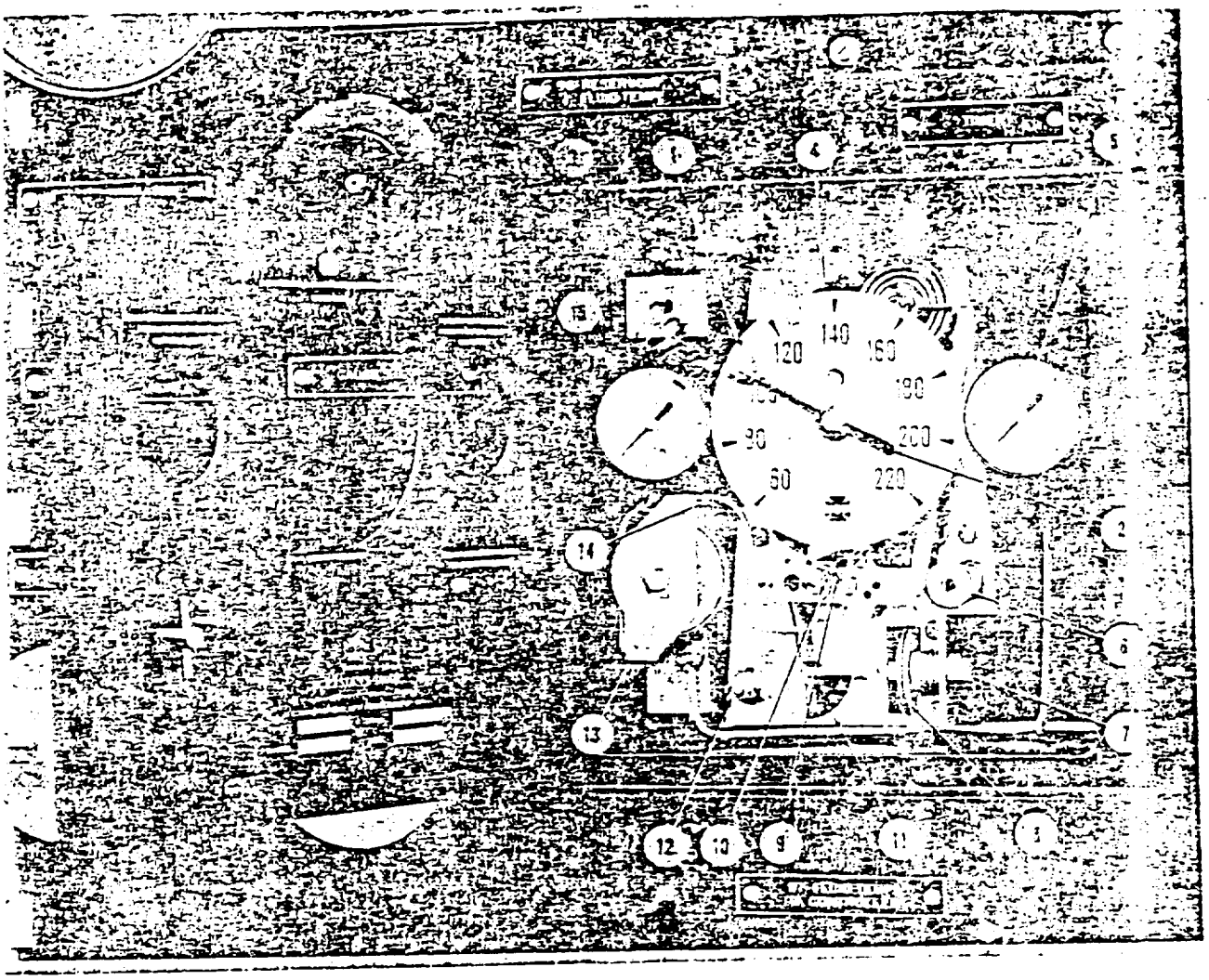

1. Red Index Pointer
2. Black Indicating Pointer
3. Process Connection Block
4. Measuring Head Assembly (mercury actuated)
5. Output Gage
6. Index Setting Knob
7. Synchronizing Nut
8. Feedback Diaphragm Assembly
9. Flapper
10. Nozzle
11. Proportional Dial
12. Proportional Band Adjustment
13. Relay Assembly
14. Orifice Cleaner Button
15. Supply Gage

Figure *Fluid Temperature Controller, Door Open*

Note

If the process can be controlled manually (steps 1 through 3) but not automatically (step 4) the trouble is in the controller. If the process cannot be controlled manually, the trouble is in the water system or the hydraulic system.

After the controller is in operation, the black indicating pointer (2) may not be directly over the red index pointer (1) since factory adjustment is based on psi output as shown on output gage (5). In normal operation the index setting knob can be turned up or down by the amount of the required black pointer change. Be sure to allow measurement to settle at the desired value before proceeding.

i. If output gage pressure is significantly different from 9 psi and the test stand is to be operated at one temperature for a long period, the red pointer may be brought to a matching position with the black pointer by turning synchronizing nut (7).

Note

When the temperatures to be controlled and the hydraulic flow in the test stand are

to be frequently varied, synchronization with each load change is not necessary; proceed as in step h above.

7-5. HYDRAULIC INDICATORS ZERO ADJUSTMENT. The pressure gages supplied with the test stand have adjustable pointers to permit recalibrating the gages. To recalibrate a gage, proceed as follows:

a. Isolate the gage from the test stand system by closing the associated shut off valve.

b. Use an independent source of pressure (hand pump) connected to a master gage of known accuracy; connect this pressure source to the test port of the gage to be calibrated.

c. Remove the ring and glass from the gage. Use a screwdriver and adjust the position of the pointer by turning the self-locking worm adjustment screw.

d. Check the calibration of the gage at several different pressures. When adjustment is satisfactory, replace the glass and ring.

e. Replace an inaccurate gage that cannot be recalibrated.

7-6. ELECTRICAL INDICATORS ZERO ADJUSTMENT. The voltmeter and ammeter are supplied with an external zero adjustment. Use a screwdriver to adjust pointer to zero with no current flow.

7-7. RESERVOIR AIR RELIEF VALVE ADJUSTMENT. The air relief valve, for the hydraulic reservoir, (93, figure 1-5) must be set to relieve if pressure in the line exceeds 125 psi. By applying regulated air, it can be determined at what psi the relief valve opens. The pressure at which the valve initially opens can be adjusted by increasing or decreasing the spring tension.

7-8. INSPECTION OF RESERVOIR LEVEL FLOAT SWITCH. The switch, S16 figure 1-6, will cut off the electric immersion heaters if the hydraulic fluid level falls below 3/4 full. If the switch does not function properly when inspected replace it. There is no adjustment.

7-9. MANOMETER CALIBRATION. The accuracy of the manometer is confirmed by initial preparation and the before use adjustment requirements contained in paragraph 3-5. 1. Further calibration is not required.

APPENDIX C

(MANUFACTURE'S INFORMATION ON MARSH GAUGES)

Marsh Standard Gauges

ANSI B40.1 Grade B accuracy is ±2% of span in middle half of scale, ±3% of span for rest of scale.

Specifications

Accuracy

Grade B Pressure and Vacuum Gauge specifications as established by ANSI Standard B40.1—1974 states that the permissible error shall not exceed 2% of span at any point between 25% and 75% of span; in the rest of the scale, 3% is permissible.

Sizes and connections

1½", 2", 2½", 3½" and 4½" dial sizes. All connections are male N.P.T. 1½" size has ⅛" bottom or center back outlet. 2" and 2½" sizes have ⅛" or ¼" bottom or center back outlets. 3½" size has ¼" bottom or center back outlet. 4½" size has ¼" bottom outlet.

Bourdon tube assembly

For Vacuum and Pressures to 600 psi Tube, tip and socket are copper alloy.

For High Pressures, 1,000 to 5,000 psi Ni-Span-C Bourdon tube; copper alloy tip and socket.

Movement

Standard movement for all 2", 2½", 3½", and 4½" gauges is the new Acculite™ 2000. It is made of glass-filled thermoplastic polyester, and is available either with or without Recalibrator in some models (see Selection Guide).

1½" Standard Gauges feature a copper alloy movement.

See page 3 for fuller descriptions of both movements.

Dial

New cupped dials are made of steel, with white enamel background and black printed matter. 2" and 2½" only.

Case patterns and construction

Plain Case, Slip Ring—drawn steel, 1½", 3½", 4½".

Plain Case, Twist-lock Ring—drawn steel, 2" and 2½".

Plain Clearfront—drawn steel, 1½".

Stainless Clearfront—drawn stainless steel, 1½" and 2".

Flush Case, Snap Ring—drawn steel, 2", 2½", 3½".

Liquid-filled Plain Case, Nonremovable Ring—phenolic, 2½".

Drawn steel cases and rings are finished in black semi-gloss enamel.

Drawn steel cases in a flush pattern have a clear zinc finish.

Drawn stainless steel cases have a brushed stainless steel finish.

Lens

All Standard Gauges are supplied with flat glass lens except for Clearfront cases, which have a molded acrylic press-fit front. 1½" Plain Case Gauges have a flat plastic crystal.

Phenolic case liquid-filled gauges—special construction features

Neoprene plug seals fill port.

Snap-in, nonremovable polypropylene retaining ring.

Accuracy is ±3% of span in middle half of scale.

300 series stainless steel internal construction is available in bottom connection in selected ranges.

2½" dial size only.

Cupped aluminum dial with black numerals on white background.

Restrictor screw is supplied as standard.

Glycerin filling dampens pulsation and vibration. Suitable for use from −30° to 150°F. Other fills available on special order.

Marsh Standard Gauge Selection Guide

DIAL SIZE			1½"						2"				
CASE MATERIAL			Steel				Stainless Steel		Steel				
CASE PATTERN			Plain		Clearfront		Clearfront		Plain				
CONNECTION LOCATION			Bottom	Center Back	Bottom	Center Back	Bottom	Center Back	Bottom			Center Back	
CONNECTION SIZE			¼"	¼"	⅛"	¼"	⅛"	¼"	¼"	¼"		¼"	¼"
RECALIBRATOR			No	No	No	No	No	No	No	No	Yes	No	No
RESTRICTOR			None	None	None	None	None	None	Yes	None	None	None	None
COPPER ALLOY BOURDON TUBE	VACUUM	30" Hg/—100 kPa	•	•	•	•	•	•	J1105	J1405	•	J1305	J2005
	COMPOUND	30" Hg x 30 psi/—100 x 210 kPa	•	•	•	•	•	•	J1112	J1412	•	•	J2012
		30" Hg x 60 psi/—100 x 400 kPa	•	•	•	•	•	•	J1114	J1414	•	J1314	•
		30" Hg x 100 psi/—100 x 700 kPa	•	•	•	•	•	•	•	•	•	•	•
		30" Hg x 150 psi/—100 x 1000 kPa	•	•	•	•	•	•	J1118	J1418	•	J1318	•
		30" Hg x 200 psi/—100 x 1400 kPa	•	•	•	•	•	•	•	•	•	•	•
		30" Hg x 300 psi/—100 x 2100 kPa	•	•	•	•	•	•	•	•	•	•	•
		30" Hg x 400 psi/—100 x 2800 kPa	•	•	•	•	•	•	•	•	•	•	•
	PRESSURE	15 psi/100 kPa	•	•	•	•	•	•	•	•	J1640	•	•
		30 psi/210 kPa	J0042	J0242	J0442	J0642	J0842	J1042	J1142	J1442	J1642	J1842	J2042
		60 psi/400 kPa	J0046	J0246	J0446	J0646	J0846	J1046	J1146	J1446	J1646	J1846	J2046
		100 psi/700 kPa	J0048	J0248	J0448	J0648	J0848	J1048	J1148	J1448	J1648	J1848	J2048
		160 psi/1,100 kPa	J0052	J0252	•	J0652	•	•	J1152	J1452	J1652	J1852	J2052
		200 psi/1,400 kPa	J0054	J0254	J0454	J0654	•	•	J1154	J1454	J1654	J1854	J2054
		300 psi/2,100 kPa	•	•	•	•	•	•	J1158	J1458	•	•	J2058
		400 psi/2,800 kPa	•	•	•	•	•	•	J1160	J1460	•	•	J2060
		500 psi/3,500 kPa	•	•	•	•	•	•	•	•	•	•	•
		600 psi/4,000 kPa	•	•	•	•	•	•	•	J1464	•	•	J2064
NI-SPAN-C BOURDON TUBE	HIGH PRESSURE	1,000 psi/7,000 kPa	•	•	•	•	•	•	•	•	J1672*	•	•
		1,500 psi/10,000 kPa	•	•	•	•	•	•	•	•	•	•	•
		2,000 psi/14,000 kPa	•	•	•	•	•	•	•	•	•	•	•
		3,000 psi/21,000 kPa	•	•	•	•	•	•	•	•	J1678*	•	•
		5,000 psi/35,000 kPa	•	•	•	•	•	•	•	•	•	•	•

(*) all high-pressure gauges have restrictors as standard equipment

TABLE V

VII. DESIGN OF STATIC REACTION GANTRY FOR AN ULTRALIGHT AIRPLANE DESTRUCTION TEST

AIAA paper #85-4022

Howard W. Smith
Professor
Department of Aerospace Engineering
University of Kansas

October 14, 1985

Partially supported by
NASA Langley Research Center
Grant #NAG 1-345

DESIGN OF STATIC REACTION GANTRY FOR AN ULTRALIGHT AIRPLANE DESTRUCTION TEST

Howard W. Smith*
University of Kansas
Lawrence, Kansas

Abstract

The steel gantry superstructure needed to perform an airplane static test is described. Standard civil engineering design practices are used to react the loads generated by an airplane in flight. Reaction columns are mounted on a structural floor to carry the wing airloads and the downward acting fuselage loads are carried directly into the floor. The gantry can accommodate a general aviation airplane or rotorcraft. An immediate use for an ultralight airplane is shown as an example configuration of the four main steel frames.

Introduction

There have been several accidents involving ultralight aircraft. In some of these the integrity of the structure was questioned,[1]**. As a result it was decided that a structural test should be performed.

Discussion

Approach

Since time and funds were limiting factors, it was decided that a structural test to destruction would be performed in the same manner as an FAA static test would be performed for certification of a new general aviation airplane. Testing was abbreviated to include only one flight condition. The "point" to be tested was chosen as point "A" on the V-n diagram.

Airplane Description

The manufacturer called the airplane an "Airmass Sunburst Model 'C'." It is nine feet high, sixteen feet long, and has a wingspan of thirty-six feet. Additional details are shown in Figures 1 and 2, and Table 1.

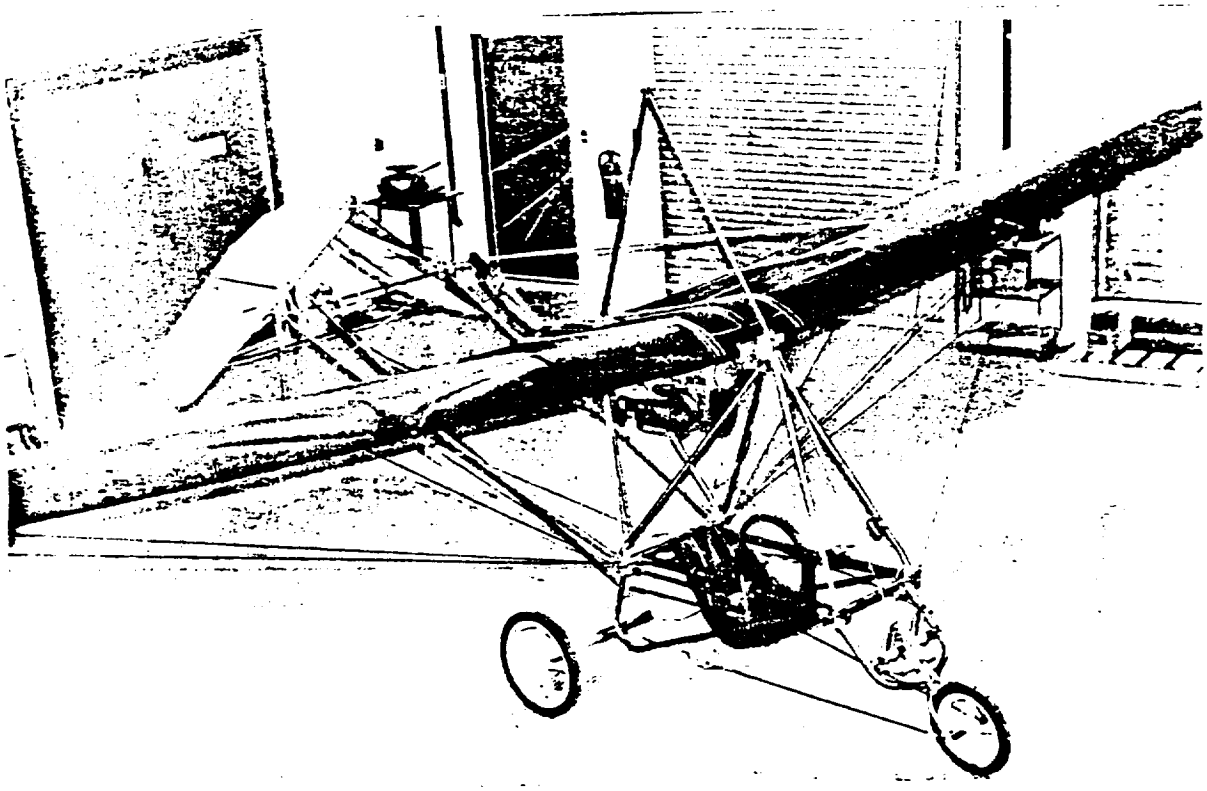

Fig. 1 Airmass Sunburst Model 'C'.

*Professor, Aerospace Engineering
Associate Fellow, AIAA

**Numerals in brackets are references.

Hangar Description

A specially designed hangar houses university-owned airplanes. The eastern half also has a structural test floor, which is a scaled version of the structural floor at the Beechcraft Plant in Wichita, Kansas. Figures 3 and 4 show the salient features of the floor. A cruciform test section is fourteen inches of reinforced concrete, with "I-Beams" embedded in floor. These embedded beams provide "up reaction" where needed, and also serve as a foundation for the steel columns of the gantry.

A major shortcoming of the hangar is the lack of an overhead crane. A clearance of twenty-one feet six inches is available for mobile crane operations.

Loads

The empty weight of the airplane is 273.9 pounds, determined by three-point weighing.

Total weight ("Basic Flight Design Weight") is:

Fuel	15.5 #
Pilot	175.0
Airp.	273.9
TOTAL	464.4

Table 1

Airmass Sunburst Ultralight Model 'C'

Geometric Specifications:

•	Length	17.58 ft
•	Height	9.69 ft
•	Wing Span	36.00 ft
	Wing Area	150.93 ft^2
	Aspect Ratio	8.59
	MGC	4.19 ft
	Wing Taper Ratio	0.92
	Incidence Angle	5.50 deg
•	Tail Area	28.04 ft^2
	Tail Span	9.33 ft
	Dihedral Angle	-40.00 deg

Performance Specifications:

•	$C_{L_{max}}$	1.45
•	OWE	277.48 lbs
•	Stall Speed	43.11 ft/sec
	Cruise Speed	50-75 ft/sec
•	Cuyuna 430 cc 30 HP engine.	

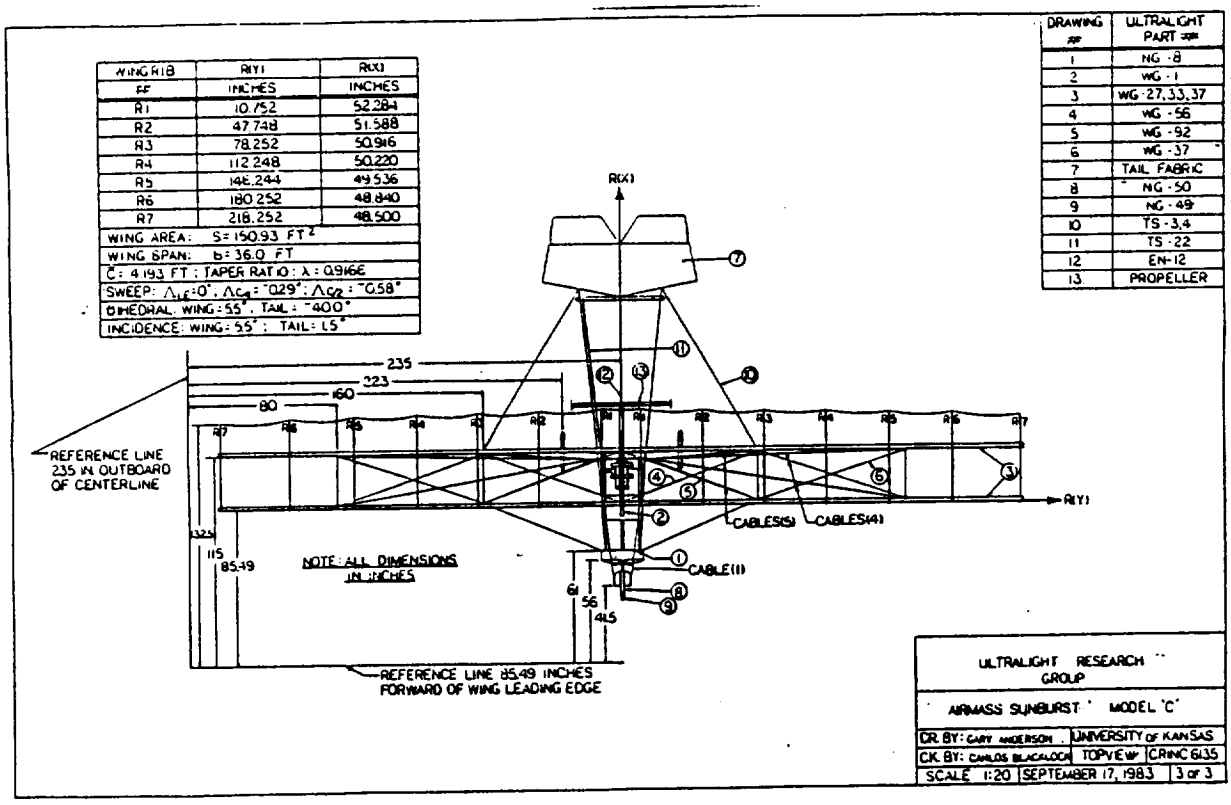

Fig. 2 Planview - "Sunburst".

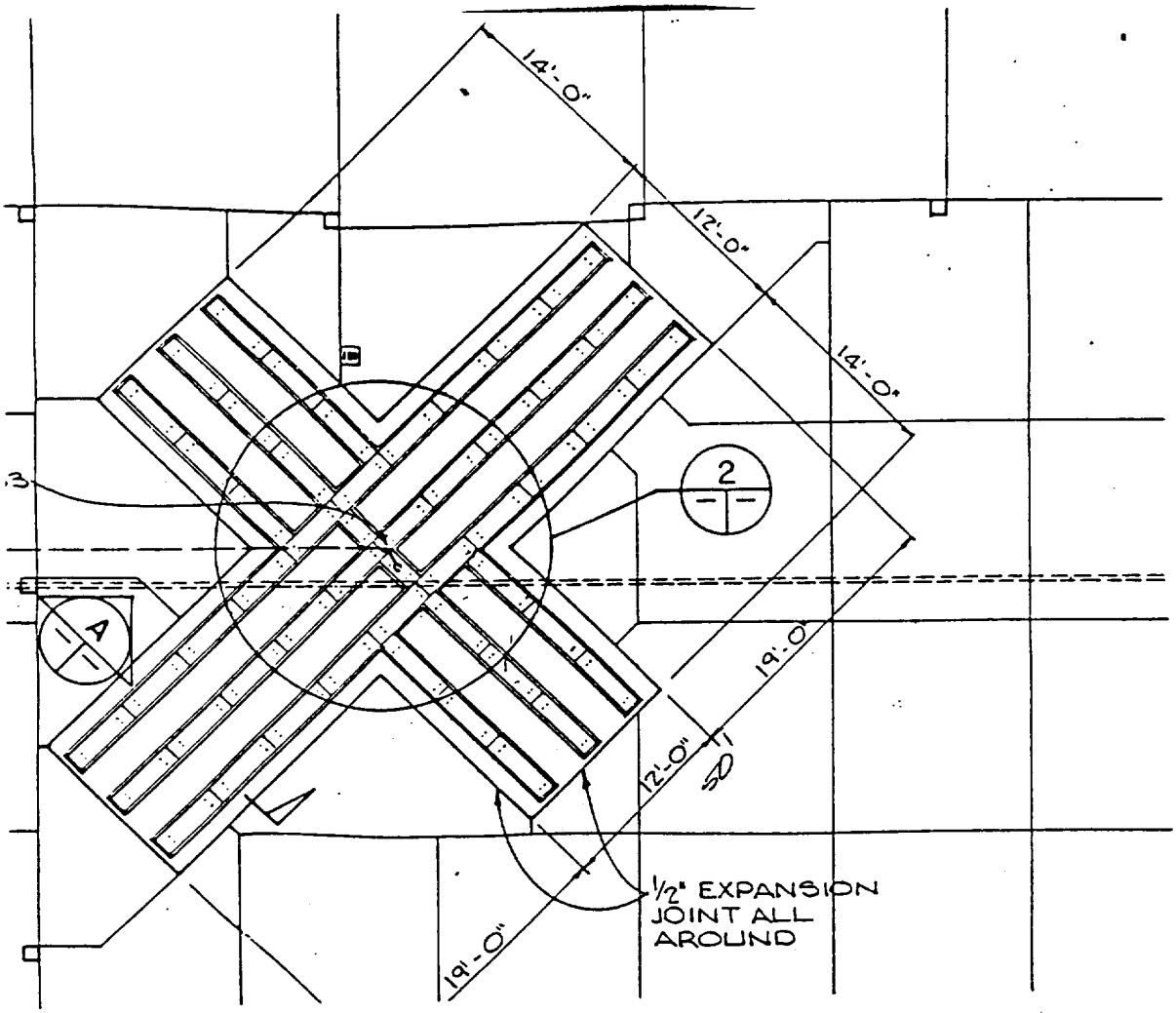

Fig. 3 Cruciform Floor.

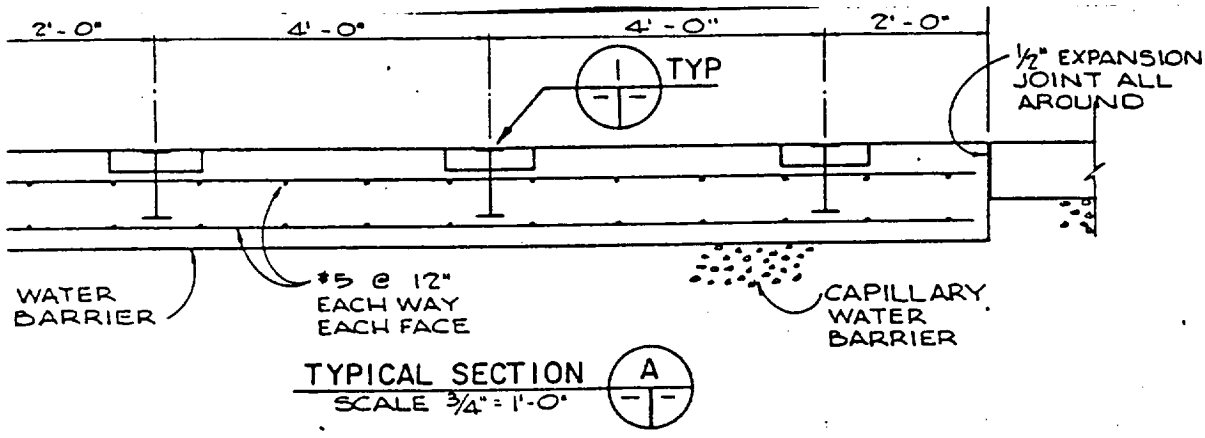

Fig. 4 Embedded Beams.

For structural test purposes, the design limit load factor was assumed to be, $n = 4.0$. A factor of safety of 1.5 was assumed,[2].

Using these values, the estimate maximum ultimate load is:

$$1.5\ (4.0)\ (464.4) = 2786.4 \text{ pounds}$$

Rounded, the design ultimate load is 2,800 lbs.

Steel Gantry

Steel used for the superstructure was designed for a general aviation airplane of the "King Air" class. Using the 12,500 lb. limit as prescribed by FAR Part 23, the ultimate load would be 1.5 x 4.0 x 12,500 = 75,000 pounds. This load can be carried by four reaction columns. Round off this number, a column load of 20,000 pounds was used for the steel design. A beam connecting each pair of columns was designed for a 40 kip load. A beam and two columns, called a "portal", was provided for each wing, the aft fuselage, and the forward fuselage. The four portals are connected to each other with beams in the water plane, Fig. 5.

Each column base plate was centered over a floor beam. Each of the three parallel floor beams is on four foot centerlines, and the columns are located on the outer beams. Since the portal height was chosen to be sixteen feet, a portal is twice as high as it is wide. Each of these portals acts as a slender frame, and requires sway bracing normal to the plane of the portal. An external brace is located on every column ten feet from the floor and extending outward and downward at a forty-five degree angle, Fig. 6. The sway brace itself consists of clevises at each end, a turnbuckle and two five-eighth inch diameter rods. Each column is tied to its nearest neighbor with a short sway brace, and the four columns near the wing-body root are diagonally tied with long sway braces, Fig. 7.

All the steel is type A36 and all bolts are type A325 per the AISC Handbook,[3]. A list of the standard steel section chosen is given in Table 2.

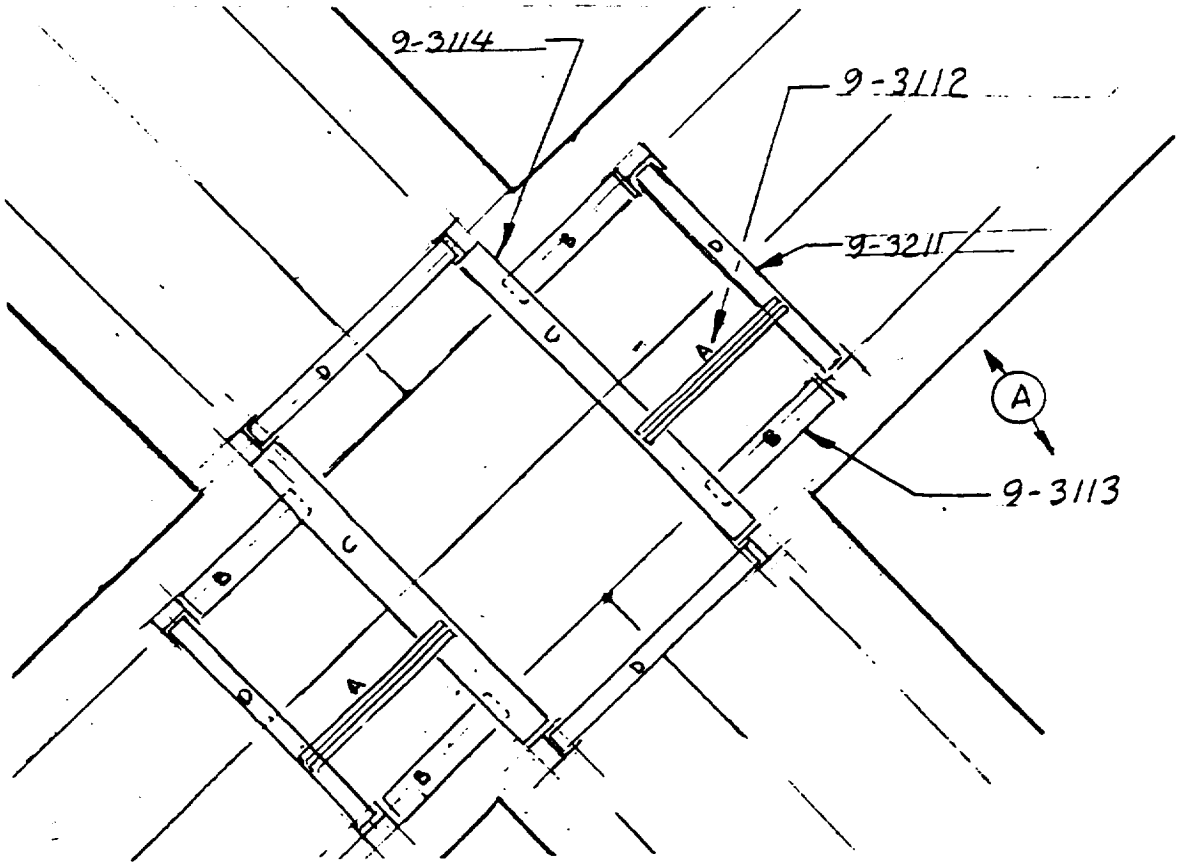

Fig. 5 Overall Steel Installation.

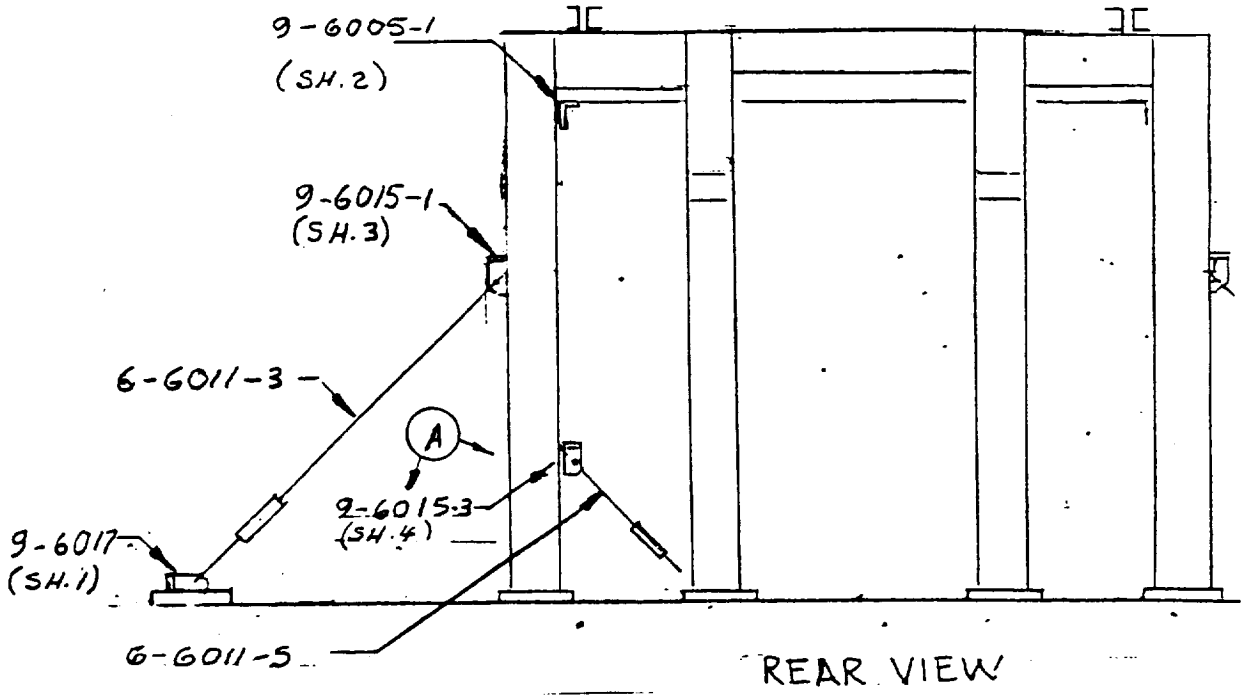

Fig. 6 External Sway Bracing.

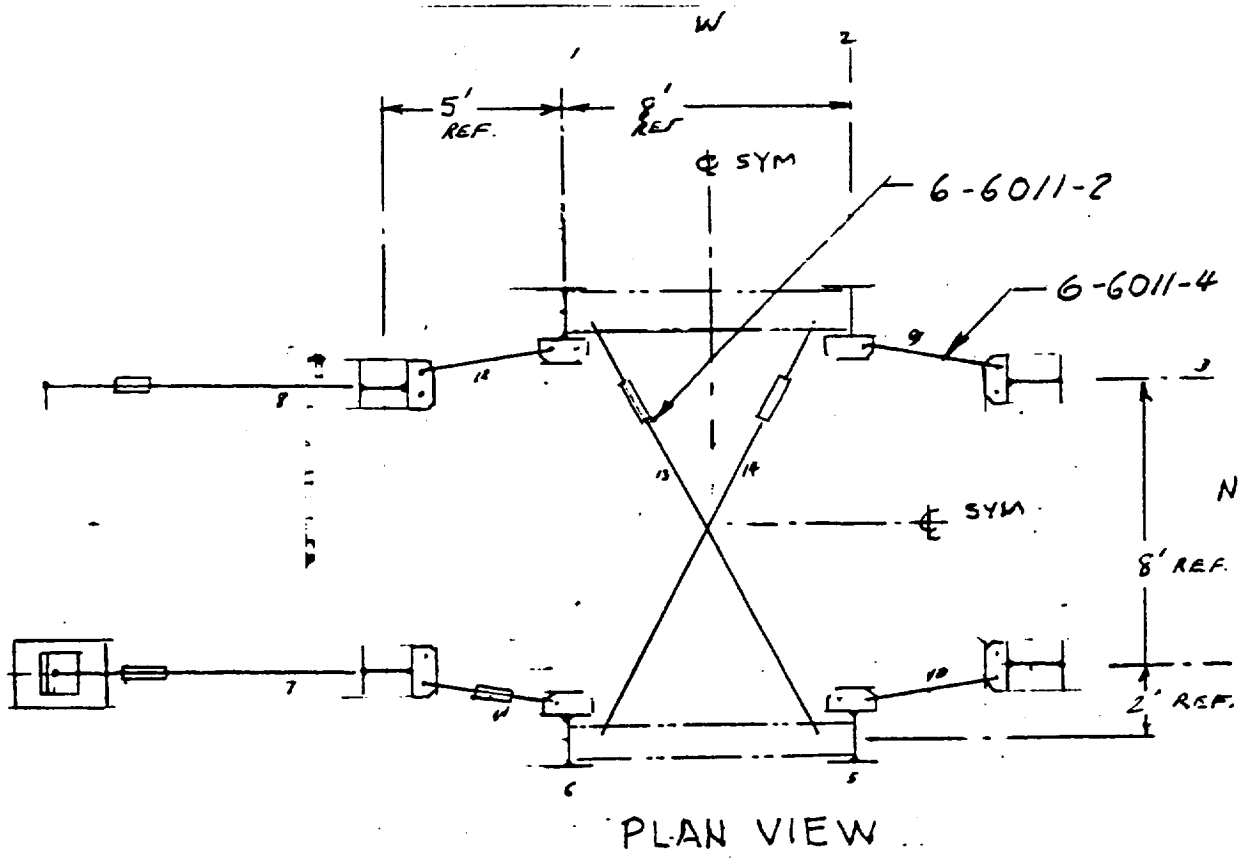

Fig. 7 Internal Sway Bracing.

Table 2. Steel Sections.

8	Columns	W8x24	16'
4	Channels	C12x20.7	5'
4	Beams	W16x40	5'
2	Beams	W18x40	12'
4	Beams	W8x24	8'

All bolts loaded in tension and shear are three-quarter inch diameter. Bolts at column base plate clamps are five-eighth inch diameter. Beam-to-beam connections are made by "good civil engineering practices." A pair of angles is fillet welded to the beam web at each end. The outstanding flange has a hole pattern that matches the repeating pattern in each column flange. Beam "seat" angles are provided for easy construction and disassembly. All assemblies were cleaned and grey primed after welding. All assemblies were painted royal blue before installation.

Acknowledgements

The work described in this paper was performed under NASA Langley Research Center Grant number LRC/NAG 1-345/3-3-83. Six students from the University of Kansas did the drawing of the steel gantry, (in alphabetical order):

Albers, Roger
Bultman, Myron
Clune, Mike
deAlmeida, Sergio
Martin, John
Robertson, Greg

There were many other people, including students, staff, faculty, and townspeople that gave freely of their time. People from Lawrence and Kansas City have given advice and services freely.

References

[1] "Ultralight Vehicle Accidents: Safety Study," NTSB/SS-85-01, Feb. 7, 1985, 405 p.

[2] "Airworthiness Standards for Powered Ultralight Vehicles," Powered Ultralight Manufacturers Association, 7535 Little River Turnpike, Suite 350, Annadale, Virginia 22003, Dec. 9, 1983.

[3] Manual of Steel Construction, AISC, Inc., 400 North Michigan Ave., Chicago, IL 60611, 8th Ed., 1980.